XX (178586.1)

Centro de Investigación y de Estudios
Avanzados del I.P.N. Unidad Guadalajara

Reducción No Lineal de Modelos de Sistemas de Potencia

Tesis que presenta:
Antonino López Ríos

Para obtener el grado de:
Maestro en Ciencias

En la especialidad de:
Ingeniería Eléctrica

Director de Tesis:
Dr. Arturo Román Messina

Guadalajara, Jalisco, Agosto de 2008

Centro de Investigación y de Estudios
Avanzados del I.P.N. Unidad Guadalajara

Nonlinear Model Reduction of Power Systems

A thesis presented by:
Antonino López Ríos

to obtain the degree of:
Master in Science

in the subject of:
Electrical Engineering

Thesis Advisors:
Dr. Arturo Román Messina

Guadalajara, Jalisco, August, 2008.

Reducción No Lineal de Modelos de Sistemas de Potencia

Tesis de Maestría en Ciencias
Ingeniería Eléctrica

Por:

Antonino López Ríos

Ingeniero Eléctrico
Instituto Tecnológico del Istmo 2001-2005

Becario del CONACYT, expediente 203032

Director de Tesis:
Dr. Arturo Román Messina

CINVESTAV del IPN Unidad Guadalajara, Agosto de 2008.

Nonlinear Model Reduction of Power Systems

Master of Science Thesis
In Electrical Engineering

By:

Antonino López Ríos

Electrical Engineer
Instituto Tecnológico del Istmo 2001-2005

Scholarship granted by CONACYT, expedient 203032

Thesis Advisors:
Dr. Arturo Román Messina

CINVESTAV del IPN Unidad Guadalajara, August, 2008.

Acknowledgments

First of all I want to thank God, to the virgin of Guadalupe, to St. Antonio and to all the saints that guided on my road. Perhaps, I know that I could not give everything of me, but I feel satisfied for all what I have achieved.

I would like to thank to:

Ph.D. Arturo Román Messina for offering me: your great support, your patience and knowledge. I want to emphasize that Ph.D. Arturo Román Messina was more than an adviser.

My parents: Roberto López Ramos and Leyda Ríos Enriquez for giving me all your love and for motivating me to study.

My brothers: Angélica, Julián, Francisco, Angel, Gilberto, Jose Antonio and to Esveydi.

My grandparents: Julián y Antonina.

My professors: Dr. Juan Manuel Ramírez Arredondo, Dr. Pablo Moreno Villalobos, Dr. Abner Israel Ramírez Vázquez, Dr. José Manuel Cañedo Castañeda, Dr. José Javier Ruíz León.

My girlfriend and friend Nayeli Martínez Ulloa.

My best friends: Dr. Jesús Héctor Hernández López, Juan Miguel Reyes, Jesús Dávila, José Francisco Herrera, Francisco Lézama, Octavio Leaños, Horacio García, Cristina Alejandra, Pablo Oñate, Omar Villaseñor, Carlos Santana, Pedro Esquivel and to all partners of the area of power systems.

Miss Aracely Calzado Michel.

Finally, I also acknowledge to the CONACYT, since this research would not have been possible without its financial assistance.

Resumen

El trabajo en esta tesis desarrolla y analiza un método para generar modelos no lineales de orden reducido de modelos físicos de sistemas de potencia, los cuales están descritos por ecuaciones algebraicas y diferenciales (DAEs). El método combina la técnica de la descomposición ortogonal propia (POD) y conceptos de la teoría de realización balanceada y puede ser usado para obtener modelos lineales y no lineales de orden reducido de modelos de sistemas de gran dimensión.

La aproximación de rango-reducido para los gramianos de controlabilidad y observabilidad se obtiene usando el método de un rango-menor de imágenes. Los modelos no lineales de orden reducido son entonces construidos mediante la proyección de las ecuaciones del movimiento del sistema, las cuales describen el comportamiento dinámico de interés sobre el espacio de más energía de las eiginfunciones dadas por la POD. El modelo de orden reducido es entonces usado para el estudio del comportamiento del sistema ante grandes y pequeñas perturbaciones.

Este método permite preservar el comportamiento dinámico del modelo original así como su pasividad y estabilidad. La técnica aunque desarrollada para procesos de sistemas de potencia, es suficientemente general para ser aplicada a cualquier proceso que es descrito por ecuaciones algebraicas-diferenciales similares.

El análisis detallado de pequeña y gran señal son desarrollados para comprobar la validez del análisis y valorar el impacto de los controles del sistema sobre el comportamiento del mismo. Los resultados de simulaciones con el de modelos de orden reducido demuestran concordancias buenas con la información de estado estable y transitorio usando modelos convencionales, con un orden de reducción de la magnitud del tiempo de cómputo.

Abstract

The work in this thesis develops and analyzes a method for generating reduced order nonlinear models from physically-based power system models described by differential-algebraic equations (DAEs). The technique combines the proper orthogonal decomposition (POD) technique and concepts from balanced realization theory and can be used to obtain linear and nonlinear reduced order models from large-scale system models.

Using the method of snapshots a low-rank, reduced-range approximation to the controllability and observability grammians is obtained. Reduced order nonlinear models are then constructed by projection of the equations of motion of the system, which describe the dynamic behavior of interest, onto the space of the most energized POD eigenfunctions. The reduced-order model is then used to study system behavior following small and large perturbations.

This method enables the reduced model to retain the dynamic behavior of the original system, as well as its passivity and stability. The technique, though developed for power system processes, is general enough to be applied to any process that is described by similar differential-algebraic equations.

Detailed small and large signal analyses are performed to check the validity of the analysis and to assess the impact of system controllers on system behavior. Simulation results with the reduced order models demonstrate good agreement with steady state and transient information using conventional models, with an order of magnitude reduction in computation time.

Index

Chapter 1

Introduction

Chapter 2

The Proper Orthogonal Decomposition Method

Chapter 3

Model Reduction using Proper Orthogonal Decomposition

Chapter 4

Power System Modeling and Analysis

Chapter 5

Modal Analysis of the Linear ROM

Chapter 6

Application

Chapter 7

Conclusions

Index of Figures and Tables

Chapter 1

Introduction

This introductory chapter presents an outline of the research work in this thesis, and defines concepts linked to reduction of the nonlinear models of the dimension large. The general introduction, the problem statement, the objectives and the study approach are presented.

The chapter concludes with an outline of the structure of the thesis.

1.1 Background and Motivation

The basic motivation for reduced-order system approximation is the need for simplified models of dynamical systems, which capture the main features of the original complex model. This need arises from limited computational, accuracy, and storage capabilities. The simplified model is then used in place of the original complex model, for either simulation or control [1].

Power system phenomena involve a complicated interaction between the dynamics of synchronous machines and system controllers. Realistic models of power grids arising from planning problems often consist of hundreds of coupled differential equations. Thus, for instance, the complexity of power system models, measured in terms of the number of coupled first-order differential equations, may reach the tens or hundreds of thousands. Therefore, simulation of the full model is not feasible or computationally demanding. Consequently, an appropriate simplification of this model is necessary, resulting in simulation with reduced computational complexity.

Power system dynamic motion involves a large number of modes and takes place over a great range of time and length scales.

Deriving from these large-scale representations, an accurate reduced-order model (ROM) is a challenging problem. To be useful, ROMs must preserve network structure, to maintain the same dynamic than the original system, and must preserve the inputs and outputs to allow for the design of controllers.

Recently, the problem of nonlinear analysis of stressed power systems has received considerable attention owing to the need to accurately describe and predict the system response to various loading conditions. However, a number of issues remain with these methods, including the dimensionality of the problem, the amount of information provided by the models, and the generation of reduced models for systems with many inputs and many outputs such as those encountered in wide-area stability analysis.

This thesis focuses on the extraction and characterization of nonlinear behavior from system models described by a set of differential-algebraic equations.

Methods to produce accurate reduced-order models are discussed and techniques to extract modal information from the derived ROMs are presented. The methods are constructive for the study of high-dimensional systems and for their application to nonlinear analysis methodologies such as normal form analysis.

1.2 Problem statement

Realistic models in power systems are quite complex systems of nonlinear differential equations. It is therefore of central importance in power system stability studies to determine cost-efficient reduced-order representations of large-scale systems that accurately describing the behavior of the underlying physical system.

Construction of low-dimensional models of various system representations by reduction of the governing differential equations has attracted significant attention in recent years. Due to the high dimensionality of the differential equations that govern dynamic power system phenomena, it is not feasible to use analytical models to solve these equations.

Low-dimensional models offer a compact description of the system dynamics, and they are potentially useful in designing, simulating, and testing control systems. Reduced-order models are particularly useful for analyzing systems with uncertain parameters and for proving stability properties in complex, high-dimensional systems.

At present, considerable research effort is concerned with feedback control design for applications described by linear models. For general systems, new methods are needed for deriving low-dimensional representations that allow the study of specific characteristics of concern.

Recently, reduced-order modeling techniques, such as those based on proper orthogonal decomposition and Galerkin projection have come to interest. The solution of such problems is challenging owing to large computational requirements of the method and the accuracy of the required representation.

Reduced-order models should offer the following characteristics [1]:

1. The approximation error should be small

2. System properties, like stability and passivity should be preserved,

3. The procedure must be computationally efficient

The ROM must be compatible with analytic methods for the analysis and control of nonlinear dynamic systems and have rigorous guarantees of quality and global error bounds on the resulting reduced model.

These issues are addressed in this work.

1.3 A Brief Review of Previous Work

Many modeling reduction techniques have been proposed in the literature. These include Krylov projection methods, proper orthogonal decomposition, Fourier reduction methods, and approximate balance truncations, among others. In what follows, we provide a brief overview of approaches for constructing ROMs in the context of this work.

There have been notable recent attempts to systematically introduce nonlinear ideas to the power system community. Among them, the POD method (also called empirical orthogonal function analysis) has been shown to be capable of representing complicated phenomena with a handful of degrees of freedom [4].

The development of mathematically rigorous order reduction techniques for DAE models such as those encountered in power system applications is an open problem. Proper orthogonal decomposition provides a systematic way for producing reduced-order models from DAE systems [6] and can be used to design system controllers.

The POD technique has been successfully applied to fluid dynamical, thermal processes, signal processing and other engineering and physical problems. However, only a handful of work exists in the area of oscillatory analysis of transient processes in power systems. Bikash and Nina [3] considered the method for identification of coherent generator groups in large interconnected power system. Messina and Vittal [2] explored the applications of the proper orthogonal decomposition to extract dynamic information from wide-area measurements. Current nonlinear reduction methods are, in general, mostly suited to small systems with little nonlinearity.

More recently, these techniques have gained wide popularity in applications related to data analysis and reduced-order modeling of various physical processes or models. Applications, for example, to unsteady fluid flow, turbulence, aerospace, optimal control, structural dynamics, microstructural design, solution of stochastic partial differential equations, heat transfer and non-destructive testing and system identification have been reported [2], [3]. Another area of interest has been in simulating and analytically approximating control systems.

This prior research forms a basis of understanding that is essential for proper interpretation of the results from the high-fidelity simulation methods surveyed here. Many of the algorithms in the literature generate features that do not fully satisfy the requirements for accurate analysis of complex systems. This research is motivated by the limitations of a wide-variety of techniques

proposed in the literature to deal with high-dimensional problems, the limitations of these techniques is that only are designed for the linear analysis while the method proposed allows us to work with nonlinear problems.

Based on this literature review, it is clear that new analytical techniques are needed to overcome the deficiencies of existing methods. The method proposed here is a step in this direction and makes an effort at closing the gaps mentioned above.

1.4 Thesis Objectives

The primary objective of this research is the development of efficient reduced-order models for large, nonlinear dynamical systems. A second direction of this thesis is to derive techniques to extract nonlinear modal information from the nonlinear ROM. The primary applications of interest are nonlinear phenomena and the analysis and design of system controllers.

Following the above problems, the specific objectives of this research are:

1. The development of a framework for model reduction of large DAE systems. In addition, to develop a systematic analysis method based on proper orthogonal decomposition and projection methods, to generate nonlinear reduced-order system representations that preserve stability and passivity properties.

2. The analysis of data-driven ROMs and its application to the analysis of wide-area system stability.

3. To extend existing approaches to include the representation of network controllers.

4. To evaluate the practical application of the method under linear and nonlinear operating conditions.

5. To address numerical issues associated with the application of these methods.

1.5 Contributions

The primary contributions of this work are as follows:

1. The development of mathematically rigorous order reduction techniques for high dimensional power system models that can be represented by a set of differential and algebraic equations. To the best of our knowledge, this work represents the first analytical application of these techniques to power systems.

2. The generalization of existing approaches to account for network structure and the inclusion of algebraic constraints in the reduction process.

3. The evaluation of alternative formulations based on singular value decomposition of the observation matrix.

4. The derivation of analytical criteria to characterize general mode-state relationships, and the extraction of modal properties.

1.6 Organization of the Thesis

The organization of this thesis is as follows:

Chapter 2 outlines the proper orthogonal decomposition technique and singular value decomposition methods, together with a description of the numerical aspects for proper orthogonal decomposition.

Chapter 3 describes the algorithm proposed for model reductions. General finite dimension approximation methods, together with the ideas behind POD reduced basis functions are discussed.

Chapter 4 introduces the nature of the adopted system model.

In Chapter 5, the modal properties of the linear ROM are examined with emphasis on the characterization of mode shapes and state-mode relationships.

Chapter 6 discusses the practical application of the developed methodologies presented in earlier chapters to the study of a practical power system.

Finally, some concluding remarks and suggestions for future research are presented in Chapter 7.

1.7 References

[1] Athanasios C. Antoulas, *Approximation of Large-Scale Dynamical Systems*, Advances in Design and Control, Siam, (2005).

[2] A. R. Messina, V. Vittal, *"Extraction of dynamics pattern from wide area measurements using empirical orthogonal functions"*, IEEE Transactions on Power Systems, vol. 22, no. 2, pp. 682-692, 2007.

[3] Bikash C. Pal, Nina F. Thornhill, *"Coherency identification in power systems through principal component analysis"*, IEEE Transactions on Power Systems, February 2005.

[4] G. Kerschen, J. C. Galinval, Alexander F. Vakaki and Lawrence A. Bergman, *"The method of proper orthogonal decomposition for dynamical characterization and order reduction of mechanical systems: An overview"*, Nonlinear Dynamics, vol. 41, pp. 147-169, 2005.

[5] Pablo A. Parrillo, Sanjay Lall, Fernando Paganini, George C. Verghese, Bernard C. Lesieutre and Jerold E. Mariden, *"Model reduction for analysis of cascading failures in power systems"*, ACC99-IEEE0267, 1999.

[6] Ricardo P. Pacheco, Valder Steffen, *"On the identification of non-linear mechanical systems using orthogonal functions"*, International Journal of Nonlinear Mechanicals, vol. 39, pp. 1147-1159, 2004.

Chapter 2

The Proper Orthogonal Decomposition Method

The proper orthogonal decomposition (POD) is a multivariate statistical method that aims at obtaining a compact representation of the data. Given a set of snapshots or observations of a system, a linear algorithm produces a series of empirical basis functions which are guaranteed to be optimal for the description of the system snapshots provided. This method may serve for two purposes, namely order reduction by projecting high-dimensional data into lower-dimensional space and feature extraction by revealing relevant but unexpected, structure hidden in the data.

The key idea of the POD is to reduce a large number of interdependent variables to a much smaller number of uncorrelated variables while retaining as much as possible of the variation in the original variables. When combined wit other techniques, proper orthogonal decomposition analysis allows model reduction and simplification.

In this chapter, we give an overview of the POD method in the context of discrete time formulations. Foundations are discussed, and several variations are outlined along with their respective capabilities. First, some mathematical preliminaries are covered following by a discussion of alternative approaches to compute the optimal basis functions. The proper orthogonal decomposition projection approach for building a reduced order model (ROM) will be presented in Chapter 3, along with ideas for extension of the methodology to allow construction of ROMs based on data generated from measurements.

2.1 Theoretical Development: The General Framework

2.1.1 Linear Expansion

Proper orthogonal decomposition (POD) is an optimal technique of finding a basis that spans an ensemble of data, collected from an experiment or a numerical simulation of a dynamical system. The mathematical formulation of the POD presented here closely follows that in the reference [1], [2].

Let $u(x,t_j)$, $j=1,\cdots,N$, denote a sequence of observations on some domain $x\in\Omega$ where x is a vector of spatial variables, and $t_j[0,T]$ is the time at which the observations are made. The POD procedure determines empirical orthogonal functions (EOFs), $\varphi_i(x), i=1,...\infty$ (a linear basis), such that the projection onto the first p EOFs (a low order representation)

$$\hat{u}(x,t_j)=\sum_{i=1}^{p}a_i(t)\varphi_i(x)\ ,\ j=1,...,N \tag{2.1}$$

is optimal in the sense that the average least squares truncation error, ε_j

$$\varepsilon_j=\left\langle\left\|u(x,t_j)-\sum_{i=1}^{p}a_i(t)\varphi_i(x)\right\|^2\right\rangle\ ,\ p\le N \tag{2.2}$$

is minimized, where $<.>$ denotes ensemble average, $\|f\|=<f,f>^{1/2}$ and $\|.\|$ denotes the L_2 norm over Ω. The a_i's are time dependent coefficients of the decomposition to be determined so that (2.1) results in a maximum for (2.2). These special orthogonal functions are called the proper orthogonal modes (POMs) of the reduced basis for the function $u(x,t_j)$.

Following [3] assume that the field is decomposed into a mean value $\mu(x,t_j)$, and a fluctuating part $\bar{u}(x,t_j)$

$$u(x,t_j)=\mu(x,t_j)+\bar{u}(x,t_j) \tag{2.3}$$

More formally, let L^2 denote the space of square integrable functions. It follows that, a normalized basis function φ is optimal if the average projection of u onto φ is maximized, i.e. [2]

$$\max_{\varphi\in\Omega}\left\langle |\,(\bar{u}(x,t_j),\varphi)\,|^2\right\rangle \text{ subject to } \|\varphi\|^2 = 1 \tag{2.4}$$

where the inner product is defined as $<U,V>=\sum_{k=0}^{p} U_k V_k^* = V^H U$, and

$$\|\varphi\|^2 = <\varphi,\varphi> = \varphi^T\varphi = \sum_{j=1}^{m}\varphi_j^2$$

The optimization problem can be recast in the form of a constrained optimization problem where the function to be maximized is given by: [1][1]

$$J[\varphi] = \left\langle |\,(\bar{u}(x,t_j),\varphi)\,|^2\right\rangle - \lambda(\|\varphi\|^2 - 1) \tag{2.5}$$

where λ is a Lagrange multiplier.

2.1.2 Autocorrelation Function

A necessary condition for the extremum of (2.5) is that the Gateaux derivative vanishes for all variations $\varphi+\delta\psi\in L^2([0,1])$, $\delta\in\Re$. This can be expressed as

$$\frac{dJ}{d\delta}[\varphi+\delta\psi]\Big|_{\delta=0} = 0 \quad , \quad \forall\psi\in L_2(\Omega) \tag{2.6}$$

From Eqn. (2.4) and for real functions μ,φ and ψ, we have that

$$\begin{aligned}&\frac{dJ}{d\delta}[\varphi+\delta\psi]\big|_{\delta=0} = 0 = \frac{dJ}{d\delta}\left[\left\langle(u,\varphi+\delta\varphi)(\varphi+\delta\varphi,u)-\lambda(\varphi+\delta\varphi,\varphi+\delta\varphi)\right\rangle\right]= \\ &2\,\mathrm{Re}\left[\left\langle(\mu,\varphi)(\varphi,u)\right\rangle-\lambda(\varphi,\psi)\right]\end{aligned} \tag{2.7}$$

where use has been made of the inner product properties.

Using the commutativity of the averaging operator and spatial integral the quantity in brackets can be written as

$$\left\langle(\mu,\psi)(\varphi,u)\right\rangle-\lambda(\varphi,\psi) = \left\langle\int u(x)\psi^*(x)dx\int\psi(x')u(x')dx'\right\rangle-\lambda\int\varphi(x)\psi^*(x)dx$$

$$= \int\left[\int u(x)\psi^*(x)dx\int\psi(x')u(x')dx'-\lambda\varphi(x)\right]\psi^*(x)dx = 0$$

---

[1]Given a function to maximize, $f(P)$, subject to the constraint $g(P)=0$, the Lagrange function can be defined as $F(P,\lambda j)=f(P)-\lambda g(P)$.

Since the function ψ can be chosen arbitrarily the basis functions must satisfy:

$$\int_{\Omega} \left\langle u(x,t_j)u(x',t_j) \right\rangle \varphi(x')dx' = \lambda\varphi(x) \tag{2.8}$$

Equation (2.8) has a finite number of orthogonal solutions $\varphi_i(x)$ (the proper orthogonal modes) with corresponding real and positive eigenvalues λ_i. Therefore, the optimal POD basis is composed of the eigenfunctions $\{\varphi_j\}$ of the integral equation (2.8), whose kernel is the averaged autocorrelation function

$$R(x,x') = \frac{1}{N}\sum_{i=1}^{N} u(x,t_j)u(x',t_j) \tag{2.9}$$

In practice the observations that form the data are only available at discrete spatial grid points herein called snapshots. In this case, the kernel $R(x,x')$ is replaced with

$$\mathbf{R(x,x')} = \begin{bmatrix} R(x_1,x_1) & \cdots & R(x_1,x_n) \\ \vdots & & \vdots \\ R(x_n,x_1) & \cdots & R(x_n,x_n) \end{bmatrix}$$

where n indicates the number of measurement positions, and

$$R(x_i,x_j) = \frac{1}{N}\sum_{k=1}^{N} u(x_i,t_k)u(x_j,t_k)\ ,\ i,j = 1,\ldots,n \tag{2.10}$$

In other words, the optimal basis is given by the eigenfunctions φ_i of (2.10) whose kernel is the autocorrelation function $\mathbf{R}(x,x') = \left\langle u(x,t_j)u(x',t_j) \right\rangle$.

2.1.3 Discrete-Time Decomposition

Observed time series are usually recorded in discrete form even though the underlying process itself is continuous. In this case, the snapshots are vectors rather than functions.

Following *Holmes et al.* [3], the integral time-average can be approximated by a sum over the set of sampled data points. In this case, the vectors

$$\mathbf{u}_j(x,t_j)=\mathbf{x}_j=[u(x_1,t_1),u(x_1,t_2),\ldots,u(x_1,t_N)]^T \quad , \quad j=1,\ldots,n \tag{2.11}$$

represent a set of snapshots obtained from the observed data at n locations $\{x_1,x_2,\ldots,x_n\}$.

The set of data can then be written as the $N\times n$-dimension ensemble matrix, **X**

$$\mathbf{X}=[\mathbf{x}_1\ \cdots\ \mathbf{x}_n]=\begin{bmatrix} u(x_1,t_1) & \cdots & u(x_n,t_1) \\ \vdots & & \vdots \\ u(x_1,t_N) & \cdots & u(x_n,t_N) \end{bmatrix} \tag{2.12}$$

where each column corresponds to the response at a specific time.

Typically, $n\neq N$. so **X** is generally rectangular. Under these assumptions, the actual integral (2.8) can be written as $\mathbf{G}\varphi=\lambda\varphi$, where $G_{ij}=1/N\sum_{k=1}^{N}u(x_i,t_k)u(x_j,t_k)$. Assuming the EOFs to be of the form $\varphi_i=\sum_{l=1}^{N}w_l^i\mathbf{x}_l$, where w_l^i is a coefficient to be determined, and substituting this expression into (2.8), the problem of minimizing (2.2) can be recast as the problem of finding the largest eigenvalue of the linear equation

$$\mathbf{C}\varphi=\lambda\varphi \tag{2.13}$$

where **C** is the autocorrelation (covariance) matrix defined as

$$\mathbf{C}=\frac{1}{N}\mathbf{X}^T\mathbf{X}=\frac{1}{N}\begin{bmatrix} x_1^Tx_1 & x_1^Tx_2 & \cdots & x_1^Tx_n \\ x_2^Tx_1 & x_2^Tx_2 & \cdots & x_2^Tx_n \\ \vdots & \vdots & . & \vdots \\ x_n^Tx_1 & x_n^Tx_2 & \cdots & x_n^Tx_n \end{bmatrix}=\frac{1}{N}\sum_{i=1}^{n}(\mathbf{x}_i-\mu_{mean})^T(\mathbf{x}_i-\mu_{mean}) \tag{2.14}$$

The resulting covariance matrix **C**, is a real, symmetric ($C_{ij}=C_{ji}$) positive and semi-definite matrix. The resulting POD modes are fully orthogonal, and are assumed to be normalized φ_i, $i=1,\ldots,n$, i.e

$$\varphi_i^T\varphi_j=\begin{cases}\delta_{ij} & i=j \\ 0, & i\neq j\end{cases}$$

Using standard linear algebra techniques the covariance matrix can be expressed in the form

$$\mathbf{C} = \mathbf{U}\,\mathbf{\Lambda}\,\mathbf{V}^{T} \tag{2.15}$$

where $\mathbf{U}$ and $\mathbf{V}$ are the matrices of right and left eigenvectors and $\mathbf{\Lambda} = diag[\lambda_1 \quad \lambda_2 \quad \cdots \quad \lambda_n]$.

The eigenvalues computed from (2.15) are real an non-negative and can be ordered such that $\lambda_1 \geq \lambda_2 \geq \cdots\cdots \geq \lambda_n \geq 0$. The eigenvectors of $\mathbf{C}$ are called proper orthogonal modes (POMs), and the associated eigenvalues are called the proper orthogonal values (POVs).

2.2 The Method of Snapshots

The method of snapshots is based on the fact that the data vectors u_i and the POD modes span the same linear space [3]. We choose the eigenfunctions φ to be a linear combination of the snapshots:

$$\varphi_l = \sum_{i=1}^{N} w_i^l \mathbf{x}_i \tag{2.16}$$

where the coefficients w_i^l are to be determined such that $\mathbf{u}$ maximizes

$$\max_{\varphi} \frac{1}{N} \sum_{j=1}^{m} \frac{\left| x_j, \varphi \right|}{< \varphi, \varphi >} \tag{2.17}$$

These l functions are assembled into an $m \times N$ matrix, φ, known as the modal matrix. In matrix form equation (2.16) becomes

$$\Phi = \mathbf{X}\mathbf{W} \tag{2.18}$$

where

$$\Phi = \begin{bmatrix} \uparrow & \uparrow & \uparrow & \uparrow \\ \varphi_1 & \varphi_2 & \cdots & \varphi_l \\ \downarrow & \downarrow & \downarrow & \downarrow \end{bmatrix};\ \mathbf{X} = \begin{bmatrix} \uparrow & \uparrow & \uparrow & \uparrow \\ x_1 & x_2 & \cdots & x_l \\ \downarrow & \downarrow & \downarrow & \downarrow \end{bmatrix};\ \mathbf{W} = \begin{bmatrix} \uparrow & \uparrow & \uparrow & \uparrow \\ w_1 & w_2 & \cdots & w_l \\ \downarrow & \downarrow & \downarrow & \downarrow \end{bmatrix}$$

and

$$w^1 = \begin{bmatrix} w_1^1 \\ w_2^1 \\ \vdots \\ w_N^1 \end{bmatrix}, \quad w^2 = \begin{bmatrix} w_1^2 \\ w_2^2 \\ \vdots \\ w_N^2 \end{bmatrix}, \ldots, \quad w^N = \begin{bmatrix} w_1^N \\ w_2^N \\ \vdots \\ w_N^N \end{bmatrix}$$

Substitution of (2.16) into the eigenvalue value problem (2.13) results in

$$\mathbf{C}\sum_{i=1}^{N} w_i^l \mathbf{x}_i = \lambda \sum_{i=1}^{N} w_i^l \mathbf{x}_i \tag{2.19}$$

where $C_{ij} = (1/N)(u_i, u_j)$. This can be written as the eigenvalue problem of dimension N

$$\mathbf{CW} = \mathbf{\Lambda W} \tag{2.20}$$

where

$$\mathbf{w} = \begin{bmatrix} w_1 & w_2 & \cdots & w_n \end{bmatrix}$$

and $\mathbf{\Lambda}$ is a diagonal matrix storing the eigenvalues λ_i of the correlation matrix $\mathbf{C}$.

In words, the first-order necessary optimality condition for φ to provide a maximum in (2.17) is given by (2.13). This completes the construction of the orthogonal set $\{\varphi_1 \quad \varphi_2 \quad \cdots \quad \varphi_n\}$.

Once the modes are found using these equations, the flow field can be reconstructed using a linear combination of the modes

$$u_k(x) = \sum_{k=1}^{\infty} a_k(t)\,\varphi_k(x) \tag{2.21}$$

for some $a_k(t) \in \Re$ [2], where the $a_k(t)$ are the time-varying amplitudes of the POD modes $\varphi_k(x)$.

The truncated POD of $\mathbf{u}$ is

[2] The extension to the complex case is discussed in Chapter 4.

$$u_k(x) = \sum_{k=1}^{p} a_k(t)\varphi_k(x) + R \tag{2.22}$$

where p is the number of dominant modes, and R is an error term. Once the relevant eigenmodes have been computed, the temporal behavior of each mode is evaluated as the inner product of the eigenmode (the POD mode φ_k) and the original data. To ensure uniqueness of the solution, the normalization condition of $< \varphi_i, \varphi_i > = 1$ is imposed $\|\varphi\| = 1$. The temporal coefficients are then expressed as

$$a_i = \left\langle \mathbf{x}, \varphi_i \right\rangle \Big/ \left\langle \varphi_i, \varphi_i \right\rangle \tag{2.23}$$

Note that the temporal modes are uncorrelated in time, i.e. $(a_j(t), a_k(t)) = \delta_{jk}\lambda_j$, where $\delta_{jk} = 1$ *for* $j = k$, 0 *else*, and that the system (2.22) is optimal in the sense that minimizes the error function

$$\varepsilon_{N_\lambda}(\varphi) = \sum_{l=1}^{p} \left\| u(t) - \sum_{j=1}^{N_\lambda} a_j(t)\varphi_j(t) \right\|$$

We remark that no conditions are imposed on the data set: the data can be a sample of a stationary process or a sample of a non-stationary process.

2.3 Energy Relationships

The use of the POD method leads naturally to a discussion of truncation criteria. Several techniques to derived truncated expansion have been proposed in the literature. Here we choose to reduce the residual terms such that the mean square value

$$R = O\left(\frac{\lambda_{p+1}}{\sum_{i=1}^{m} \lambda_i} \right) \tag{2.24}$$

be as small as possible.

Among the POD eigenvalues obtained, the most significant eigenmodes contain most of the energy of the dynamics and correspond to the largest

eigenvalues. Let the total energy be expressed as the sum of the energy of every eigenvalue

$$E = \sum_{k=1}^{n} \lambda_k \tag{2.25}$$

The associated percentage of total energy contributed by each mode can be expressed as

$$E_k = \frac{\lambda_k}{\sum_{j=1}^{n} \lambda_j} \tag{2.26}$$

Thus, for instance, we can select the order p of the reduced basis φ such that the predetermined level of the total energy E of the snapshot ensemble is captured. The p-dominant eigenfunctions are then obtained as

$$\frac{\sum_{i=1}^{p} \lambda_i}{\sum_{j=1}^{n} \lambda_j} \geq E \tag{2.27}$$

for the smallest integer p, were E is an appropriate energy level.

2.4 The Singular Value Decomposition

The POD method may also be formulated as a singular value problem in terms of the observation matrix. Let $\mathbf{A}$ be a real $m \times n$ matrix. The singular value decomposition theorem states that $\mathbf{A}$ can be decomposed into the following form:

$$\mathrm{A} = \mathbf{U}\boldsymbol{\Sigma}\mathbf{V}^T \tag{2.28}$$

where $\mathbf{U} = col[\mathbf{u}_1 \quad \mathbf{u}_2 \quad \cdots \quad \mathbf{u}_m]$ is an $m \times m$ orthonormal matrix ($\mathbf{U}^T = \mathbf{U}^{-1}$), $\boldsymbol{\Sigma}$ is an $m \times n$ pseudo-diagonal and semi-positive definite matrix with diagonal entries containing the singular values, and $\mathbf{V} = col[\mathbf{v}_1 \quad \mathbf{v}_2 \quad \cdots \quad \mathbf{v}_n]$ is an $n \times n$ orthonormal matrix ($\mathbf{V}^T = \mathbf{V}^{-1}$). The columns of $\mathbf{U}$ and $\mathbf{V}$ are called left and right singular vectors for $\mathbf{A}$. The diagonal entries of $\boldsymbol{\Sigma}$, that is the $\Sigma_{ii} = \sigma_i$, can be arranged to be non-negative and in order of decreasing magnitude

$\sigma_1 \geq \sigma_2 \geq \cdots \geq \sigma_m \geq 0$. The decomposition (2.28) is called the SVD of the matrix $\mathbf{A}$.

Theorem 2.1 The largest singular value of a matrix $\mathbf{A}$ is equal to its induced 2-norm: $\sigma_1 = \|\mathbf{A}\|_2$, in addition, every matrix $\mathbf{A}$ with entries in C has a SVD.

2.4.1 Properties of the SVD

Assume that in (2.28) $\sigma_r > 0$, while $\sigma_{r+1} = 0$; the matrices $\mathbf{U}, \mathbf{\Sigma}, \mathbf{V}$ are partitioned compatibly in two blocks, the first having r columns:

$$\mathbf{U} = [\mathbf{U}_1 \quad \mathbf{U}_2], \quad \mathbf{\Sigma} = \begin{bmatrix} \mathbf{\Sigma}_1 & \\ & \mathbf{\Sigma}_2 \end{bmatrix} \in \mathrm{R}^{n \times m} \quad \text{and} \quad \mathbf{V} = [\mathbf{V}_1 \quad \mathbf{V}_2] \tag{2.29}$$

$$\mathbf{\Sigma}_1 = \begin{bmatrix} \sigma_1 & & \\ & \ddots & \\ & & \sigma_r \end{bmatrix} > \mathbf{0}, \quad \mathbf{\Sigma}_2 = \mathbf{0} \in \mathrm{R}^{(n-r)\times(m-r)}$$

where $\mathbf{U}_1, \mathbf{U}_2$ have $r, n-r$ columns and $\mathbf{V}_1, \mathbf{V}_2$ have $r, m-r$ columns, respectively.

It can be readily proved that:

1. Rank $\mathbf{A} = r$

2. The four fundamental spaces associated with $\mathbf{A}$ are:

$$\text{span col } \mathbf{A} = \text{span col } \mathbf{U}_1, \quad \ker \mathbf{A}^{*} = \text{span col } \mathbf{U}_2$$
$$\text{span col } \mathbf{A}^{*} = \text{span col } \mathbf{V}_1, \quad \ker \mathbf{A} = \text{span col } \mathbf{V}_2$$

3. **Dyadic decomposition.** Matrix $\mathbf{A}$ can be decomposed as a sum of r outer products of rank one:

$$\mathbf{A} = \sum_{i=1}^{k} \sigma_i \left(\mathbf{u}_i \mathbf{v}_i^T \right)$$

4. The orthogonal projection onto the span of the columns of $\mathbf{A}$ is $\mathbf{U}_1 \mathbf{U}_1^{*}$.

5. The orthogonal projection onto the kernel of $\mathbf{A}^{*}$ is $\mathbf{I}_n - \mathbf{U}_1 \mathbf{U}_1^{*} = \mathbf{U}_2 \mathbf{U}_2^{*}$.

6. The orthogonal projection onto the span of the columns of $\mathbf{A}^{\dagger}$ is $\mathbf{V}_1\mathbf{V}_1^*$

7. The orthogonal projection onto the kernel of $\mathbf{A}$ is $\mathbf{I}_n - \mathbf{V}_1\mathbf{V}_1^* = \mathbf{V}_2\mathbf{V}_2^*$.

8. The Frobenius norm of $\mathbf{A}$ is $\|\mathbf{A}\|_F = \sqrt{\sigma_1^2 + \sigma_2^2 + \cdots + \sigma_r^2}$

2.4.2 Relation to the Eigenvalue Problem

An interesting interpretation of the POD modes can be obtained from the singular value analysis of the response matrix $\mathbf{X}$.

Using the notation in section 2.1 let the response matrix $\mathbf{X}$ be given by

$$\mathbf{X} = \begin{bmatrix} u(x_1,t_1) & \cdots & u(x_n,t_1) \\ \vdots & & \vdots \\ u(x_1,t_N) & \cdots & u(x_n,t_N) \end{bmatrix} \tag{2.30}$$

where the columns correspond to a response at time.

It then follows from (2.28) that the SVD of the response matrix $\mathbf{X}$ may be written as

$$\mathbf{X} = \mathbf{U}\boldsymbol{\Sigma}\mathbf{V}^T \tag{2.31}$$

In terms of the notation above for SVD, it can be seen directly from (2.15) that the correlation matrix defined previously is given by

$$\mathbf{X}\mathbf{X}^T = (\mathbf{U}\boldsymbol{\Sigma}\mathbf{V})(\mathbf{U}\boldsymbol{\Sigma}\mathbf{V})^T = \mathbf{U}\boldsymbol{\Sigma}^2\mathbf{U}^T \tag{2.32}$$

and

$$\mathbf{X}^T\mathbf{X} = (\mathbf{U}\boldsymbol{\Sigma}\mathbf{V})^T(\mathbf{U}\boldsymbol{\Sigma}\mathbf{V}) = \mathbf{V}\boldsymbol{\Sigma}^2\mathbf{V}^T \tag{2.33}$$

Hence (2.32) becomes

$$\mathbf{X}^T\mathbf{X}\mathbf{U} = \mathbf{U}\begin{bmatrix} \lambda_1 & & & \\ & \lambda_2 & & \\ & & & \lambda_n \end{bmatrix} = \mathbf{U}\begin{bmatrix} \sigma_1^2 & & & \\ & \sigma_2^2 & & \\ & & & \sigma_n^2 \end{bmatrix} \tag{2.34}$$

From (2.32)-(2.34), the singular values of $\mathbf{X}$ are the square roots of the eigenvalues of $\mathbf{X}\mathbf{X}^T$ or $\mathbf{X}^T\mathbf{X}$. In addition, the left and right eigenvectors of $\mathbf{X}$ are the eigenvectors of $\mathbf{X}\mathbf{X}^T$ and $\mathbf{X}^T\mathbf{X}$, respectively.

The POMs, defined as the eigenvectors of the sample correlation matrix $\mathbf{C}$ are thus equal to the left singular vectors of $\mathbf{X}$. the POVs, defined as the eigenvalues of matrix $\mathbf{C}$ are the squares of the singular values divided by the number of samples N

The k first empirical eigenfunctions are obtained of the relations of the energy, as follows:

$$\frac{\sum_{i=1}^{k}\sigma_i}{\sum_{i=1}^{n}\sigma_i}\times 100 \le (\%) \tag{2.35}$$

where σ_i is the ith singular value, and $(\%)$ is the percentage of captured energy.

2.5 References

[1] R. Messina, V. Vittal, *"Extraction of dynamics pattern from wide area measurements using empirical orthogonal functions"*, *IEEE Transactions on Power Systems*, vol. 22, no. 2, pp. 682-692, 2007.

[2] G. Kerschen, J. C. Galinval, Alexander F. Vakakis and Lawrence A. Bergman, *"The method of proper orthogonal decomposition for dynamical characterization and order reduction of mechanical systems: An overview"*, *Nonlinear Dynamics*, vol. 41, pp. 147-169, 2005.

[3] Philip Holmes, John L. Lumley, Gal Berkooz, *"Turbulence, coherent structures, dynamical systems and symmetry"* New York: Cambridge University Press, 1996.

Chapter 3

Model Reduction using Proper Orthogonal Decomposition

Nonlinear model reduction is emerging as an issue of strategic importance to the analysis of large power system models. Solving the differential algebraic equations (DAEs) simultaneously in simulation and control applications can pose a numerical challenge. Other motivations for model reduction are for storage and retrieval of optimal control trajectories, insight into the model structure, and analysis of dynamic degrees of freedom.

This chapter describes an approach based on proper orthogonal decomposition for model reduction of nonlinear dynamic systems that can be expressed in an explicit state space form. A method for producing reduced-order models of nonlinear systems described by DAE models based on proper orthogonal decomposition is presented. This approach makes use of the proper orthogonal decomposition and is well suited for applications that require large-scale model reduction.

Based on this theoretical framework, a new algorithm for model reduction is proposed. The analysis procedure begins with the introduction of the perturbation model that enables the representation of higher order nonlinear effects. First, the system equations are expanded in a truncated series around a given operating condition. Then, a set of basis functions is obtained by generating a set of observations through simulations of the nonlinear process. Using the computed eigenfunctions as basis functions in a truncated series representation of the system model, a nonlinear reduced-order model is obtained. The model can be used to estimate nonlinear system response, or be used as an auxiliary technique to other nonlinear analysis methods such as the method of normal forms.

3.1 Background

Power system dynamical models are often large and complex, requiring a great deal of computational resources. High- dimensional models are not amenable to dynamic analysis and controller design. A challenging problem is that of determining a ROM that preserves physical aspects of interest.

In this chapter, a mathematical modeling approach for obtaining low-order models for the power system is presented that retains the input-output properties of the system. The method relies on proper orthogonal decomposition of measured data and can be used to study linear and nonlinear behavior.

Consider a general high dimensional system, Σ, described by an implicit mixed set of differential and algebraic equations (DAEs) of the form:

$$\Sigma : \begin{cases} \dot{\mathbf{x}} = \mathbf{f}(\mathbf{x}, \mathbf{y}, \mathbf{u}) \\ \mathbf{0} = \mathbf{g}(\mathbf{x}, \mathbf{y}) \\ \mathbf{E} = \mathbf{h}(\mathbf{x}, \mathbf{y}, \mathbf{u}) \end{cases} \tag{3.1}$$

In the preceding equation $\mathbf{u} \in \mathrm{R}^m$ is the input or excitation vector, $\mathbf{x} \in \mathrm{R}^n$, is the state vector, $\mathbf{g} \in \mathrm{R}^p$ is the vector of algebraic constraints; and $\mathbf{E} \in \mathrm{R}^q$ is the vector of outputs or observations. The output function $\mathbf{h}$, can be linear or nonlinear, depending on the system model and the outputs of interest.

Model reduction techniques seek to produce a similar system (the reduced order system)

$$\hat{\Sigma} : \begin{cases} \dot{\hat{\mathbf{x}}} = \hat{\mathbf{f}}(\hat{\mathbf{x}}, \mathbf{y}, \mathbf{u}) \\ \mathbf{0} = \mathbf{g}(\hat{\mathbf{x}}, \mathbf{y}) \\ \mathbf{E} = \mathbf{h}(\hat{\mathbf{x}}, \mathbf{y}, \mathbf{u}) \end{cases} \tag{3.2}$$

of order k much smaller than the original order , but for which the outputs $\mathbf{E}$ and $\hat{\mathbf{E}}$ are approximately equal for inputs of interest $\mathbf{u}$.

Figure 3.1 illustrates the concept of reduced-order-modeling from computational power system dynamics models whilst Fig. 3.2 shows the input-

output representation. Starting from a physical model of the system, the goal is to construct a reduced-order system representation that can be used for simulation or control.

If possible the input-out mapping should be preserved as discussed in our numerical application of the method. The complexity n of such system is measured by the number of internal variables involved (assumed finite); that is, n is the size of $\mathbf{x} = [x_1 \quad x_2 \quad \cdots \quad x_n]^*$ [3]. This idea will be explored further in the next subsection.

It will be demonstrated in the sequel that a projection procedure employing basis functions which are computed from the proper orthogonal decomposition of the full system response can efficiently reduce the infinite-dimensional systems to finite-dimensional dynamical models while maintaining high-fidelity and reducing system complexity.

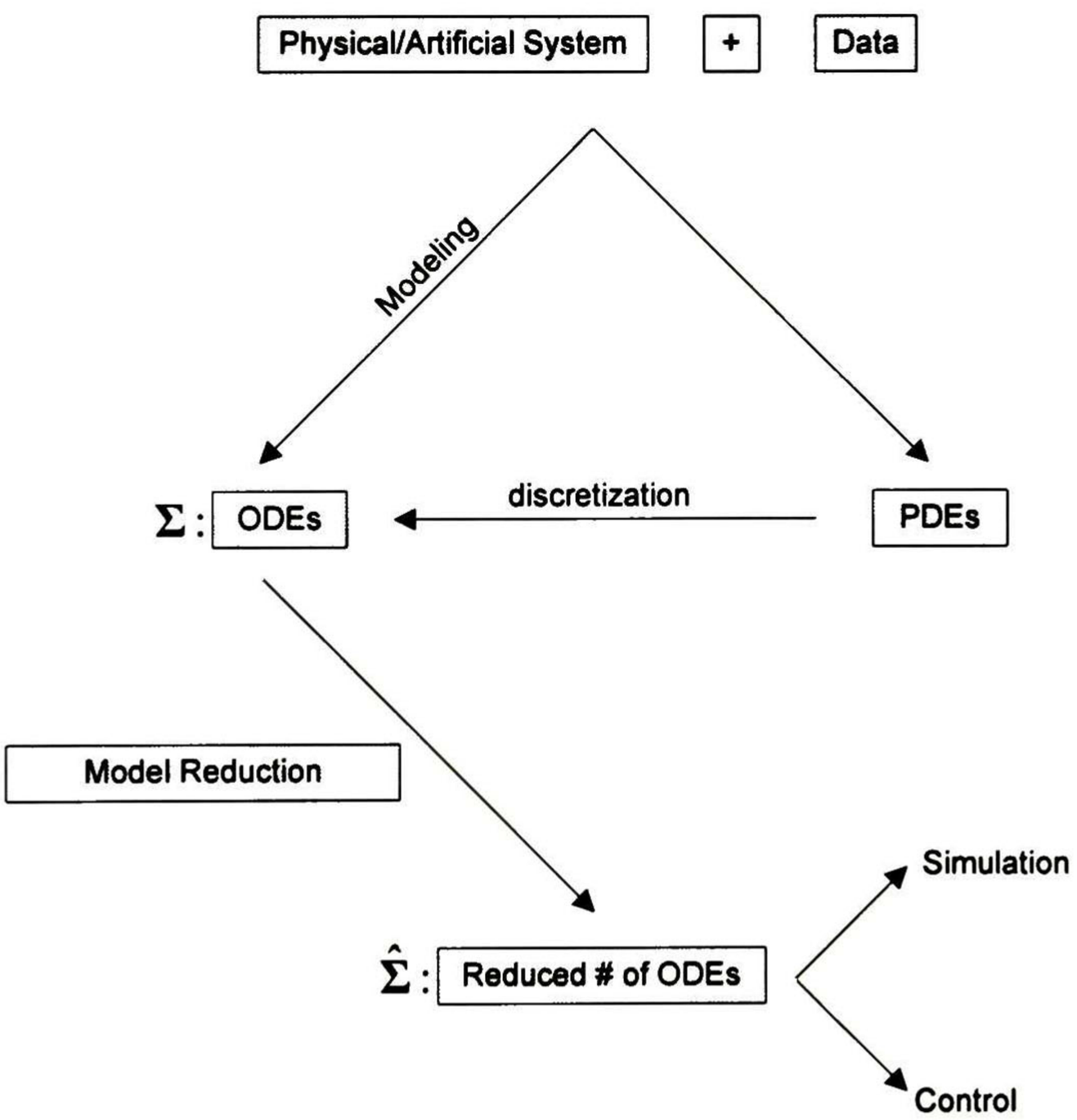

Figure 3.1. Pictorial representation of the concept of reduced-order modeling.

[3] Given a vector or matrix with real entries, the superscript * denotes its transpose. If the entries are complex, the same superscript denotes conjugation with transposition.

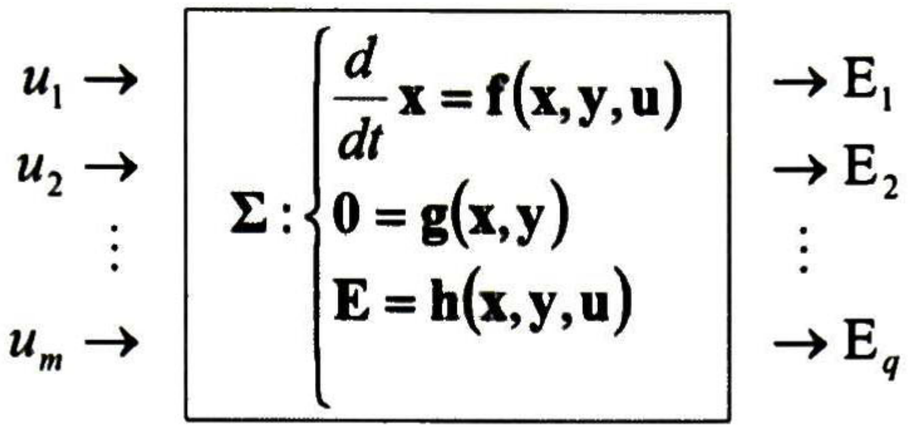

Figure 3.2. Explicit finite-dimensional dynamical system.

We now formalize the notion of the dynamical system Σ.

3.1.1 Problem Statement

Following the above definitions, the problem can be stated as follows. Given a nonlinear dynamical system $\Sigma = (\mathbf{f},\mathbf{g},\mathbf{h})$ with $\mathbf{u} \in \mathrm{U}$, $\mathbf{x} \in \mathrm{X}$, $\mathbf{y} \in \mathrm{Y}$, $\mathbf{h} \in \mathrm{H}$ find a reduced order system $\hat{\Sigma} = (\hat{\mathbf{f}},\hat{\mathbf{g}},\hat{\mathbf{h}})$, $\mathbf{u} \in \mathrm{U}$, $\mathbf{y} \in \mathrm{Y}$, and $\hat{\mathrm{X}} = \{\hat{\mathbf{x}} : \mathrm{T} \rightarrow \mathrm{R}^k\}$, where $k < n$, T is a transformation matrix; such that (some of or all) the following conditions are satisfied:

1. The approximation error is small, and there exists a global error bound.

2. Stability and passivity are preserved.

3. The procedure is computationally stable and efficient.

Over the last few years, several alternate analytical approaches to the determination of reduced-order system representations have been proposed. The following sections describe a general approach based on proper orthogonal analysis for systematically obtaining reduced-order system representations.

3.2 Reduced-Order Dynamic Modeling

3.2.1 Projection onto Optimal Basis

The central idea of POD is to determine a family of subspaces, of increasing (finite) dimension, that optimally span the data, in the sense that the error in the projection onto each subspace is minimized. In what follows a brief mathematical development is given and the method is outlined.

Consider a dynamic system described by the nonlinear plant equation (3.1). The projection-based approach is based on a special linear change of

variables $\bar{\mathbf{x}} = \mathbf{T}\mathbf{x}$ derived from empirical orthogonal function analysis of the observation matrix. See Chapter 2.

Consider that nonsingular left and right transformation matrices are partitioned as

$$\bar{\mathbf{x}} = \begin{pmatrix} \hat{\mathbf{x}} \\ \tilde{\mathbf{x}} \end{pmatrix}, \quad \mathbf{T}^{-1} = \begin{bmatrix} \mathbf{S} & \mathbf{T}_1 \end{bmatrix}, \quad \mathbf{T} = \begin{bmatrix} \mathbf{W}^* \\ \mathbf{T}_2^* \end{bmatrix} \quad \text{where} \quad \hat{\mathbf{x}} \in \mathrm{R}^k, \quad \tilde{\mathbf{x}} \in \mathrm{R}^{n-k}, \quad \mathbf{S}, \mathbf{W} \in \mathrm{R}^{n \times k}$$

Since $\mathbf{W}^*\mathbf{S} = \mathbf{I}_k$, it follows that

$$\mathbf{\Pi} = \mathbf{S}\mathbf{W}^* \in \mathrm{R}^{n \times n} \tag{3.3}$$

is an oblique projection onto the k-dimensional subspace spanned by the columns $\mathbf{S}$ along the kernel of $\mathbf{W}^*$

Using the transform $\bar{\mathbf{x}} = \mathbf{T}\mathbf{x}$, (3.1) may be represented by the following system of DAEs:

$$\dot{\bar{\mathbf{x}}} = \mathbf{T}\mathbf{f}\left(\mathbf{T}^{-1}\bar{\mathbf{x}}, \mathbf{y}, \mathbf{u}\right) \tag{3.4}$$

$$\mathbf{0} = \mathbf{g}\left(\mathbf{T}^{-1}\bar{\mathbf{x}}, \mathbf{y}\right) \tag{3.5}$$

and

$$\mathbf{E} = \mathbf{h}\left(\mathbf{T}^{-1}\bar{\mathbf{x}}, \mathbf{y}, \mathbf{u}\right) \tag{3.6}$$

As discussed in our introductory section, the objective of model reduction is to replace the nonlinear system (3.4)-(3.6) by an equivalent system

$$\hat{\mathbf{\Sigma}} : \begin{cases} \dot{\hat{\mathbf{x}}}(t) = \mathbf{W}^*\mathbf{f}\left(\mathbf{S}\hat{\mathbf{x}}(t), \mathbf{y}, \mathbf{u}(t)\right) \\ 0 = \mathbf{g}\left(\mathbf{S}\hat{\mathbf{x}}(t), \mathbf{y},\right) \\ \mathbf{E} = \mathbf{h}\left(\mathbf{S}\hat{\mathbf{x}}(t), \mathbf{y}, \mathbf{u}\right) \end{cases} \tag{3.7}$$

where $\hat{\mathbf{x}}(t)$ is a k ($k << n$) vector of dominant states.

Several different approaches exist for defining the basis $\mathbf{T}$ Before proceeding with the development of the method, the nature of the nonlinear system model is reviewed.

3.3 Nonlinear System Representation

A key issue in the proposed formulation is that we must have a representation of the nonlinear part that can be efficiently stored and evaluated [5]. Such a representation can be viewed as an extension to linearization theory to the nonlinear model of the power system. In the succeeding sections we explore the use of linearized models to generate a projection-based ROM.

3.3.1 DAE Model

Consider a general nonlinear system containing quadratic and higher-order nonlinearities. For clarity of illustration we assume that the system model can be expressed in compact form as

$$\hat{\Sigma}: \begin{cases} \dfrac{d}{dt}\hat{\mathbf{x}}(t) = \mathbf{W}^{*}\mathbf{f}\left(\mathbf{S}\hat{\mathbf{x}}(t), \mathbf{y}, \mathbf{u}(t)\right) \\ 0 = \mathbf{g}\left(\mathbf{S}\hat{\mathbf{x}}(t), \mathbf{y},\right) \end{cases} \tag{3.8}$$

This model lends itself to physically-based power system formulations and is general enough to allow the study of various physical systems.

Expanding in a Taylor series around the origin gives [3]

$$\begin{aligned} \dot{x}_i = f_{i0} &+ \frac{\partial f_{i0}}{\partial x_1}\Delta x_1 + \cdots + \frac{\partial f_{i0}}{\partial x_n}\Delta x_n + \frac{\partial f_{i0}}{\partial y_1}\Delta y_1 + \cdots + \frac{\partial f_{i0}}{\partial y_p}\Delta y_p \\ &+ \frac{\partial f_{i0}}{\partial u_1}\Delta u_1 + \cdots + \frac{\partial f_{i0}}{\partial u_m}\Delta u_m + \cdots \\ f_{i0} &= f_i\left(\mathbf{x}_0, \mathbf{y}_0, \mathbf{u}_0\right) \end{aligned} \tag{3.9}$$

Equation (3.9) can be written in a more convenient form using the Kronecker product of two matrices [4], this is:

$$\begin{bmatrix} \Delta x_1 & \cdots & \Delta x_n \end{bmatrix}^T \otimes \begin{bmatrix} \Delta x_1 & \cdots & \Delta x_n \end{bmatrix}^T = \begin{bmatrix} \Delta x_1^2 & \cdots & \Delta x_1 \Delta x_n & \cdots & \Delta x_n \Delta x_1 & \cdots & \Delta x_n^2 \end{bmatrix}^T$$

We start by defining the following theorem.

Theorem 3.1. Let A, B, C, D, G, H, R be matrices of dimension $p \times q$, $s \times t$, $r \times l$, $q \times s$, $t \times u$, $p \times q$ and $s \times t$ respectively. Then,

$$(\mathbf{A} \otimes \mathbf{B}) \otimes \mathbf{C} = \mathbf{A} \otimes (\mathbf{B} \otimes \mathbf{C})$$

$$(\mathbf{A}+\mathbf{H})\otimes(\mathbf{B}+\mathbf{R})=\mathbf{A}\otimes\mathbf{B}+\mathbf{A}\otimes\mathbf{R}+\mathbf{H}\otimes\mathbf{B}+\mathbf{H}\otimes\mathbf{R}$$

$$(\mathbf{A}+\mathbf{H})\otimes(\mathbf{B}+\mathbf{R})=\mathbf{A}\otimes\mathbf{B}+\mathbf{A}\otimes\mathbf{R}+\mathbf{H}\otimes\mathbf{B}+\mathbf{H}\otimes\mathbf{R}$$

$$(\mathbf{A}\otimes\mathbf{B})(\mathbf{D}\otimes\mathbf{G})=\mathbf{AD}\otimes\mathbf{BG}$$

$$\mathbf{B}\otimes\mathbf{A}=\mathbf{U}_{s\times p}(\mathbf{A}\otimes\mathbf{B})\mathbf{U}_{q\times t}$$

Making use of the Kronecker produc identities given by Theorem 3.1, we can approximate (3.1) up to second order terms as

$$\begin{aligned}\Delta\dot{\mathbf{x}}=&\mathbf{A}_x\Delta\mathbf{x}+\mathbf{A}_y\Delta\mathbf{y}+\mathbf{A}_u\Delta\mathbf{u}+\mathbf{H}_{xx}(\Delta\mathbf{x}\otimes\Delta\mathbf{x})+\mathbf{H}_{xy}(\Delta\mathbf{x}\otimes\Delta\mathbf{y})\\&+\mathbf{H}_{xu}(\Delta\mathbf{x}\otimes\Delta\mathbf{u})+\mathbf{H}_{yx}(\Delta\mathbf{y}\otimes\Delta\mathbf{x})+\mathbf{H}_{yy}(\Delta\mathbf{y}\otimes\Delta\mathbf{y})+\mathbf{H}_{yu}(\Delta\mathbf{y}\otimes\Delta\mathbf{u})\\&+\mathbf{H}_{ux}(\Delta\mathbf{u}\otimes\Delta\mathbf{x})+\mathbf{H}_{uy}(\Delta\mathbf{u}\otimes\Delta\mathbf{y})+\mathbf{H}_{uu}(\Delta\mathbf{u}\otimes\Delta\mathbf{u})\end{aligned}\quad(3.10)$$

where

$$H_{xxi}=\frac{1}{2}\frac{\partial^2 f_{i0}}{\partial x_1^2}(\Delta x_1)^2+\cdots+\frac{1}{2}\frac{\partial^2 f_{i0}}{\partial x_1\partial x_n}\Delta x_1\Delta x_n+\cdots+\frac{1}{2}\frac{\partial^2 f_{i0}}{\partial x_n\partial x_1}\Delta x_n\Delta x_1$$
$$+\cdots+\frac{1}{2}\frac{\partial^2 f_{i0}}{\partial x_n^2}(\Delta x_n)^2$$

$$H_{xyi}=\frac{1}{2}\frac{\partial^2 f_{i0}}{\partial x_1\partial y_1}\Delta x_1\Delta y_1+\cdots+\frac{1}{2}\frac{\partial^2 f_{i0}}{\partial x_1\partial y_p}\Delta x_1\Delta y_p+\cdots+\frac{1}{2}\frac{\partial^2 f_{i0}}{\partial x_n\partial y_1}\Delta x_n\Delta y_1$$
$$+\cdots+\frac{1}{2}\frac{\partial^2 f_{i0}}{\partial x_n\partial y_p}\Delta x_n\Delta y_p$$

$$H_{xui}=\frac{1}{2}\frac{\partial^2 f_{i0}}{\partial x_1\partial u_1}\Delta x_1\Delta u_1+\cdots+\frac{1}{2}\frac{\partial^2 f_{i0}}{\partial x_1\partial u_m}\Delta x_1\Delta u_m+\cdots+\frac{1}{2}\frac{\partial^2 f_{i0}}{\partial x_n\partial u_1}\Delta x_n\Delta u_1$$
$$+\cdots+\frac{1}{2}\frac{\partial^2 f_{i0}}{\partial x_n\partial u_m}\Delta x_n\Delta u_m$$

$$H_{yxi}=\frac{1}{2}\frac{\partial^2 f_{i0}}{\partial y_1\partial x_1}\Delta y_1\Delta x_1+\cdots+\frac{1}{2}\frac{\partial^2 f_{i0}}{\partial y_1\partial x_n}\Delta y_1\Delta x_n+\cdots+\frac{1}{2}\frac{\partial^2 f_{i0}}{\partial y_p\partial x_1}\Delta y_p\Delta x_1$$
$$+\cdots+\frac{1}{2}\frac{\partial^2 f_{i0}}{\partial y_p\partial x_n}\Delta y_p\Delta x_n$$

$$H_{yyi} = \frac{1}{2}\frac{\partial^2 f_{i0}}{\partial y_1^2}(\Delta y_1)^2 + \cdots + \frac{1}{2}\frac{\partial^2 f_{i0}}{\partial y_1 \partial y_p}\Delta y_1 \Delta y_p + \cdots + \frac{1}{2}\frac{\partial^2 f_{i0}}{\partial y_p \partial y_1}\Delta y_p \Delta y_1$$
$$+ \cdots + \frac{1}{2}\frac{\partial^2 f_{i0}}{\partial y_p^2}(\Delta y_p)^2$$

$$H_{yui} = \frac{1}{2}\frac{\partial^2 f_{i0}}{\partial y_1 \partial u_1}\Delta y_1 \Delta u_1 + \cdots + \frac{1}{2}\frac{\partial^2 f_{i0}}{\partial y_1 \partial u_m}\Delta y_1 \Delta u_m + \cdots + \frac{1}{2}\frac{\partial^2 f_{i0}}{\partial y_p \partial u_1}\Delta y_p \Delta u_1$$
$$+ \cdots + \frac{1}{2}\frac{\partial^2 f_{i0}}{\partial y_p \partial u_m}\Delta y_p \Delta u_m$$

$$H_{uxi} = \frac{1}{2}\frac{\partial^2 f_{i0}}{\partial u_1 \partial x_1}\Delta u_1 \Delta x_1 + \cdots + \frac{1}{2}\frac{\partial^2 f_{i0}}{\partial u_1 \partial x_n}\Delta u_1 \Delta x_n + \cdots + \frac{1}{2}\frac{\partial^2 f_{i0}}{\partial u_m \partial x_1}\Delta u_m \Delta x_1$$
$$+ \cdots + \frac{1}{2}\frac{\partial^2 f_{i0}}{\partial u_m \partial x_n}\Delta u_m \Delta x_n$$

$$H_{uyi} = \frac{1}{2}\frac{\partial^2 f_{i0}}{\partial u_1 \partial y_1}\Delta u_1 \Delta y_1 + \cdots + \frac{1}{2}\frac{\partial^2 f_{i0}}{\partial u_1 \partial y_p}\Delta u_1 \Delta y_p + \cdots + \frac{1}{2}\frac{\partial^2 f_{i0}}{\partial u_m \partial y_1}\Delta u_m \Delta y_1$$
$$+ \cdots + \frac{1}{2}\frac{\partial^2 f_{i0}}{\partial u_m \partial y_p}\Delta u_m \Delta y_p$$

$$H_{uui} = \frac{1}{2}\frac{\partial^2 f_{i0}}{\partial u_1^2}(\Delta u_1)^2 + \cdots + \frac{1}{2}\frac{\partial^2 f_{i0}}{\partial u_1 \partial u_m}\Delta u_1 \Delta u_m + \cdots + \frac{1}{2}\frac{\partial^2 f_{i0}}{\partial u_m \partial u_1}\Delta u_m \Delta u_1$$
$$+ \cdots + \frac{1}{2}\frac{\partial^2 f_{i0}}{\partial u_m^2}(\Delta u_m)^2$$

Further, linearization of the constraint equations assuming that all motions are small [2], results in the following equations:

$$\frac{\partial \mathbf{g}}{\partial \mathbf{x}}\frac{\mathbf{dx}}{\mathbf{dx}} + \frac{\partial \mathbf{g}}{\partial \mathbf{y}}\frac{\mathbf{dy}}{\mathbf{dx}} = \mathbf{0} \tag{3.11}$$

Solving (3.11) for **dy** yields

$$\mathbf{dy} = -\left[\frac{\partial \mathbf{g}}{\partial \mathbf{y}}\right]^{-1}\frac{\partial \mathbf{g}}{\partial \mathbf{x}}\mathbf{dx} \tag{3.12}$$

or, for incremental changes,

$$\Delta \mathbf{y} = -\mathbf{B}_y^{-1}\mathbf{B}_x \Delta \mathbf{x} \tag{3.13}$$

where

$$\mathbf{B}_y = \frac{\partial \mathbf{g}}{\partial \mathbf{y}}$$

$$\mathbf{B}_x = \frac{\partial \mathbf{g}}{\partial \mathbf{x}}$$

provided that the inverse of $\left[\frac{\partial \mathbf{g}}{\partial \mathbf{y}}\right]$ exist, the no singularity of this equation depend of the network variables. A measurement is the stress of the system, i.e., this implicate that program of power flow no converge and therefore this matrix is singular.

Noting that

$$\Delta\mathbf{y} \otimes \Delta\mathbf{y} = \left(-\mathbf{B}_y^{-1}\mathbf{B}_x \otimes -\mathbf{B}_y^{-1}\mathbf{B}_x\right)(\Delta\mathbf{x} \otimes \Delta\mathbf{x}) = \mathbf{C}_{yy}(\Delta\mathbf{x} \otimes \Delta\mathbf{x})$$

$$\Delta\mathbf{x} \otimes \Delta\mathbf{y} = \left(\mathbf{I}_{n\times n} \otimes -\mathbf{B}_y^{-1}\mathbf{B}_x\right)(\Delta\mathbf{x} \otimes \Delta\mathbf{x}) = \mathbf{C}_{xy}(\Delta\mathbf{x} \otimes \Delta\mathbf{x})$$

$$\Delta\mathbf{y} \otimes \Delta\mathbf{x} = \left(-\mathbf{B}_y^{-1}\mathbf{B}_x \otimes \mathbf{I}_{n\times n}\right)(\Delta\mathbf{x} \otimes \Delta\mathbf{x}) = \mathbf{C}_{yx}(\Delta\mathbf{x} \otimes \Delta\mathbf{x})$$

$$\Delta\mathbf{y} \otimes \Delta\mathbf{u} = \left(-\mathbf{B}_y^{-1}\mathbf{B}_x \otimes \mathbf{I}_{m\times m}\right)(\Delta\mathbf{x} \otimes \Delta\mathbf{u}) = \mathbf{C}_{yu}(\Delta\mathbf{x} \otimes \Delta\mathbf{u})$$

$$\Delta\mathbf{u} \otimes \Delta\mathbf{y} = \left(\mathbf{I}_{m\times m} \otimes -\mathbf{B}_y^{-1}\mathbf{B}_x\right)(\Delta\mathbf{u} \otimes \Delta\mathbf{x}) = \mathbf{C}_{uy}(\Delta\mathbf{u} \otimes \Delta\mathbf{x})$$

and substituting these expressions into (3.10) yields the perturbed model

$$\begin{aligned}\Delta\dot{\mathbf{x}} = {} & \left(\mathbf{A}_x - \mathbf{A}_y\mathbf{B}_y^{-1}\mathbf{B}_x\right)\Delta\mathbf{x} + \mathbf{A}_u\Delta\mathbf{u} + \left(\mathbf{H}_{xx} + \mathbf{H}_{xy}\mathbf{C}_{xy} + \mathbf{H}_{yx}\mathbf{C}_{yx}\right)(\Delta\mathbf{x} \otimes \Delta\mathbf{x}) + \\ & \left(\mathbf{H}_{xu} + \mathbf{H}_{yu}\mathbf{C}_{yu}\right)(\Delta\mathbf{x} \otimes \Delta\mathbf{u}) + \left(\mathbf{H}_{ux} + \mathbf{H}_{uy}\mathbf{C}_{uy}\right)(\Delta\mathbf{u} \otimes \Delta\mathbf{x}) + \mathbf{H}_{uu}(\Delta\mathbf{u} \otimes \Delta\mathbf{u})\end{aligned}$$

or, equivalently,

$$\begin{aligned}\Delta\dot{\mathbf{x}} = {} & \mathbf{A}_{xc}\Delta\mathbf{x} + \mathbf{A}_{uc}\Delta\mathbf{u} + \mathbf{H}_{xxc}(\Delta\mathbf{x} \otimes \Delta\mathbf{x}) + \mathbf{H}_{xuc}(\Delta\mathbf{x} \otimes \Delta\mathbf{u}) + \\ & \mathbf{H}_{uxc}(\Delta\mathbf{u} \otimes \Delta\mathbf{x}) + \mathbf{H}_{uuc}(\Delta\mathbf{u} \otimes \Delta\mathbf{u})\end{aligned} \tag{3.14}$$

and

$$\Delta\mathbf{y} = \mathbf{B}_{yx}\Delta\mathbf{x} \tag{3.15}$$

where:

$$\mathbf{A}_{xc} = \mathbf{A}_x - \mathbf{A}_y \mathbf{B}_y^{-1} \mathbf{B}_x$$
$$\mathbf{A}_{uc} = \mathbf{A}_u$$
$$\mathbf{H}_{xxc} = \mathbf{H}_{xx} + \mathbf{H}_{xy} \mathbf{C}_{xy} + \mathbf{H}_{yx} \mathbf{C}_{yx}$$
$$\mathbf{H}_{xuc} = \mathbf{H}_{xu} + \mathbf{H}_{yu} \mathbf{C}_{yu}$$
$$\mathbf{H}_{uxc} = \mathbf{H}_{ux} + \mathbf{H}_{uy} \mathbf{C}_{uy}$$
$$\mathbf{H}_{uuc} = \mathbf{H}_{uu}$$
$$\mathbf{B}_{yx} = -\mathbf{B}_y^{-1} \mathbf{B}_x$$

Analogous results to those described above, can be shown to hold for higher-order representations. Subsequent transformation of this description to the reduced-order form is described below.

3.3.2 Projection-Based ROM Generation

Consider the system model (3.14)-(3.15). Let now the linear transformation $\bar{\mathbf{x}} = \mathbf{T}\mathbf{x}$ be introduced. Substitution of this expression into (3.14) yields the transformed system

$$\begin{aligned} \Delta\dot{\bar{\mathbf{x}}} = {} & \bar{\mathbf{A}}_{xc} \Delta\bar{\mathbf{x}} + \bar{\mathbf{A}}_{uc} \Delta\mathbf{u} + \bar{\mathbf{H}}_{xxc} \left(\Delta\bar{\mathbf{x}} \otimes \Delta\bar{\mathbf{x}} \right) + \bar{\mathbf{H}}_{xuc} \left(\Delta\bar{\mathbf{x}} \otimes \Delta\mathbf{u} \right) + \\ & \bar{\mathbf{H}}_{uxc} \left(\Delta\mathbf{u} \otimes \Delta\bar{\mathbf{x}} \right) + \bar{\mathbf{H}}_{uuc} \left(\Delta\mathbf{u} \otimes \Delta\mathbf{u} \right) \end{aligned} \tag{3.16}$$

$$\Delta\mathbf{y} = \bar{\mathbf{B}}_{yx} \Delta\bar{\mathbf{x}} \tag{3.17}$$

where

$$\bar{\mathbf{A}}_{xc} = \mathbf{T}\mathbf{A}_{xc}\mathbf{T}^{-1}$$
$$\bar{\mathbf{A}}_{uc} = \mathbf{T}\mathbf{A}_{uc}$$
$$\bar{\mathbf{B}}_{yx} = \mathbf{B}_{yx}\mathbf{T}^{-1}$$
$$\bar{\mathbf{H}}_{xxc} = \mathbf{T}\mathbf{H}_{xxc} \left(\mathbf{T}^{-1} \otimes \mathbf{T}^{-1} \right)$$
$$\bar{\mathbf{H}}_{xuc} = \mathbf{T}\mathbf{H}_{xuc} \left(\mathbf{T}^{-1} \otimes \mathbf{I}_m \right)$$
$$\bar{\mathbf{H}}_{uxc} = \mathbf{T}\mathbf{H}_{uxc} \left(\mathbf{I}_m \otimes \mathbf{T}^{-1} \right)$$
$$\bar{\mathbf{H}}_{uuc} = \mathbf{T}\mathbf{H}_{uuc}$$

and use has been made of the identities

$$(\Delta\mathbf{x}\otimes\Delta\mathbf{x})=\left(\mathbf{T}^{-1}\Delta\bar{\mathbf{x}}\otimes\mathbf{T}^{-1}\Delta\bar{\mathbf{x}}\right)=\left(\mathbf{T}^{-1}\otimes\mathbf{T}^{-1}\right)(\Delta\bar{\mathbf{x}}\otimes\Delta\bar{\mathbf{x}})$$
$$(\Delta\mathbf{x}\otimes\Delta\mathbf{u})=\left(\mathbf{T}^{-1}\Delta\bar{\mathbf{x}}\otimes\mathbf{I}_m\Delta\mathbf{u}\right)=\left(\mathbf{T}^{-1}\otimes\mathbf{I}_m\right)(\Delta\bar{\mathbf{x}}\otimes\Delta\mathbf{u})$$
$$(\Delta\mathbf{u}\otimes\Delta\mathbf{x})=\left(\mathbf{I}_m\Delta\mathbf{u}\otimes\mathbf{T}^{-1}\Delta\bar{\mathbf{x}}\right)=\left(\mathbf{I}_m\otimes\mathbf{T}^{-1}\right)(\Delta\mathbf{u}\otimes\Delta\bar{\mathbf{x}})$$

The result is a ROM that contains fewer states than the original system. As discussed below, the number of states that can be truncated depends on the system itself and on the accuracy that is required for system behavior.

It should be emphasized that the methodology presented here is general and can be extended to accommodate higher dimensional systems.

It remains to choose the transformation matrix $\mathbf{T}$ such that the reduction is optimal.

3.4 Development of Low-Order Model

As discussed in Chapter 2, proper orthogonal decomposition is used to obtain a reduced dynamical model of the systems. The POD technique selects an orthogonal set of spatial modes that is optimal in terms of retained kinetic energy.

A step-by-step algorithm used to obtain the reduced-order representation is presented here.

1. For a given fault scenario, determine the time trajectories of the system states. Build the observation matrix $\mathbf{x}\in\mathrm{R}^{n\times N}$, i.e.,

$$\mathbf{x}=\begin{bmatrix}\mathbf{x}_1 & \mathbf{x}_2 & \cdots & \mathbf{x}_N\end{bmatrix}$$

$$\mathbf{x}_i=\begin{bmatrix}x_1(t_i)\\ \vdots\\ x_n(t_i)\end{bmatrix}\in\mathrm{R}^n,\quad i=1,\ldots,N.$$

through numerical solution of the full system model.

2. Find an optimal low-dimensional linear subspace of the state space. More formally, we seek a set of orthonormal basis vectors $\mathbf{u}_j \in \mathrm{R}^n, \quad j = 1,\ldots,N$, such that $\mathbf{x}_i = \sum_{j=1}^{n} \gamma_{ji}\mathbf{u}_j, \quad i = 1,\ldots,N$, that is,

$$\underbrace{\begin{bmatrix}\mathbf{x}_1 & \cdots & \mathbf{x}_N\end{bmatrix}}_{\mathbf{x}} = \underbrace{\begin{bmatrix}\mathbf{u}_1 & \cdots & \mathbf{u}_n\end{bmatrix}}_{\mathbf{u}} \overbrace{\begin{bmatrix}\gamma_{11} & \cdots & \gamma_{1N} \\ \vdots & & \vdots \\ \gamma_{n1} & \cdots & \gamma_{nN}\end{bmatrix}}^{\Gamma}, \quad \mathbf{U}^*\mathbf{U} = \mathbf{I}_n$$

where

$$\mathbf{x} = \mathbf{U}\,\boldsymbol{\Sigma}\mathbf{V}^T$$
$$\boldsymbol{\Gamma} = \boldsymbol{\Sigma}\mathbf{V}^T$$

The $\mathbf{u}_j$ are sometimes referred to as empirical eigenfunctions or principal directions of the "cloud" of data $\{\mathbf{x}_i\}$.

3. The snapshots reconstructed from only k empirical eigenfunctions, $\hat{\mathbf{x}}_i = \sum_{j=1}^{k} \gamma_{ji}\mathbf{u}_j, \quad i = 1,\ldots,N$, this is

$$\underbrace{\begin{bmatrix}\hat{\mathbf{x}}_1 & \cdots & \hat{\mathbf{x}}_N\end{bmatrix}}_{\hat{\mathbf{x}}} = \underbrace{\begin{bmatrix}\mathbf{u}_1 & \cdots & \mathbf{u}_k\end{bmatrix}}_{\hat{\mathbf{u}}} \overbrace{\begin{bmatrix}\gamma_{11} & \cdots & \gamma_{1N} \\ \vdots & & \vdots \\ \gamma_{k1} & \cdots & \gamma_{kN}\end{bmatrix}}^{\hat{\Gamma}} \in \mathrm{R}^{n\times N}, \quad k < N$$

$$\hat{\boldsymbol{\Gamma}} = \hat{\boldsymbol{\Sigma}}\hat{\mathbf{V}}^T$$

In order to determine the appropriate number of modes to be used in the reduced order system calculate the percentage of total energy captured in the first k modes:

$$\frac{\sum_{i=1}^{k}\sigma_i}{\sum_{i=1}^{n}\sigma_i} \times 100 \le (\%)$$

where σ_i is the i th singular value, and $(\%)$ is the percentage of captured energy, normally is 99.99%. Project the data back onto the physical states to give the time history of each state. The subspace constructed using the corresponding k singular vectors are optimal in approximating the data set.

4. Once the modes are calculated and the number of modes to be used is determined, the dynamics of the original system is projected onto the low-dimensional subspace, using the transformation

$$\mathbf{S} = \mathbf{W} = \mathbf{U}_k \in \mathrm{R}^{n \times k}$$
$$\mathbf{W}^* \mathbf{S} = \mathbf{I}_k$$

where $\mathbf{W}$ is the transformation matrix that has the empirical eigenfunctions of the greater energy.

5. Obtain the nonlinear ROM using the theory in section 3.3.2. Denote

$$\mathbf{T}^{-1} = \begin{bmatrix} \mathbf{W} & \mathbf{T}_1 \end{bmatrix}, \qquad \mathbf{T} = \begin{bmatrix} \mathbf{W}^* \\ \mathbf{T}_2 \end{bmatrix}$$

as the transformation matrix.

Given explicit expressions for the nonlinear terms, the power series expansions in (3.14) are obtained in a straightforward manner. The nonlinear state-space model now takes the form

$$\begin{aligned} \Delta\dot{\hat{\mathbf{x}}} = {} & \mathbf{W}^* \mathbf{A}_{xc} \left(\mathbf{W}\Delta\hat{\mathbf{x}} + \mathbf{T}_1 \Delta\tilde{\mathbf{x}} \right) + \mathbf{W}^* \mathbf{A}_{uc} \Delta\mathbf{u} + \mathbf{W}^* \mathbf{H}_{xxc} \left[(\mathbf{W} \otimes \mathbf{W})(\Delta\hat{\mathbf{x}} \otimes \Delta\hat{\mathbf{x}}) + \right. \\ & (\mathbf{W} \otimes \mathbf{T}_1)(\Delta\hat{\mathbf{x}} \otimes \Delta\tilde{\mathbf{x}}) + (\mathbf{T}_1 \otimes \mathbf{W})(\Delta\tilde{\mathbf{x}} \otimes \Delta\hat{\mathbf{x}}) + (\mathbf{T}_1 \otimes \mathbf{T}_1)(\Delta\tilde{\mathbf{x}} \otimes \Delta\tilde{\mathbf{x}}) \left. \right] + \\ & \mathbf{W}^* \mathbf{H}_{xuc} \left[(\mathbf{W} \otimes \mathbf{I}_{m \times m})(\Delta\hat{\mathbf{x}} \otimes \Delta\mathbf{u}) + (\mathbf{T}_1 \otimes \mathbf{I}_{m \times m})(\Delta\tilde{\mathbf{x}} \otimes \Delta\mathbf{u}) \right] + \\ & \mathbf{W}^* \mathbf{H}_{uxc} \left[(\mathbf{I}_{m \times m} \otimes \mathbf{W})(\Delta\mathbf{u} \otimes \Delta\hat{\mathbf{x}}) + (\mathbf{I}_{m \times m} \otimes \mathbf{T}_1)(\Delta\mathbf{u} \otimes \Delta\tilde{\mathbf{x}}) \right] + \\ & \mathbf{W}^* \mathbf{H}_{uuc} (\Delta\mathbf{u} \otimes \Delta\mathbf{u}) \end{aligned} \tag{3.18}$$

$$\Delta\mathbf{y} = \mathbf{B}_{yx} \mathbf{W}\Delta\hat{\mathbf{x}} + \mathbf{B}_{yx} \mathbf{T}_1 \Delta\tilde{\mathbf{x}} \tag{3.19}$$

Neglecting the terms in $\Delta\tilde{\mathbf{x}}$, we have

$$\Delta\dot{\hat{\mathbf{x}}} = \hat{\mathbf{A}}_{xc}\Delta\hat{\mathbf{x}} + \hat{\mathbf{A}}_{uc}\Delta\mathbf{u} + \hat{\mathbf{H}}_{xxc}\left(\Delta\hat{\mathbf{x}} \otimes \Delta\hat{\mathbf{x}}\right) + \hat{\mathbf{H}}_{xuc}\left(\Delta\hat{\mathbf{x}} \otimes \Delta\mathbf{u}\right) + \hat{\mathbf{H}}_{uxc}\left(\Delta\mathbf{u} \otimes \Delta\hat{\mathbf{x}}\right) + \hat{\mathbf{H}}_{uuc}\left(\Delta\mathbf{u} \otimes \Delta\mathbf{u}\right) \tag{3.20}$$

$$\Delta\mathbf{y} = \hat{\mathbf{B}}_{yx}\Delta\hat{\mathbf{x}} \tag{3.21}$$

Hence, we have

$$\begin{aligned}
\Delta\mathbf{x} &= \mathbf{W}\Delta\hat{\mathbf{x}} \\
\hat{\mathbf{A}}_{xc} &= \mathbf{W}^{*}\mathbf{A}_{xc}\mathbf{W} \\
\hat{\mathbf{A}}_{uc} &= \mathbf{W}^{*}\mathbf{A}_{uc} \\
\hat{\mathbf{B}}_{yx} &= \mathbf{B}_{yx}\mathbf{W} \\
\hat{\mathbf{H}}_{xxc} &= \mathbf{W}^{*}\mathbf{H}_{xxc}\left(\mathbf{W} \otimes \mathbf{W}\right) \\
\hat{\mathbf{H}}_{xuc} &= \mathbf{W}^{*}\mathbf{H}_{xuc}\left(\mathbf{W} \otimes \mathbf{I}_{m}\right) \\
\hat{\mathbf{H}}_{uxc} &= \mathbf{W}^{*}\mathbf{H}_{uxc}\left(\mathbf{I}_{m} \otimes \mathbf{W}\right) \\
\hat{\mathbf{H}}_{uuc} &= \mathbf{W}^{*}\mathbf{H}_{uuc}
\end{aligned}$$

This is the basic model used in this research. It is worth noting that the model is general and could be used to accommodate for more complex system representations.

We remark that, in this model, the original physical variables are represented as a linear combination of the ROM states, i.e.

$$\mathbf{x}_k = \sum_{j=1}^{n} w_{kj}\hat{\mathbf{x}}_k$$

This allows to relate the ROM solution to the physical states as discussed in Chapter 6.

The flowchart in Fig. 3.3 illustrates the proposed procedure. Generation of nonlinear ROMs is broken down into four major steps as discussed above:

1. The derivation of an analytical model of the power system
2. The generation of the POD basis functions,
3. The extraction of modal properties, and

4. The computation of the nonlinear ROM

Chapter 4 describes the power system model used in the procedure.

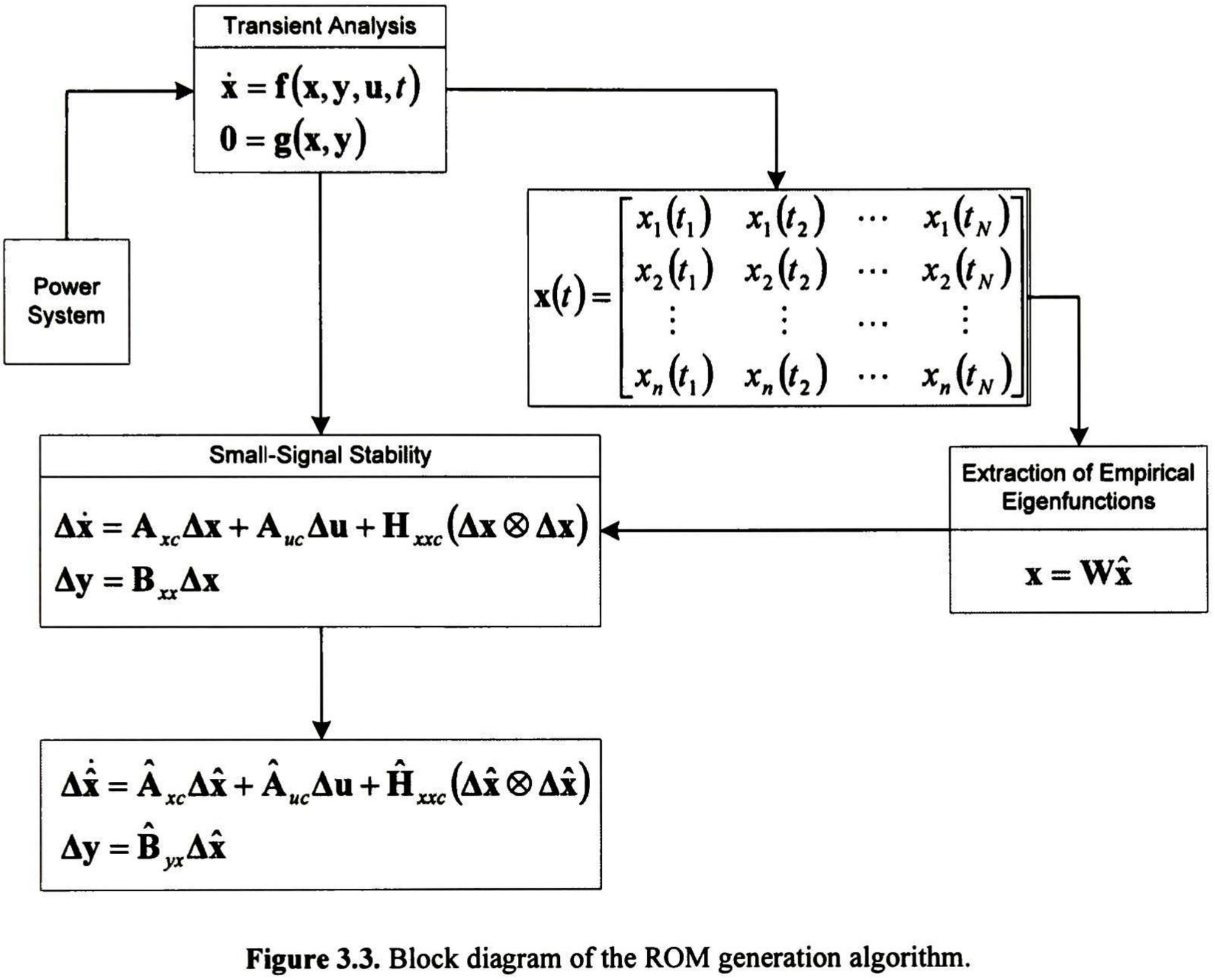

Figure 3.3. Block diagram of the ROM generation algorithm.

3.5 References

[1] Athanasios C. Antoulas, *Approximation of Large-Scale Dynamical Systems,* Advances in Design and Control, Siam, (2005).

[2] James Stewart, *Calculus: Concepts and Contexts, 3rd. Edition* Thomson, 11:774-786 (2006).

[3] Prabha Kundur, *Power System Stability and Control* Mc-Graw-Hill, Inc., 12: 703-704.

[4] W. Brewer John, *"Kronecker Products and Matrix Calculus in System Theory"*, IEEE Transactions on Circuits and Systems, Vol. cas-25, No. 9, September 1978.

[5] G. Kershen J. C. Galinval, Alexander F. Vakakis and Lawrence A. Bergman, *"The method of proper orthogonal decomposition for dynamical characterization and order reduction of mechanical systems: An overview"*, Nonlinear Dynamics, vol. 41, pp. 147-169, 2005.

Chapter 4

Power System Modeling and Analysis

The study of systems governed by a set of differential-algebraic equations with periodic coefficients is of great importance in diverse branches of science and engineering. Dynamic models described by an implicit mixed set of differential and algebraic equations (DAEs) arise when modeling physical system processes.

In this chapter, a modeling framework based on perturbation theory is proposed for analyzing the nonlinear behavior of power systems modeled as differential-algebraic systems. An advanced nonlinear linear model of the power system is first developed that allows detailed evaluation of the impact of machine controls on system behavior, as well as the identification of reduced-order system representations. The method makes use of perturbation theory and enables detailed representation of machines and their controllers and the transmission system. Only the second-order nonlinear effect is retained in the analysis.

On the basis of this model, normal form theory is used to study nonlinear power system behavior following large disturbances. The technique uses a series of observations of a system to build a linear basis for approximating system behavior. The approach is general enough to include the representation of various controllers and can be used in conjunction with efficient techniques for the analysis of complex systems.

The theory and analysis methods can be easily generalized to other types of nonlinear systems and higher-dimensional representations.

4.1 The Adopted Power System Formulation

Power system phenomena involve a complicated interaction between the dynamics of synchronous machines and system controllers. In this section, a general, nonlinear dynamic model of the power system is proposed which preserves network structure and load characteristics.

The power system is her seen as constituted of the dynamic models of synchronous machines and their controllers interacting through the steady-state representation of the network. In this model, each machine is represented by a d-q model and a simple excitation system; loads are treated as constant impedances but the model is general and could be used to accommodate more complex system representations.

For dynamic stability analysis, both machine stator and network transients are neglected. This has the advantage of simplifying the algebraic theory very significantly. As a consequence, the entire interconnected power system can be represented by a set of differential equations together with a set of algebraic equations of the form

$$\begin{aligned} \dot{\mathbf{x}} &= \mathbf{f}(\mathbf{x},\mathbf{y},\mathbf{u}) \quad , \quad \mathbf{x} \in \mathrm{R}^{n} , \mathbf{u} \in \mathrm{R}^{m} , \mathbf{y} \in \mathrm{R}^{p} \\ \mathbf{0} &= \mathbf{g}(\mathbf{x},\mathbf{y}) \end{aligned} \tag{4.1}$$

where $\mathbf{x}$ is the vector of state variables, $\mathbf{y}$ is the vector of algebraic variables, and $\mathbf{u}$ is the input vector.

Several representations to obtain the above system model have been proposed in the literature. In the succeeding sections, a systematic technique to build the state representation is introduced. Based on this representation, a second-order system representation is derived for the analysis of nonlinear system behavior.

4.1.1 Generator Dynamic Equations

We assume that each synchronous generator is represented using the two-axis model and a static excitation system. In this representation, machine saturation is neglected.

For clarity of illustration, we assume that each generator is represented by a fourth-order d-q axis model. Generalizations to this model are discussed in the derivation of the model.

The differential equations describing the dynamic behavior of the *ith* generator and the excitation system are given by Eqs. (4.2)-(4.6) [1].

A block diagram of the excitation system model is shown in Fig. 4.1.

Rotor swing

$$\frac{2H_i}{\omega_s}\frac{d\omega_i}{dt} = P_{mi} - E'_{di}\,I_{di} - E'_{qi}\,I_{qi} - \left(X'_{qi} - X'_{di}\right)I_{di}\,I_{qi} - D_i\left(\omega_i - \omega_s\right) \quad i = 1,\ldots,ng \tag{4.2}$$

$$\frac{d\delta_i}{dt} = \omega_0\left(\omega_i - \omega_s\right) \quad i = 1,\ldots,ng \tag{4.3}$$

Static excitation system

$$T_{Ai}\frac{dE_{fdi}}{dt} = -E_{fdi} + K_{Ai}\left(V_{refi} - V_i\right) \quad i = 1,\ldots,ng \tag{4.4}$$

Internal voltage equations

$$T'_{d0i}\frac{dE'_{qi}}{dt} = -E'_{qi} - \left(X_{di} - X'_{di}\right)I_{di} + E_{fdi} \quad i = 1,\ldots,ng \tag{4.5}$$

$$T'_{q0i}\frac{dE'_{di}}{dt} = -E'_{di} + \left(X_{qi} - X'_{qi}\right)I_{qi} \quad i = 1,\ldots,ng \tag{4.6}$$

In the equations above, δ is the angular position of the rotor in electrical rad, ω. is the rotor angle velocity in electrical rad/s, P_m is the mechanical input power un pu, and ng is the number of the generators, The other symbols have the usual meaning.

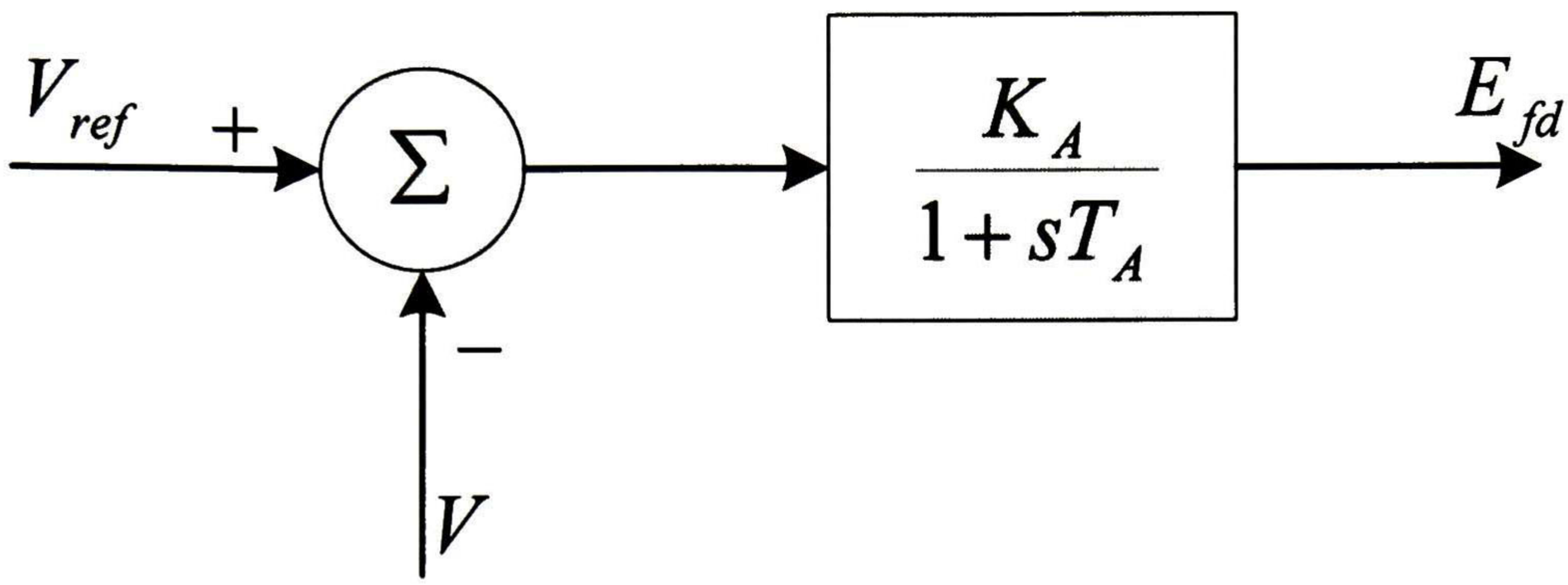

Figure 4.1. Exciter model

Let $\mathbf{x} = \begin{bmatrix} \mathbf{x}_{g1} & \mathbf{x}_{g2} & \cdots & \mathbf{x}_{gng} \end{bmatrix}^T$, be the vector of dynamic states, where

$$\mathbf{x}_{gk} = \begin{bmatrix} E'_{qk} & E'_{dk} & E_{fdk} & \delta_k & \omega_k \end{bmatrix}^T \tag{4.7}$$

The partial state space representation can then be written as

$$\dot{\mathbf{x}} = \mathbf{f}_0\left(\mathbf{x}, \mathbf{I}_{d-q}, \overline{\mathbf{V}}, \mathbf{u}\right) \tag{4.8}$$

where $\mathbf{f}_0$ represents an m-dimensional vector field in the theory of dynamical systems.

4.1.2 Algebraic Equations

Consider a general network with n nodes and ng generators. In this model, the network is represented by a quasi-stationary model and loads are treated as voltage-dependent functions.

Figure 4.2 depicts the general nature of the adopted system model whilst Fig. 4.3 shows a schematic diagram of the interface generator-network equations.

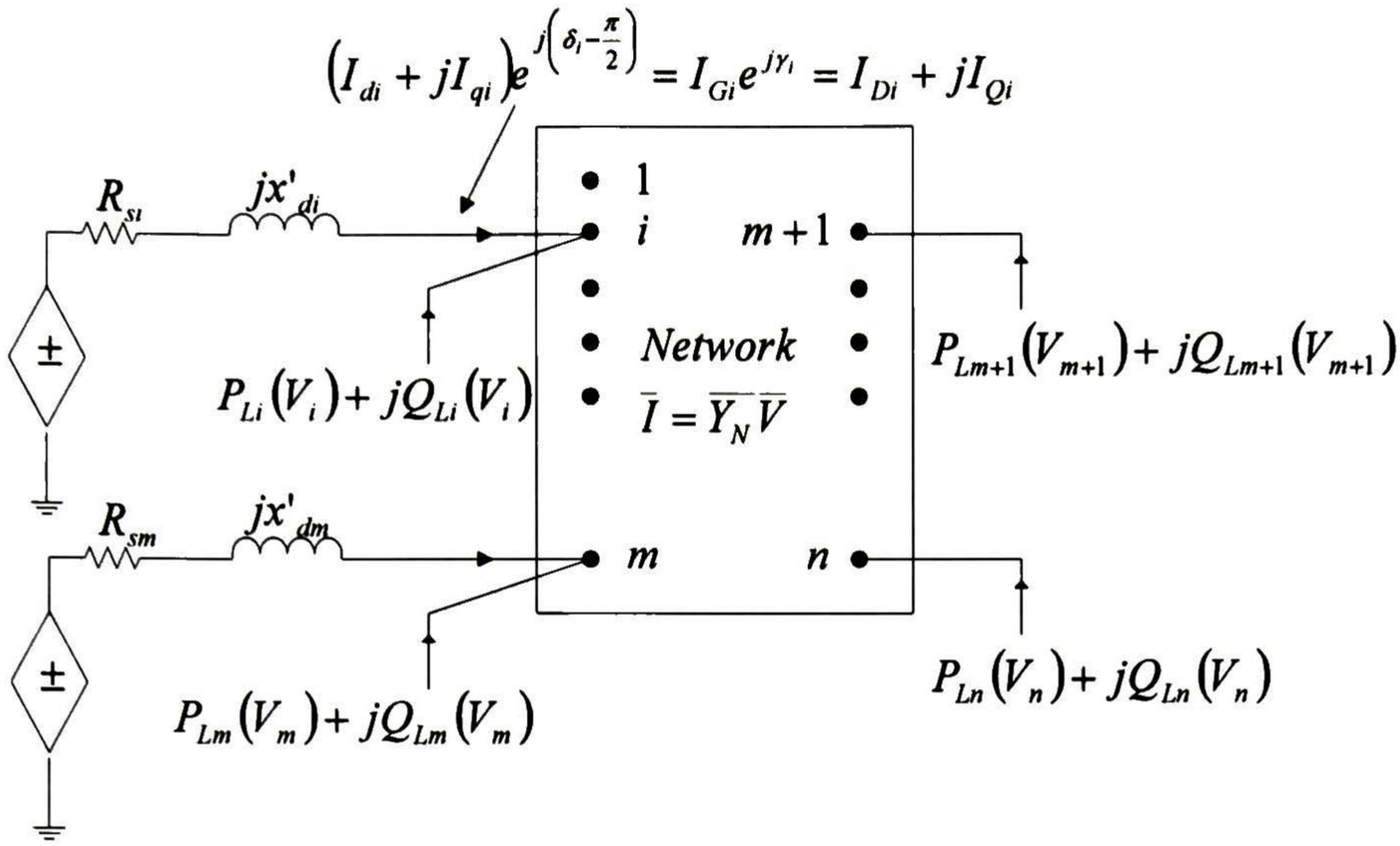

Figure 4.2. Interconnection of synchronous machine dynamic circuit and the rest of the network.

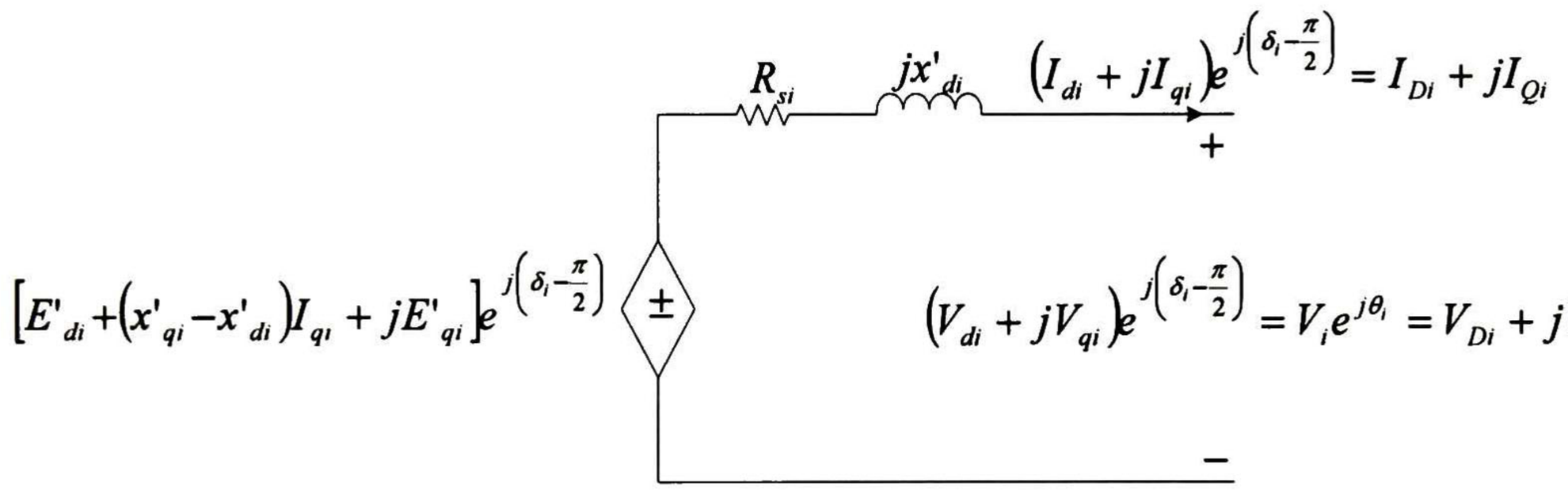

Figure 4.3. Synchronous machine two-axis model circuit,, $i = 1,\ldots,ng$.

With reference to Fig. 4.2, the interface generator-network and load-network equations are:

Load flow mismatches at generation buses

$$V_i e^{j\theta_i}\left(I_{di} - jI_{qi}\right)e^{-j\left(\delta_i - \frac{\pi}{2}\right)} + P_{Li}(V_i) + jQ_{Li}(V_i) = \sum_{k=1}^{n} V_i V_k Y_{ik} e^{j(\theta_i - \theta_k - \alpha_{ik})}, \qquad (4.9)$$

$$i = 1,\ldots,ng$$

Load flow mismatches at load buses

$$P_{Li}(V_i) + jQ_{Li}(V_i) = \sum_{k=1}^{n} V_i V_k Y_{ik} e^{j(\theta_i - \theta_k - \alpha_{ik})} \qquad i = ng+1,\ldots,n \qquad (4.10)$$

The corresponding algebraic machine equations are:

$$0 = V_i e^{j\theta_i} + (R_{si} + jX'_{di})(I_{di} + jI_{qi})e^{j\left(\delta_i - \frac{\pi}{2}\right)} - \left[E'_{di} + (X'_{qi} - X'_{di})I_{qi} + jE'_{qi}\right]e^{j\left(\delta_i - \frac{\pi}{2}\right)} \quad \text{for} \quad i = 1, \ldots, ng \tag{4.11}$$

Equations (4.1) through (4.11) describe system behavior and are used in this research to derive analytical reduced-order representations of the system. Techniques to cast these equations in the nonlinear state space form (4.1) are discussed below.

4.2 Transmission Network Model

4.2.1 Interface Generator-Network Equations

In order to express the machine equations in network coordinates, we multiply (4.11) by $e^{-j\left(\delta_i - \frac{\pi}{2}\right)}$ The d- and q-axis components of stator voltage can be written as

$$E'_{di} - V_i \sin(\delta_i - \theta_i) - R_{si} I_{di} + X'_{qi} I_{qi} = 0 \quad i = 1, \ldots, ng \tag{4.12}$$

and

$$E'_{qi} - V_i \cos(\delta_i - \theta_i) - R_{si} I_{qi} - X'_{di} I_{di} = 0 \quad i = 1, \ldots, ng \tag{4.13}$$

Defining

$$\mathbf{Z}_{d-q,i} = \begin{bmatrix} R_{si} & -X'_{qi} \\ X'_{di} & R_{si} \end{bmatrix}$$

equations (4.10) and (4.11) can be rewritten as

$$\mathbf{I}_{d-q,i} = \begin{bmatrix} I_{di} \\ I_{qi} \end{bmatrix} = \left[\mathbf{Z}_{d-q,i}\right]^{-1} \begin{bmatrix} E'_{di} - V_i \sin(\delta_i - \theta_i) \\ E'_{qi} - V_i \cos(\delta_i - \theta_i) \end{bmatrix} \quad i = 1, \ldots, ng \tag{4.14}$$

Thus,

$$\mathbf{I}_{d-q,i} = \mathbf{h}_i(\mathbf{x}_i, V_i, \theta_i) = \mathbf{h}_i(\mathbf{x}_i, \overline{\mathbf{V}}_i) \quad i = 1,\ldots,ng \tag{4.15}$$

where

$$\mathbf{h}_i(\mathbf{x}_i, V_i, \theta_i) = \left[\mathbf{Z}_{d-q,i}\right]^{-1}\begin{bmatrix} E'_{di} - V_i \sin(\delta_i - \theta_i) \\ E'_{qi} - V_i \cos(\delta_i - \theta_i) \end{bmatrix} \quad , i = 1,\ldots,ng$$

$$\overline{\mathbf{V}}_i = (V_i, \theta_i)$$

4.2.2 Transmission Network Equations

Solving (4.9) for the real and imaginary components yields

$$\begin{aligned} &I_{di}V_i \sin(\delta_i - \theta_i) + I_{qi}V_i \cos(\delta_i - \theta_i) + P_{Li}(V_i) \\ &-\sum_{k=1}^{n} V_i V_k Y_{ik} \cos(\theta_i - \theta_k - \alpha_{ik}) = 0 \end{aligned} \tag{4.16}$$

$$\begin{aligned} &I_{di}V_i \cos(\delta_i - \theta_i) - I_{qi}V_i \sin(\delta_i - \theta_i) + Q_{Li}(V_i) \\ &-\sum_{k=1}^{n} V_i V_k Y_{ik} \sin(\theta_i - \theta_k - \alpha_{ik}) = 0 \end{aligned} \tag{4.17}$$

for $i = 1,\ldots,ng$. Similarly,

$$P_{Li}(V_i) - \sum_{k=1}^{n} V_i V_k Y_{ik} \cos(\theta_i - \theta_k - \alpha_{ik}) = 0 \tag{4.18}$$

$$Q_{Li}(V_i) - \sum_{k=1}^{n} V_i V_k Y_{ik} \sin(\theta_i - \theta_k - \alpha_{ik}) = 0 \tag{4.19}$$

for $i = ng+1,\ldots,n$.

Note that, in this model, loads can be represented at generator and load buses.

Collecting real and imaginary components we have:

Real Power Equations

$$\begin{aligned} &I_{di}V_i \sin(\delta_i - \theta_i) + I_{qi}V_i \cos(\delta_i - \theta_i) + P_{Li}(V_i) \\ &-\sum_{k=1}^{n} V_i V_k Y_{ik} \cos(\theta_i - \theta_k - \alpha_{ik}) = 0 \quad i = 1,\ldots,ng \end{aligned} \tag{4.20}$$

$$P_{Li}(V_i) - \sum_{k=1}^{n} V_i V_k Y_{ik} \cos(\theta_i - \theta_k - \alpha_{ik}) = 0 \quad i = ng+1, \ldots, n \tag{4.21}$$

Reactive Power Equations

$$\begin{aligned} & I_{di} V_i \cos(\delta_i - \theta_i) - I_{qi} V_i \sin(\delta_i - \theta_i) + Q_{Li}(V_i) \\ & - \sum_{k=1}^{n} V_i V_k Y_{ik} \sin(\theta_i - \theta_k - \alpha_{ik}) = 0 \quad i = 1, \ldots, ng \end{aligned} \tag{4.22}$$

$$Q_{Li}(V_i) - \sum_{k=1}^{n} V_i V_k Y_{ik} \sin(\theta_i - \theta_k - \alpha_{ik}) = 0 \quad i = ng+1, \ldots, n \tag{4.23}$$

These equations allow us to obtain the nonlinear power system model as described in successive sections of this chapter.

4.3 Power System DAE Model

The overall system model is obtained by combining the machines equations (4.2)-(4.6) with the network representation. Let to this end, the state vector be defined as

$$\mathbf{x} = \begin{bmatrix} E'_{q1} & E'_{d1} & E_{fd1} & \delta_1 & \omega_1 & \cdots & E'_{qng} & E'_{dng} & E_{fdng} & \delta_{ng} & \omega_{ng} \end{bmatrix}^T$$

The corresponding current injections can be expressed in vector form as

$$\mathbf{I}_{d-q} = \begin{bmatrix} \mathbf{I}_{d-q,1} & \cdots & \mathbf{I}_{d-q,ng} \end{bmatrix}^T$$

$$\mathbf{I}_{d-q,k} = \begin{bmatrix} I_{dk} & I_{qk} \end{bmatrix}^T$$

and

$$\overline{\mathbf{V}} = \begin{bmatrix} \overline{\mathbf{V}}_1 & \cdots & \overline{\mathbf{V}}_{ng} & \overline{\mathbf{V}}_{ng+1} & \cdots & \overline{\mathbf{V}}_n \end{bmatrix}^T$$

$$\overline{\mathbf{V}}_k = \begin{bmatrix} V_k & \theta_k \end{bmatrix}^T$$

where, $\mathbf{I}_{d-q,k}$ is the current vector in d and q axis of the stator circuit of the *k*th generator; $\overline{\mathbf{V}}_k$ is the voltage vector in the *k*th bus; $\mathbf{u}_k$ is the excitation of the *k*th generator.

The input vector is:

$$\mathbf{u} = \begin{bmatrix} \mathbf{u}_1 & \cdots & \mathbf{u}_{ng} \end{bmatrix}^T$$

$$\mathbf{u}_k = \begin{bmatrix} P_{mk} & V_{refk} \end{bmatrix}^T$$

Combining the system equations (4.2) through (4.21) results in the DAE system

$$\dot{\mathbf{x}} = \mathbf{f}_0\left(\mathbf{x}, \mathbf{I}_{d-q}, \overline{\mathbf{V}}, \mathbf{u}\right) \tag{4.24}$$

$$\mathbf{I}_{d-q} = \mathbf{h}\left(\mathbf{x}, \overline{\mathbf{V}}\right) \tag{4.25}$$

$$\mathbf{0} = \mathbf{g}_0\left(\mathbf{x}, \mathbf{I}_{d-q}, \overline{\mathbf{V}}\right) \tag{4.26}$$

Substituting the Equation (4.25) into (4.24) and (4.26), we obtain

$$\dot{\mathbf{x}} = \mathbf{f}\left(\mathbf{x}, \overline{\mathbf{V}}, \mathbf{u}\right) \tag{4.27}$$

$$\mathbf{0} = \mathbf{g}\left(\mathbf{x}, \overline{\mathbf{V}}\right) \tag{4.28}$$

The proposed method allows for the detailed representation of the dynamics of machines, FACTS devices and load characteristics in a systematic manner. The nonlinear nature of this model makes it very difficult to find general analytical solutions. Conventional ways of analyzing nonlinear system behavior either rely on linear analysis or are based on detailed simulation of the nonlinear model (4.27)-(4.28).

For systems of the form (4.27), (4.28), the fundamental task of qualitative analysis reduces to determining a truncated model that approximates system behavior around a given operating condition.

4.4 Second-Order System Representation

Assuming that $\mathbf{f}(\mathbf{x})$ is continuous and can be expanded, the Taylor power series expansion up to order 2 of Eqn. (4.27) about a stable equilibrium point results in

$$\begin{aligned}\Delta\dot{\mathbf{x}} = {} & \mathbf{A}_x\Delta\mathbf{x} + \mathbf{A}_G\Delta\bar{\mathbf{V}}_G + \mathbf{A}_u\Delta\mathbf{u} + \mathbf{H}_{xx}(\Delta\mathbf{x}\otimes\Delta\mathbf{x}) + \mathbf{H}_{xG}(\Delta\mathbf{x}\otimes\Delta\bar{\mathbf{V}}_G) \\ & + \mathbf{H}_{xu}(\Delta\mathbf{x}\otimes\Delta\mathbf{u}) + \mathbf{H}_{Gx}(\Delta\bar{\mathbf{V}}_G\otimes\Delta\mathbf{x}) + \mathbf{H}_{GG}(\Delta\bar{\mathbf{V}}_G\otimes\Delta\bar{\mathbf{V}}_G) \\ & + \mathbf{H}_{Gu}(\Delta\bar{\mathbf{V}}_G\otimes\Delta\mathbf{u}) + \mathbf{H}_{ux}(\Delta\mathbf{u}\otimes\Delta\mathbf{x}) + \mathbf{H}_{uG}(\Delta\mathbf{u}\otimes\Delta\bar{\mathbf{V}}_G) \\ & + \mathbf{H}_{uu}(\Delta\mathbf{u}\otimes\Delta\mathbf{u})\end{aligned} \tag{4.29}$$

$$\mathbf{0} = \mathbf{B}_x\Delta\mathbf{x} + \mathbf{B}_G\Delta\bar{\mathbf{V}}_G + \mathbf{B}_L\Delta\bar{\mathbf{V}}_L \tag{4.30}$$

$$\mathbf{0} = \mathbf{C}_G\Delta\bar{\mathbf{V}}_G + \mathbf{C}_L\Delta\bar{\mathbf{V}}_L \tag{4.31}$$

where:

$$\Delta\mathbf{x} = \begin{bmatrix}\Delta\mathbf{x}_1 & \Delta\mathbf{x}_2 & \Delta\mathbf{x}_3 & \Delta\mathbf{x}_4 & \Delta\mathbf{x}_5\end{bmatrix}^T$$

$$\Delta\mathbf{x}_1 = \begin{bmatrix}\Delta E'_{q1} & \cdots & \Delta E'_{qng}\end{bmatrix}^T$$

$$\Delta\mathbf{x}_2 = \begin{bmatrix}\Delta E'_{d1} & \cdots & \Delta E'_{dng}\end{bmatrix}^T$$

$$\Delta\mathbf{x}_3 = \begin{bmatrix}\Delta E_{fd1} & \cdots & \Delta E_{fdng}\end{bmatrix}^T$$

$$\Delta\mathbf{x}_4 = \begin{bmatrix}\Delta\delta_1 & \cdots & \Delta\delta_{ng}\end{bmatrix}^T$$

$$\Delta\mathbf{x}_5 = \begin{bmatrix}\Delta\omega_1 & \cdots & \Delta\omega_{ng}\end{bmatrix}^T$$

$$\Delta\bar{\mathbf{V}}_G = \begin{bmatrix}\Delta\theta_1 & \cdots & \Delta\theta_{ng} & \Delta V_1 & \cdots & \Delta V_{ng}\end{bmatrix}^T$$

$$\Delta\bar{\mathbf{V}}_L = \begin{bmatrix}\Delta\theta_{ng+1} & \cdots & \Delta\theta_n & \Delta V_{ng+1} & \cdots & \Delta V_n\end{bmatrix}^T$$

$$\mathbf{B}_x = \begin{bmatrix}\dfrac{\partial\mathbf{g}_1}{\partial\mathbf{x}} & \cdots & \dfrac{\partial\mathbf{g}_{ng}}{\partial\mathbf{x}}\end{bmatrix}^T$$

$$\mathbf{B}_G = \begin{bmatrix}\dfrac{\partial\mathbf{g}_1}{\partial\bar{\mathbf{V}}_G} & \cdots & \dfrac{\partial\mathbf{g}_{ng}}{\partial\bar{\mathbf{V}}_G}\end{bmatrix}^T$$

$$\mathbf{B}_L = \begin{bmatrix}\dfrac{\partial\mathbf{g}_1}{\partial\bar{\mathbf{V}}_L} & \cdots & \dfrac{\partial\mathbf{g}_{ng}}{\partial\bar{\mathbf{V}}_L}\end{bmatrix}^T$$

$$\mathbf{C}_G = \left[\frac{\partial \mathbf{g}_{ng+1}}{\partial \bar{\mathbf{V}}_G} \quad \cdots \quad \frac{\partial \mathbf{g}_n}{\partial \bar{\mathbf{V}}_G} \right]^T$$

$$\mathbf{C}_L = \left[\frac{\partial \mathbf{g}_{ng+1}}{\partial \bar{\mathbf{V}}_L} \quad \cdots \quad \frac{\partial \mathbf{g}_n}{\partial \bar{\mathbf{V}}_L} \right]^T$$

Further, the constraint (algebraic equations) (4.30 and 4.31) are related as follows

$$\begin{aligned} \Delta \bar{\mathbf{V}}_L &= \mathbf{C}_{GL} \Delta \bar{\mathbf{V}}_G \\ \Delta \bar{\mathbf{V}}_G &= \mathbf{B}_{xG} \Delta \mathbf{x} \end{aligned} \tag{4.32}$$

where

$$\begin{aligned} \mathbf{C}_{GL} &= -\mathbf{C}_L^{-1} \mathbf{C}_G \\ \mathbf{B}_{xG} &= -\left(\mathbf{B}_G + \mathbf{B}_L \mathbf{C}_{GL} \right)^{-1} \mathbf{B}_x \end{aligned}$$

Substituting (4.32) in (4.29), leads to

$$\begin{aligned} \Delta \dot{\mathbf{x}} = \mathbf{A}_{xc} \Delta \mathbf{x} + \mathbf{A}_{uc} \Delta \mathbf{u} + \mathbf{H}_{xxc} (\Delta \mathbf{x} \otimes \Delta \mathbf{x}) + \mathbf{H}_{xuc} (\Delta \mathbf{x} \otimes \Delta \mathbf{u}) + \\ \mathbf{H}_{uxc} (\Delta \mathbf{u} \otimes \Delta \mathbf{x}) + \mathbf{H}_{uuc} (\Delta \mathbf{u} \otimes \Delta \mathbf{u}) \end{aligned} \tag{4.33}$$

In Eqn. 4.33, matrices $\mathbf{H}_{xuc}$, $\mathbf{H}_{uxc}$ and $\mathbf{H}_{uu}$ are zero for the classic and detailed model. Therefore, Eqn. (4.33) can be written alternatively as

$$\Delta \dot{\mathbf{x}} = \mathbf{A}_{xc} \Delta \mathbf{x} + \mathbf{A}_{uc} \Delta \mathbf{u} + \mathbf{H}_{xxc} (\Delta \mathbf{x} \otimes \Delta \mathbf{x}) \tag{4.34}$$

$$\begin{bmatrix} \Delta \bar{\mathbf{V}}_G \\ \Delta \bar{\mathbf{V}}_L \end{bmatrix} = \begin{bmatrix} \mathbf{B}_{xG} \\ \mathbf{C}_{GL} \mathbf{B}_{xG} \end{bmatrix} \Delta \mathbf{x} \tag{4.35}$$

Equations (4.34) and (4.35) constitute the analytical model used in this research.

4.5 References

[1] Peter W. Sauer and M. A. Pai, *Power System Dynamics and Stability*, Prentice Hall, 1998.

[2] Prabha Kundur, *Power System Stability and Control* Mc-Graw-Hill, Inc.

Chapter 5

Modal Analysis of the Linear ROM

In the previous chapter, a general second-order representation of the power system was developed. In this chapter the properties of the POD-based reduced order dynamical model for the power system are investigated with emphasis on the ability of the model to capture key modal properties of the full system representation.

Measures are introduced that provide information about the relative controllability and observability of the linear ROM. Also, measures providing the participation of each generator and load to the modal oscillation can be calculated.

First, the nature of the power system model is examined. A discussion is then given on the relationship between states and modes.

The method can also be extended to consider higher-order nonlinearities, which may arise from stressed operating conditions.

5.1 State-Space Realizations of the System Model

Based on the nonlinear model in Chapter 4, a second-order normal form procedure is considered here that allows the study of large DAE models.

In the discussion that follows, we assume that system behavior can be represented by a DAE model [3], of the form

$$\dot{\mathbf{x}} = \mathbf{f}\left(\mathbf{x}, \overline{\mathbf{V}}, \mathbf{u}\right) \tag{5.1}$$

$$\mathbf{0} = \mathbf{g}\left(\mathbf{x}, \overline{\mathbf{V}}\right) \tag{5.2}$$

where $\mathbf{x} \in \mathrm{R}^n$ is state vector of the system, $\mathbf{u} \in \mathrm{R}^m$ is the vector of inputs, and $\overline{\mathbf{V}} \in \mathrm{R}^p$ is the vector of algebraic variables.

For clarity of illustration, let the vector of voltage pseudo states be partitioned in the form

$$\overline{\mathbf{V}} = \begin{bmatrix} \overline{\mathbf{V}}_G \\ \overline{\mathbf{V}}_L \end{bmatrix}$$

where

$$\overline{\mathbf{V}}_G = \begin{bmatrix} \theta_1 & \cdots & \theta_m & V_1 & \cdots & V_m \end{bmatrix}^*$$

$$\overline{\mathbf{V}}_L = \begin{bmatrix} \theta_{m+1} & \cdots & \theta_{nb} & V_{m+1} & \cdots & V_{nb} \end{bmatrix}^*$$

represent the bus terminal voltages at the generator and load buses.

Expanding (5.1) into a second-order series expansion and using the notation in Chapter 4 the system model is then written as

$$\begin{aligned} \Delta\dot{\mathbf{x}} = {} & \mathbf{A}_x \Delta\mathbf{x} + \mathbf{A}_G \Delta\overline{\mathbf{V}}_G + \mathbf{A}_u \Delta\mathbf{u} + \mathbf{H}_{xx}(\Delta\mathbf{x} \otimes \Delta\mathbf{x}) + \mathbf{H}_{xG}(\Delta\mathbf{x} \otimes \Delta\overline{\mathbf{V}}_G) \\ & + \mathbf{H}_{xu}(\Delta\mathbf{x} \otimes \Delta\mathbf{u}) + \mathbf{H}_{Gx}(\Delta\overline{\mathbf{V}}_G \otimes \Delta\mathbf{x}) + \mathbf{H}_{GG}(\Delta\overline{\mathbf{V}}_G \otimes \Delta\overline{\mathbf{V}}_G) \\ & + \mathbf{H}_{Gu}(\Delta\overline{\mathbf{V}}_G \otimes \Delta\mathbf{u}) + \mathbf{H}_{ux}(\Delta\mathbf{u} \otimes \Delta\mathbf{x}) + \mathbf{H}_{uG}(\Delta\mathbf{u} \otimes \Delta\overline{\mathbf{V}}_G) \\ & + \mathbf{H}_{uu}(\Delta\mathbf{u} \otimes \Delta\mathbf{u}) \end{aligned} \tag{5.3}$$

and

$$\mathbf{0} = \mathbf{B}_x \Delta\mathbf{x} + \mathbf{B}_G \Delta\overline{\mathbf{V}}_G + \mathbf{B}_L \Delta\overline{\mathbf{V}}_L \tag{5.4}$$

$$\mathbf{0} = \mathbf{C}_G \Delta\overline{\mathbf{V}}_G + \mathbf{C}_L \Delta\overline{\mathbf{V}}_L \tag{5.5}$$

where matrices $\mathbf{B}_x, \mathbf{B}_G, \mathbf{B}_L, \mathbf{C}_G$ and $\mathbf{C}_L$ are the Jacobian matrices of the augmented system defined as

$$\mathbf{B}_x = \begin{bmatrix} \dfrac{\partial \mathbf{g}_1}{\partial \mathbf{x}} & \cdots & \dfrac{\partial \mathbf{g}_{ng}}{\partial \mathbf{x}} \end{bmatrix}^T$$

$$\mathbf{B}_G = \begin{bmatrix} \dfrac{\partial \mathbf{g}_1}{\partial \overline{\mathbf{V}}_G} & \cdots & \dfrac{\partial \mathbf{g}_{ng}}{\partial \overline{\mathbf{V}}_G} \end{bmatrix}^T$$

$$\mathbf{B}_L = \left[\frac{\partial \mathbf{g}_1}{\partial \bar{\mathbf{V}}_L} \quad \cdots \quad \frac{\partial \mathbf{g}_{ng}}{\partial \bar{\mathbf{V}}_L} \right]^T$$

$$\mathbf{C}_G = \left[\frac{\partial \mathbf{g}_{ng+1}}{\partial \bar{\mathbf{V}}_G} \quad \cdots \quad \frac{\partial \mathbf{g}_n}{\partial \bar{\mathbf{V}}_G} \right]^T$$

$$\mathbf{C}_L = \left[\frac{\partial \mathbf{g}_{ng+1}}{\partial \bar{\mathbf{V}}_L} \quad \cdots \quad \frac{\partial \mathbf{g}_n}{\partial \bar{\mathbf{V}}_L} \right]^T$$

The set of equations (5.4) and (5.5) may be rewritten in the form

$$\begin{bmatrix} \mathbf{0} \\ \mathbf{0} \end{bmatrix} = \begin{bmatrix} \mathbf{B}_G & \mathbf{B}_L \\ C_G & C_L \end{bmatrix} \begin{bmatrix} \Delta \bar{\mathbf{V}}_G \\ \Delta \bar{\mathbf{V}}_L \end{bmatrix} + \begin{bmatrix} \mathbf{B}_x \\ \mathbf{0} \end{bmatrix} \Delta \mathbf{x}$$

Solving (5.4) and (5.5) for $\Delta \bar{\mathbf{V}}_L$ and $\Delta \bar{\mathbf{V}}_G$ yields

$$\Delta \bar{\mathbf{V}}_L = -\mathbf{C}_L^{-1} \mathbf{C}_G \Delta \bar{\mathbf{V}}_G = \mathbf{C}_{GL} \Delta \bar{\mathbf{V}}_G \tag{5.6}$$

$$\Delta \bar{\mathbf{V}}_G = -\left(\mathbf{B}_G + \mathbf{B}_L \mathbf{C}_{GL}\right)^{-1} \mathbf{B}_x \Delta \mathbf{x} = \mathbf{B}_{xG} \Delta \mathbf{x} \tag{5.7}$$

The existence of the inverses of the matrices given by the equations (5.6) and (5.7) determines the stress level of the network. Substituting (5.6) and (5.7) in (5.3), leads to

$$\begin{aligned} \Delta \dot{\mathbf{x}} = \mathbf{A}_{xc} \Delta \mathbf{x} + \mathbf{A}_{uc} \Delta \mathbf{u} + \mathbf{H}_{xxc} (\Delta \mathbf{x} \otimes \Delta \mathbf{x}) + \mathbf{H}_{xuc} (\Delta \mathbf{x} \otimes \Delta \mathbf{u}) + \\ \mathbf{H}_{uxc} (\Delta \mathbf{u} \otimes \Delta \mathbf{x}) + \mathbf{H}_{uuc} (\Delta \mathbf{u} \otimes \Delta \mathbf{u}) \end{aligned} \tag{5.8}$$

Here $\mathbf{H}_{xuc}$, $\mathbf{H}_{uxc}$ and $\mathbf{H}_{uu}$ are zero for the classic and fifth-order model: In this case, the system model (5.8) reduces to

$$\Delta \dot{\mathbf{x}} = \mathbf{A}_{xc} \Delta \mathbf{x} + \mathbf{A}_{uc} \Delta \mathbf{u} + \mathbf{H}_{xxc} (\Delta \mathbf{x} \otimes \Delta \mathbf{x}) \tag{5.9}$$

Equations (5.9) and (5.6), (5.7) describe system behavior.

The goal is to obtain a ROM that preserves modal characteristics and input-output characteristics. Let, to this end, $\mathbf{W} \in \mathrm{R}^{n \times k}$ be the transformation matrix, such that $\mathbf{W}^* \mathbf{W} = \mathbf{I}_k$, where the asterisk denotes complex conjugation and $\mathbf{I}_k$ is the kth order identity matrix. The corresponding projection matrix is

$$\Delta \mathbf{x} = \mathbf{W}\Delta \hat{\mathbf{x}} \tag{5.10}$$

Substitution of (5.10) into (5.9) and rearranging yields

$$\Delta \dot{\hat{\mathbf{x}}} = \mathbf{W}^{*}\mathbf{A}_{xc}\mathbf{W}\Delta \hat{\mathbf{x}} + \mathbf{W}^{*}\mathbf{A}_{uc}\Delta \mathbf{u} + \mathbf{W}^{*}\mathbf{H}_{xxc}(\mathbf{W} \otimes \mathbf{W})(\Delta \hat{\mathbf{x}} \otimes \Delta \hat{\mathbf{x}})$$

or equivalently,

$$\Delta \dot{\hat{\mathbf{x}}} = \hat{\mathbf{A}}_{xc}\Delta \hat{\mathbf{x}} + \hat{\mathbf{A}}_{uc}\Delta \mathbf{u} + \hat{\mathbf{H}}_{xxc}(\Delta \hat{\mathbf{x}} \otimes \Delta \hat{\mathbf{x}}) \tag{5.11}$$

and

$$\Delta \overline{\mathbf{V}}_{G} = \mathbf{B}_{xG}\mathbf{W}\Delta \hat{\mathbf{x}} = \hat{\mathbf{B}}_{xG}\Delta \hat{\mathbf{x}} \tag{5.12}$$

$$\Delta \overline{\mathbf{V}}_{L} = \mathbf{C}_{GL}\mathbf{B}_{xG}\mathbf{W}\Delta \hat{\mathbf{x}} = \mathbf{C}_{GL}\hat{\mathbf{B}}_{xG}\Delta \hat{\mathbf{x}} = \hat{\mathbf{C}}_{xL}\Delta \hat{\mathbf{x}} \tag{5.13}$$

where

$$\hat{\mathbf{A}}_{xc} = \mathbf{W}^{*}\mathbf{A}_{xc}\mathbf{W}$$
$$\hat{\mathbf{A}}_{uc} = \mathbf{W}^{*}\mathbf{A}_{uc}$$
$$\hat{\mathbf{H}}_{xxc} = \mathbf{W}^{*}\mathbf{H}_{xxc}(\mathbf{W} \otimes \mathbf{W})$$

and $\mathbf{W}^{*}$ is the inverse matrix $\mathbf{W}$

Remark 5.1. Matrices $\hat{\mathbf{B}}_{xG}$ and $\hat{\mathbf{C}}_{xL}$ give a description of the way in which variations in the states appears on the bus voltage deviations.

Further simplification can be obtained by noting that the nonlinear term in Eq. (5.11), can be represented by its Carleman representation

$$\hat{\mathbf{H}}_{xxc}(\Delta \hat{\mathbf{x}} \otimes \Delta \hat{\mathbf{x}}) = \begin{bmatrix} \Delta \hat{\mathbf{x}}^{*}\hat{\mathbf{H}}_{xx1}\Delta \hat{\mathbf{x}} \\ \vdots \\ \Delta \hat{\mathbf{x}}^{*}\hat{\mathbf{H}}_{xxk}\Delta \hat{\mathbf{x}} \end{bmatrix} = \Delta \hat{\mathbf{x}}^{*}\begin{bmatrix} \hat{\mathbf{H}}_{xx1} \\ \vdots \\ \hat{\mathbf{H}}_{xxk} \end{bmatrix}\Delta \hat{\mathbf{x}} \tag{5.14}$$

where $\hat{\mathbf{H}}_{xxi} \in \mathrm{R}^{k\times k}$ and $\Delta \hat{\mathbf{x}} \in \mathrm{R}^{k}$ The functions $\hat{\mathbf{H}}_{xxi} \in \mathrm{R}^{k\times k}$ may be though of as a second-order corrections to system behavior and contain information on modal interaction involving the primary (linear) modes.

The system model contains $2m$ differential equations, $2m$ algebraic equations for the generation buses, and $2(nb-m)$ algebraic equations for the load buses, for a classical system representation. A number of properties of the proposed model that are relevant to the subsequent analysis will now be presented.

5.2 Modal Analysis of the linear ROM

Let $\Delta\hat{\mathbf{x}} = \hat{\boldsymbol{\varphi}}\hat{\mathbf{z}}$ be a transformation that eliminates the cross-coupling between the state variables, consider a new state vector $\hat{\mathbf{z}}$, where $\hat{\boldsymbol{\varphi}}$ is the modal matrix of $\hat{\mathbf{A}}_{xc}$.

Substituting the above expression for $\Delta\hat{\mathbf{x}}$ in the equations (5.11-5.13), we have

$$\dot{\hat{\mathbf{z}}} = \hat{\boldsymbol{\psi}}\hat{\mathbf{A}}_{xc}\hat{\boldsymbol{\varphi}}\hat{\mathbf{z}} + \hat{\boldsymbol{\psi}}\hat{\mathbf{A}}_{uc}\Delta\mathbf{u} + \hat{\boldsymbol{\psi}}\hat{\mathbf{H}}_{xxc}\left(\hat{\boldsymbol{\varphi}}\otimes\hat{\boldsymbol{\varphi}}\right)\left(\hat{\mathbf{z}}\otimes\hat{\mathbf{z}}\right)$$

Upon simplification,

$$\dot{\hat{\mathbf{z}}} = \hat{\boldsymbol{\Lambda}}\hat{\mathbf{z}} + \hat{\boldsymbol{\psi}}\hat{\mathbf{A}}_{uc}\Delta\mathbf{u} + \hat{\mathbf{H}}_{xxc\Lambda}\left(\hat{\mathbf{z}}\otimes\hat{\mathbf{z}}\right) \tag{5.15}$$

where

$$\hat{\boldsymbol{\varphi}} = \begin{bmatrix}\hat{\boldsymbol{\varphi}}_1 & \hat{\boldsymbol{\varphi}}_2 & \cdots & \hat{\boldsymbol{\varphi}}_k\end{bmatrix} \tag{5.16}$$

$$\hat{\boldsymbol{\psi}} = \begin{bmatrix}\hat{\boldsymbol{\psi}}_1^{\,T} & \hat{\boldsymbol{\psi}}_2^{\,T} & \cdots & \hat{\boldsymbol{\psi}}_k^{\,T}\end{bmatrix}^T \tag{5.17}$$

and matrix $\hat{\boldsymbol{\Lambda}}$ is a diagonal matrix with the eigenvalues $\hat{\lambda}_1, \hat{\lambda}_2, \ldots, \hat{\lambda}_k$ as diagonal elements. We assume that $\hat{\boldsymbol{\psi}}$ and $\hat{\boldsymbol{\varphi}}$ are normalized such that,

$$\hat{\boldsymbol{\psi}}\hat{\boldsymbol{\varphi}} = \mathbf{I}_k, \quad \hat{\boldsymbol{\psi}} = \hat{\boldsymbol{\varphi}}^{-1}$$

Application of this transformation to the nonlinear part in (5.15) yields

$$\hat{\mathbf{H}}_{xxc\Lambda}\left(\hat{\mathbf{z}}\otimes\hat{\mathbf{z}}\right) = \hat{\mathbf{z}}^*\begin{bmatrix}\hat{\mathbf{H}}_{xx\Lambda 1}\\ \vdots \\ \hat{\mathbf{H}}_{xx\Lambda k}\end{bmatrix}\hat{\mathbf{z}} = \hat{\mathbf{z}}^*\begin{bmatrix}\hat{\boldsymbol{\varphi}}_{H1}\hat{\boldsymbol{\Lambda}}_{H1}\hat{\boldsymbol{\psi}}_{H1}\\ \vdots \\ \hat{\boldsymbol{\varphi}}_{Hk}\hat{\boldsymbol{\Lambda}}_{Hk}\hat{\boldsymbol{\psi}}_{Hk}\end{bmatrix}\hat{\mathbf{z}} \tag{5.18}$$

where $\hat{\Lambda}_{Hi}$ is a diagonal matrix with the eigenvalues $\hat{\lambda}_{Hi,1}, \hat{\lambda}_{Hi,2}, \ldots, \hat{\lambda}_{Hi,k}$ as diagonal elements.

These equations have the same structure for nonlinear analysis.

5.3 Mode Shape, Sensitivity, and Participation Factor

5.3.1 Mode Shape and Eigenvectors

In the previous section, we expressed the system response in terms of the state vectors $\Delta\hat{\mathbf{x}}$ and $\hat{\mathbf{z}}$, namely

$$\begin{aligned}\Delta\hat{\mathbf{x}}(t) &= \hat{\boldsymbol{\varphi}}\hat{\mathbf{z}}(t) \\ &= \begin{bmatrix}\hat{\boldsymbol{\varphi}}_1 & \hat{\boldsymbol{\varphi}}_2 & \cdots & \hat{\boldsymbol{\varphi}}_k\end{bmatrix}\hat{\mathbf{z}}(t)\end{aligned} \tag{5.19}$$

$$\begin{aligned}\hat{\mathbf{z}}(t) &= \hat{\boldsymbol{\psi}}\Delta\hat{\mathbf{x}}(t) \\ &= \begin{bmatrix}\hat{\boldsymbol{\psi}}_1 & \hat{\boldsymbol{\psi}}_2 & \cdots & \hat{\boldsymbol{\psi}}_k\end{bmatrix}\Delta\hat{\mathbf{x}}(t)\end{aligned} \tag{5.20}$$

The variables $\Delta\hat{x}_1, \Delta\hat{x}_2, \ldots, \Delta\hat{x}_k$ are the original state variables chosen to represent the dynamic performance of the reduced system. The variables $\hat{z}_1, \hat{z}_2, \ldots, \hat{z}_k$ are the transformed state variables such that each variable is associated with only one mode. In other words, the transformed variables $\hat{\mathbf{z}}$ are directly related to the modes.

The right eigenvector gives the mode shape, i.e., the relative activity of the state variables when a particular mode is excited. For example, the degree of activity of the state variable $\hat{x}_k$ in the ith mode is given by the element $\hat{\varphi}_{ki}$ of the right eigenvector $\hat{\boldsymbol{\varphi}}_i$.

The magnitudes of the elements of $\hat{\boldsymbol{\varphi}}_i$ give the extents of the activities of the k state variables in the ith mode, and the angles of the elements give phase displacements of the state variables with regard to the mode.

The left eigenvector $\hat{\boldsymbol{\psi}}_i$ identifies which combination of the original state variables displays only the ith mode. Thus the kth element of the right eigenvector $\hat{\boldsymbol{\varphi}}_i$ measures the activity of the variable $\hat{x}_k$ in the ith mode, and the

*k*th element of the left eigenvector $\hat{\psi}_i$ weighs the contribution of this activity to the *i*th mode.

5.3.2 Eigenvalue Sensitivity

Let us now examine the sensitivity of eigenvalues to the elements of the state matrix. Consider the equation that follows [2]:

$$\hat{\mathbf{A}}_{xc}\hat{\boldsymbol{\varphi}}_i = \hat{\lambda}_i\hat{\boldsymbol{\varphi}}_i \tag{5.21}$$

Differentiating with respect to a_{kj} (the element of $\hat{\mathbf{A}}_{xc}$ in the *k*th row and *j*th column) yields

$$\frac{\partial\hat{\mathbf{A}}_{xc}}{\partial a_{kj}}\hat{\boldsymbol{\varphi}}_i + \hat{\mathbf{A}}_{xc}\frac{\partial\hat{\boldsymbol{\varphi}}_i}{\partial a_{kj}} = \frac{\partial\hat{\lambda}_i}{\partial a_{kj}}\hat{\boldsymbol{\varphi}}_i + \hat{\lambda}_i\frac{\partial\hat{\boldsymbol{\varphi}}_i}{\partial a_{kj}}$$

Premultiplying by $\hat{\boldsymbol{\psi}}_i$, and noting that $\hat{\boldsymbol{\psi}}_i\hat{\boldsymbol{\varphi}}_i = 1$ and $\hat{\boldsymbol{\psi}}_i\left(\hat{\mathbf{A}}_{xc} - \lambda_i\mathbf{I}\right) = 0$, in addition all elements of $\frac{\partial\hat{\mathbf{A}}_{xc}}{\partial a_{kj}}$ are zero, except for the element in the *k*th row and *j*th column which is equal to 1. Hence we see that the above equation simplifies to

$$\frac{\partial\hat{\lambda}_i}{\partial a_{kj}} = \hat{\psi}_{ik}\hat{\varphi}_{ji} \tag{5.22}$$

Equation (5.22) shows that the sensitivity of the eigenvalue $\hat{\lambda}_i$ to the element a_{kj} of the state matrix is equal to the product of the left eigenvector element $\hat{\psi}_{ik}$ and the right eigenvector element $\hat{\varphi}_{ji}$.

5.3.3 Participation Factor

Following Verghese et al. [1], the relative participation of state k in mode i can be determined via the participation factor.

Let the participation matrix ($\hat{\mathbf{P}}$), which combines the right and left eigenvectors, which is a measure of the association between the state variables and the modes, be defined as

$$\hat{\mathbf{P}} = \begin{bmatrix} \hat{\mathbf{P}}_1 & \hat{\mathbf{P}}_2 & \cdots & \hat{\mathbf{P}}_k \end{bmatrix} \tag{5.23}$$

with

$$\hat{\mathbf{P}}_i = \begin{bmatrix} \hat{P}_{1i} \\ \hat{P}_{2i} \\ \vdots \\ \hat{P}_{ki} \end{bmatrix} = \begin{bmatrix} \hat{\varphi}_{1i}\hat{\psi}_{i1} \\ \hat{\varphi}_{2i}\hat{\psi}_{i2} \\ \vdots \\ \hat{\varphi}_{ki}\hat{\psi}_{ik} \end{bmatrix} \tag{5.24}$$

where $\hat{\varphi}_{ki}$ is denotes the kth entry of the right eigenvector $\hat{\boldsymbol{\varphi}}_i$, and $\hat{\psi}_{ik}$ is denotes the kth entry of the left eigenvector $\hat{\boldsymbol{\psi}}_i$.

The element $\hat{P}_{ki} = \hat{\varphi}_{ki}\hat{\psi}_{ik}$ is termed the participation factor [2]. It is a measure of the relative participation of the kth state variable in the ith mode and vice versa. In addition, the participation factor $\hat{P}_{ki}$ is actually equal to the sensitivity of the eigenvalue $\hat{\lambda}_i$ to the diagonal element a_{kk} of the state matrix $\hat{\mathbf{A}}_{xc}$

$$\hat{P}_{ki} = \frac{\partial \lambda_i}{\partial a_{kk}} \tag{5.25}$$

5.4 Controllability and Observability Formulation

Let the system model (5.15) be rewritten in the form

$$\dot{\hat{\mathbf{z}}} = \hat{\mathbf{\Lambda}}\hat{\mathbf{z}} + \hat{\boldsymbol{\psi}}\hat{\mathbf{A}}_{uc}\Delta\mathbf{u} + \hat{\mathbf{H}}_{xxc\Lambda}\left(\hat{\mathbf{z}} \otimes \hat{\mathbf{z}}\right)$$

or more explicitly,

$$\dot{\hat{\mathbf{z}}} = \hat{\mathbf{\Lambda}}\hat{\mathbf{z}} + \hat{\boldsymbol{\psi}}\hat{\mathbf{A}}_{uc}\Delta\mathbf{u} + \hat{\mathbf{z}}^* \begin{bmatrix} \hat{\boldsymbol{\varphi}}_{H1}\hat{\mathbf{\Lambda}}_{H1}\hat{\boldsymbol{\psi}}_{H1} \\ \hat{\boldsymbol{\varphi}}_{H2}\hat{\mathbf{\Lambda}}_{H2}\hat{\boldsymbol{\psi}}_{H2} \\ \vdots \\ \hat{\boldsymbol{\varphi}}_{Hk}\hat{\mathbf{\Lambda}}_{Hk}\hat{\boldsymbol{\psi}}_{Hk} \end{bmatrix} \hat{\mathbf{z}}$$

with

$$\Delta\overline{\mathbf{V}}_G = \hat{\mathbf{B}}_{xG}\hat{\boldsymbol{\varphi}}\hat{\mathbf{z}}$$

$$\Delta\overline{\mathbf{V}}_L = \hat{\mathbf{C}}_{xL}\hat{\boldsymbol{\varphi}}\hat{\mathbf{z}}$$

These equations may be rewritten as

$$\dot{\hat{\mathbf{z}}} = \hat{\boldsymbol{\Lambda}}\hat{\mathbf{z}} + \hat{\mathbf{M}}_c\Delta\mathbf{u} + \hat{\mathbf{z}}^* \begin{bmatrix} \hat{\boldsymbol{\varphi}}_{H1}\hat{\boldsymbol{\Lambda}}_{H1}\hat{\boldsymbol{\Psi}}_{H1} \\ \hat{\boldsymbol{\varphi}}_{H2}\hat{\boldsymbol{\Lambda}}_{H2}\hat{\boldsymbol{\Psi}}_{H2} \\ \vdots \\ \hat{\boldsymbol{\varphi}}_{Hk}\hat{\boldsymbol{\Lambda}}_{Hk}\hat{\boldsymbol{\Psi}}_{Hk} \end{bmatrix} \hat{\mathbf{z}} \tag{5.26}$$

$$\Delta\overline{\mathbf{V}}_G = \hat{\mathbf{M}}_{oG}\hat{\mathbf{z}} \tag{5.27}$$

$$\Delta\overline{\mathbf{V}}_L = \hat{\mathbf{M}}_{oL}\hat{\mathbf{z}} \tag{5.28}$$

Referring to Equation (5.26), it is clear that if the *i*th row of matrix $\hat{\mathbf{M}}_c$ is zero, the inputs have no effect on the *i*th mode. In such a case, the *i*th mode is said to be uncontrollable.

From Equations (5.27) and (5.28), it is seen that the *i*th column of matrices $\hat{\mathbf{M}}_{oG}$ and $\hat{\mathbf{M}}_{oL}$ determines whether or not the variable $\hat{z}_i$ contributes to the formation of the outputs. If the column is zero, then the corresponding mode is unobservable. This explains why some poorly damped modes are sometimes not detected by observing the transient response of a few monitored quantities.

Based on the above model, controllability and observability measures are defined for the linear ROM as follows.

Definition 5.1. Consider the system model (5.26)-(5.27). The $k \times m$ matrix $\hat{\mathbf{M}}_c = \hat{\boldsymbol{\psi}}\hat{\mathbf{A}}_{uc}$ is defined as the mode controllability matrix.

Definition 5.2. The $2m \times k$ matrix $\hat{\mathbf{M}}_{oG} = \hat{\mathbf{B}}_{xG}\hat{\boldsymbol{\varphi}}$ and the $2(nb-m)\times k$ matrix $\hat{\mathbf{M}}_{oL} = \hat{\mathbf{C}}_{xL}\hat{\boldsymbol{\varphi}}$ are defined as the observability matrices.

These measures are the counterpart of the controllability and observability matrices used in conventional linear formulations.

In the sequel, a computer algorithm to determine controllability measures is discussed.

5.5 Numerical Algorithm

Based on the above theoretical framework, the actual calculation of the relevant modal quantities now is accomplished by performing the following algorithm.

1. Determine the most energetic modes using the POD approach in section 3.4. These modes are related to the physical state space variables through the transformation

$$\Delta \mathbf{x} = \mathbf{W}\Delta\hat{\mathbf{x}} = \mathbf{W}\hat{\boldsymbol{\varphi}}\hat{\mathbf{z}} = \bar{\boldsymbol{\varphi}}\hat{\mathbf{z}} \tag{5.29}$$

where $\bar{\boldsymbol{\varphi}}$ gives the modes with the most energy.

2. Compute modal controllability and observability matrices. Let the system behavior be expressed in the form $\hat{\mathbf{z}} = \hat{\boldsymbol{\psi}}\mathbf{W}^{*}\Delta\mathbf{x} = \bar{\boldsymbol{\psi}}\Delta\mathbf{x}$. Matrix $\bar{\boldsymbol{\psi}}_i$ identifies that combination of the original state variables displays only the *i*th mode, i.e., the *k*th element of the $\bar{\boldsymbol{\psi}}_i$ weighs the contribution of the activity of the variable x_k to *i*th mode of greater energy.

3. Compute the matrix of participation factors, P

$$\mathbf{P} = \begin{bmatrix} \bar{\varphi}_{11}\bar{\psi}_{11} & \bar{\varphi}_{12}\bar{\psi}_{21} & \cdots & \bar{\varphi}_{1k}\bar{\psi}_{k1} \\ \bar{\varphi}_{21}\bar{\psi}_{12} & \bar{\varphi}_{22}\bar{\psi}_{22} & \cdots & \bar{\varphi}_{2k}\bar{\psi}_{k2} \\ \vdots & \vdots & \vdots & \vdots \\ \bar{\varphi}_{n1}\bar{\psi}_{1n} & \bar{\varphi}_{n2}\bar{\psi}_{2n} & \cdots & \bar{\varphi}_{nk}\bar{\psi}_{kn} \end{bmatrix} \tag{5.30}$$

4. Calculate the observability matrix. For the generation and load buses, the matrix is used that provide the reduced model, because the outputs do not lose their physical meaning, which provides us a direct relation with the modes of greater energy and of this form we can see how observable is a mode anywhere of the network of the system.

$$\mathbf{M}_{oG} = \hat{\mathbf{B}}_{xG}\hat{\boldsymbol{\varphi}} \tag{5.31}$$

$$\mathbf{M}_{oL} = \hat{\mathbf{C}}_{xL}\hat{\boldsymbol{\varphi}} \tag{5.32}$$

5. Determine the controllability matrix.

$$\mathbf{M}_c = \hat{\boldsymbol{\psi}}\hat{\mathbf{A}}_{uc} \tag{5.33}$$

In interpreting of the expression given by Equation 5.33, is important to emphasize that the controllability matrix, provides us a direct relation of the modes with the excitations of the system, this indicates to us of so controllable is a mode from the inputs of the system.

5.6 Modal Solutions

Further insight into the nature of the proposed model can be obtained from modal analysis of the system model (5.15).

Let the ROM representation be given by

$$\dot{\bar{\mathbf{x}}} = \overline{\mathbf{A}}_{xc}\bar{\mathbf{x}} + \overline{\mathbf{A}}_{uc}\Delta\mathbf{u} + \overline{\mathbf{H}}_{xxc}\left(\bar{\mathbf{x}} \otimes \bar{\mathbf{x}}\right) \tag{5.34}$$

The transformation $\hat{\mathbf{x}} = \hat{\boldsymbol{\varphi}}\hat{\mathbf{z}}$, transforms the ROM into the modal form

$$\dot{\hat{\mathbf{z}}} = \hat{\boldsymbol{\Lambda}}\hat{\mathbf{z}} + \hat{\boldsymbol{\psi}}\hat{\mathbf{A}}_{uc}\Delta\mathbf{u} + \hat{\mathbf{H}}_{xxc\Lambda}\left(\hat{\mathbf{z}} \otimes \hat{\mathbf{z}}\right) \tag{5.35}$$

Neglecting higher order terms and assuming a solution to Eqn. (5.35) of the form

$$\dot{\hat{\mathbf{z}}}(t) = e^{\hat{\boldsymbol{\Lambda}}t}\hat{\mathbf{z}}_o \tag{5.36}$$

we can obtain mode-state relationships.

Modal solutions (5.34) are then transformed back into the original physical domain by using the inverse transformation

$$\begin{aligned} \mathbf{x} &= \boldsymbol{\varphi}\mathbf{z} \\ \mathbf{x} &= \mathbf{W}\hat{\mathbf{x}} \end{aligned} \tag{5.37}$$

Combining (5.36) and (5.37) yields

$$\mathbf{x}(t) = \mathbf{W}\hat{\boldsymbol{\varphi}}\hat{\mathbf{z}}(t) = \mathbf{W}\hat{\boldsymbol{\varphi}}e^{\hat{\boldsymbol{\Lambda}}t}\hat{\mathbf{z}}_o \tag{5.38}$$

where $\mathbf{W}\hat{\boldsymbol{\varphi}}$ denotes is the transformation matrix mapping $\hat{\mathbf{z}}(t)$ to $\mathbf{x}(t)$.

Remark 5.1. At any instant t, Eqn. (5.38) enables the time evolution of the physical states, $x(t)$, to be expressed as a linear combination of the system oscillation modes .

Remark 5.2. The effect of system modes on the network variables can be then obtained from Eqns. (5.12) and (5.13).

Note that no information is lost in the reconstruction process, since the sum of all individual contributions gives back the original time series.

5.7 Reduced-Order Model Validation

In this section, we examine the accuracy and efficiency of the low-dimensional dynamical model obtained from the projection procedure.

Let $\bar{\mathbf{x}}$ be an approximation of $\Delta\mathbf{x}$ in a space of dimension n, i.e.,

$$\bar{\mathbf{x}} = \mathbf{W}\Delta\hat{\mathbf{x}}$$

$$\dot{\bar{\mathbf{x}}} = \mathbf{W}\hat{\mathbf{A}}_{xc}\mathbf{W}^{*}\bar{\mathbf{x}} + \mathbf{W}\hat{\mathbf{A}}_{uc}\Delta\mathbf{u} + \mathbf{W}\hat{\mathbf{H}}_{xxc}\left(\mathbf{W}^{*}\otimes\mathbf{W}^{*}\right)\left(\bar{\mathbf{x}}\otimes\bar{\mathbf{x}}\right)$$

$$\dot{\bar{\mathbf{x}}} = \bar{\mathbf{A}}_{xc}\bar{\mathbf{x}} + \bar{\mathbf{A}}_{uc}\Delta\mathbf{u} + \bar{\mathbf{H}}_{xxc}\left(\bar{\mathbf{x}}\otimes\bar{\mathbf{x}}\right) \tag{5.39}$$

$$\Delta\mathbf{V}_{G} = \hat{\mathbf{B}}_{xG}\mathbf{W}^{*}\bar{\mathbf{x}} = \bar{\mathbf{B}}_{xG}\bar{\mathbf{x}} \tag{5.40}$$

$$\Delta\mathbf{V}_{L} = \hat{\mathbf{C}}_{xL}\mathbf{W}^{*}\bar{\mathbf{x}} = \bar{\mathbf{C}}_{xL}\bar{\mathbf{x}} \tag{5.41}$$

The system of DAEs of above, has advantage of that state variables $\bar{\mathbf{x}}$, has the same physical meaning that of state variables $\Delta\mathbf{x}$ of the original system, in addition, it preserves the same dynamic behavior. The validation consists of comparing the results of the model reduced with those of this model.

5.8 References

[1] G. C. Verghese, I. J. Perez-Arriaga, and F. C. Schweppe, *"Selective Modal Analysis with Application to Electric Power Systems, Part I: Heuristic Introduction, Part II: The Dynamic Stability Problem"*, *IEEE Transactions*, Vol., PAS-101, No. 9, pp. 3117-3134, September 1982.

[2] Prabha Kundur, *Power System Stability and Control* Mc-Graw-Hill, Inc., 12: 699-717.

[3] Peter W. Sauer and M. A. Pai, *Power System Dynamics and Stability*, Prentice Hall, 1998.

Chapter 6
Application

This chapter describes the application of the proposed technique to the analysis and characterization of nonlinear behavior in a test power system. The performance of the proposed technique is tested on a 16-machine, 68 bus test power system. In particular, the developed technique is used to analyze the influence of the modes with the greatest energy in the dynamic behavior of the system.

Several case studies are presented and discussed to in which both conventional eigenanalysis and reduction techniques are used to analyze the ability of nonlinear ROMs to capture system behavior following large perturbations.

The main interest is focused on determining ROMs for stressed operating conditions and large-signal perturbations. Numerical issues associated with the application of the technique are also discussed.

The accuracy and efficiency of the reduction method is quantified by comparing the reduced-order system simulations with those from commercial stability software. Detailed dynamic simulations demonstrate that reduced-order models yield accurate predictions over a wide range of operating scenarios.

6.1 Outline of the Study

The proposed method was tested on the NPCC system of test system has 68 buses, 16 generators and 86 transmission lines shown in Fig. 6.1. The base case condition in the analysis is essentially that given in Ref. [1].

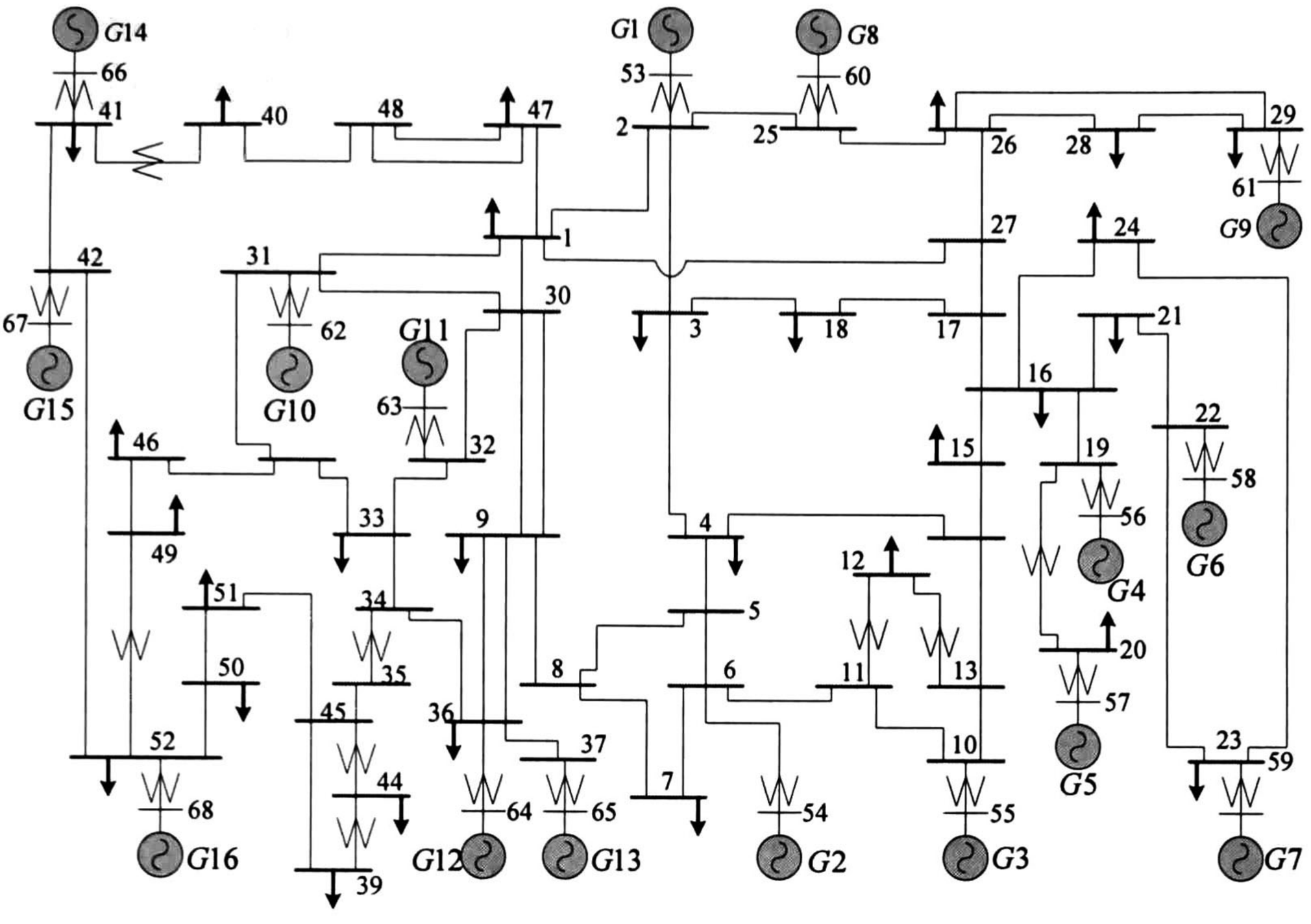

Figure 6.1. Single line diagram 16 generator system, 68 buses and 86 lines.

Two system representations are considered in the analysis:

1. A classical system representation, and

2. A detailed system representation.

6.2 Classical System Representation

6.2.1 Modeling Considerations

The classical system representation has 32 states. For this model, the state vector and input vectors is of the original unreduced system are

$$\mathbf{x} = \begin{bmatrix} \delta_1 & \cdots & \delta_{16} & \omega_1 & \cdots & \omega_{16} \end{bmatrix}^T$$

$$\mathbf{u} = \begin{bmatrix} T_{m1} & \cdots & T_{m16} \end{bmatrix}^T$$

The dynamic behavior of the system is described by the following differential-algebraic equations of motion:

$$\begin{aligned} \frac{d}{dt}\mathbf{x} &= \mathbf{f}(\mathbf{x},\mathbf{y},\mathbf{u}) \\ \mathbf{0} &= \mathbf{g}(\mathbf{x},\mathbf{y}) \end{aligned} \tag{6.1}$$

with initial conditions $\mathbf{x}(0) = \mathbf{x}_o$. The Equation 6.1 represent a system of 32 differential equations with 136 algebraic equations, this is the reason by that no represent in the text.

The goal is to represent the dynamic behavior of the system by a low-order nonlinear ROM of the form

$$\begin{aligned} \Delta\dot{\hat{\mathbf{x}}} &= \hat{\mathbf{A}}_{xc}\Delta\hat{\mathbf{x}} + \hat{\mathbf{A}}_{uc}\Delta\mathbf{u} + \hat{\mathbf{H}}_{xxc}(\Delta\hat{\mathbf{x}} \otimes \Delta\hat{\mathbf{x}}) \\ \Delta\mathbf{y} &= \hat{\mathbf{B}}_{yx}\Delta\hat{\mathbf{x}} \end{aligned} \tag{6.2}$$

where $\Delta\hat{\mathbf{x}}$ is the reduced state vector and the matrices $\hat{\mathbf{A}}_{xc}$, $\hat{\mathbf{H}}_{xxc}$ are the linear and second-order approximations in the ROM, respectively; matrix $\hat{\mathbf{B}}_{yx}$ is a linear approximation that relationship the algebraic variables of the system with the reduced state vector.

6.2.2 Application to Transient Stability Data

To verify the ability of the method to determine accurate ROMs, we consider output data from transient stability simulations. To this end, several perturbations were conducted including small and large signal perturbations.

Figure 6.2 shows the system response to a three-phase fault at bus 28. This fault is seen to excite an oscillation in which machines Gen 14 and Gen 15 swing, mainly, in opposition to machine Gen 16. The other machines have a minor contribution to the observed oscillation.

As pointed out in Chapter 3, the accuracy of the technique is improved when the mean value is removed from the original signals; this also makes the

model more efficient. In the developed model, this is accomplished by referring the system behavior to the inertia center. Figure 6.3 shows system behavior in the center of angle formulation (COI).

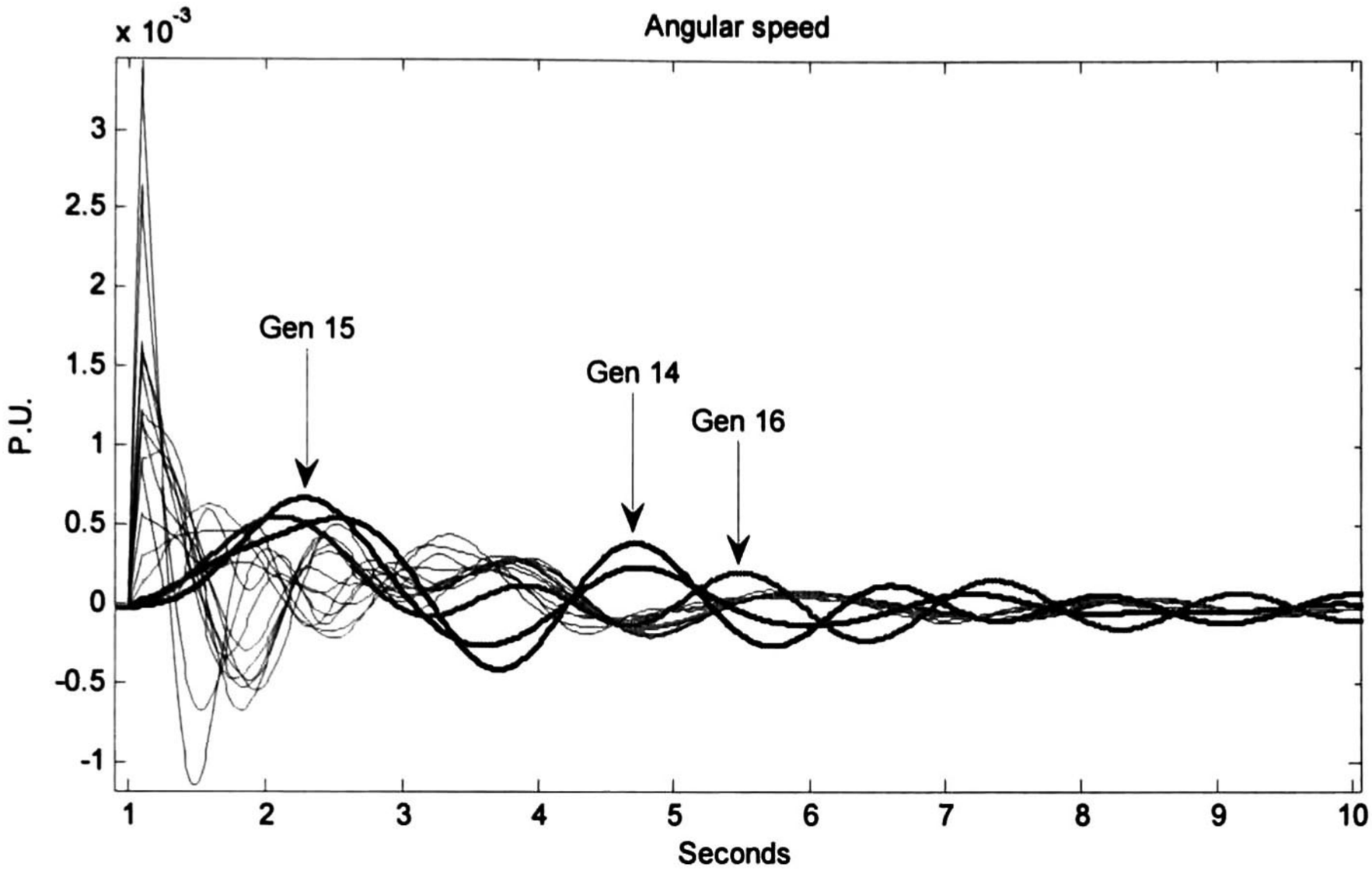

Figure 6.2. Dynamic behavior of the angular speed to a three-phase fault at bus 28.

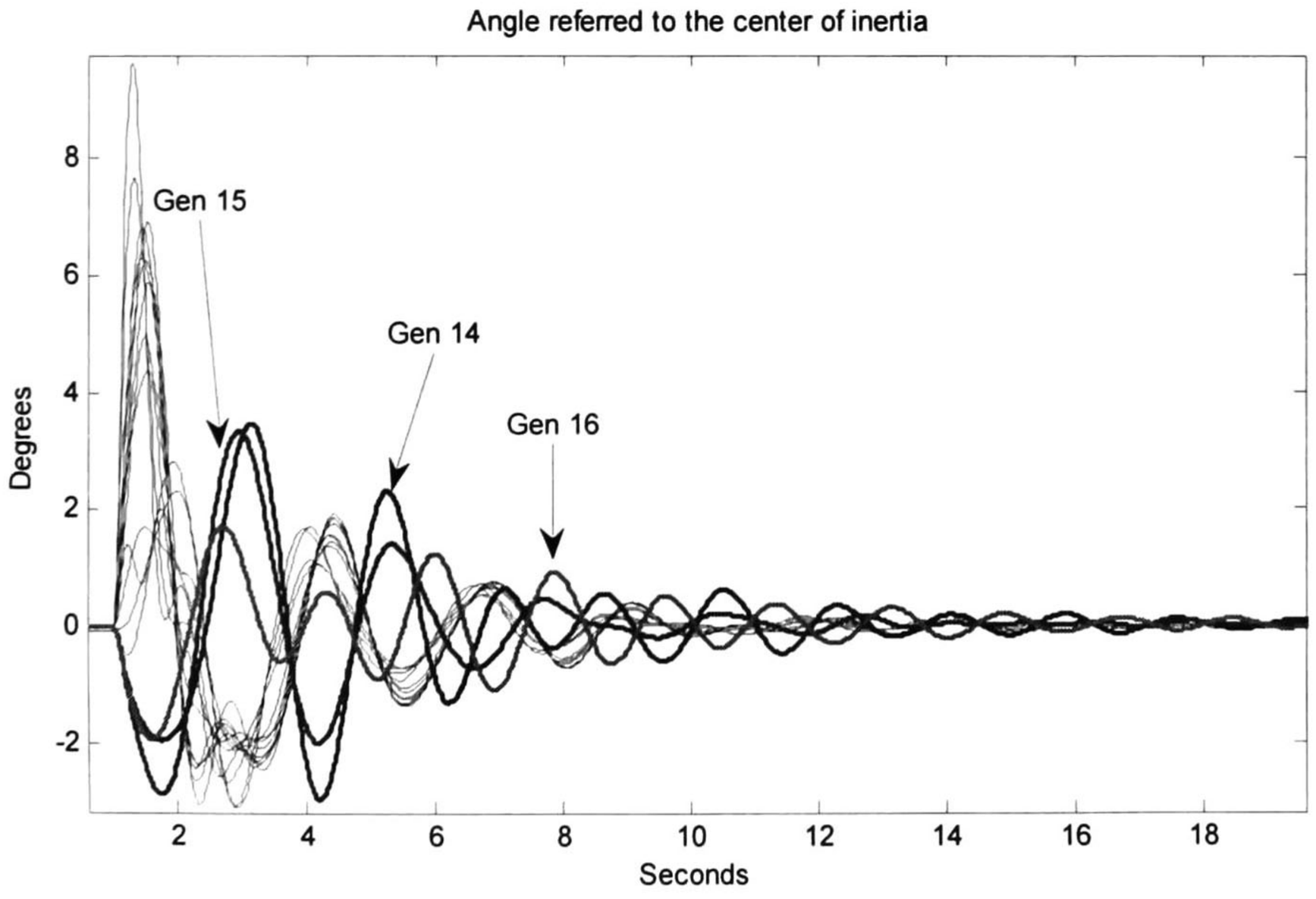

Figure 6.3. Dynamic behavior of the angle referred to the inertia center for a three-phase fault at bus 28.

Here, solid lines represent the time evolution of the original model while broken lines correspond to the time evolution of the ROM with an energy percentage of 99.99%. See Fig. 6.4. In addition in all simulations, the signals that represent the time evolution of the original model (solid lines) are overlapping to the signals that represent the time evolution of the ROM (broken lines).

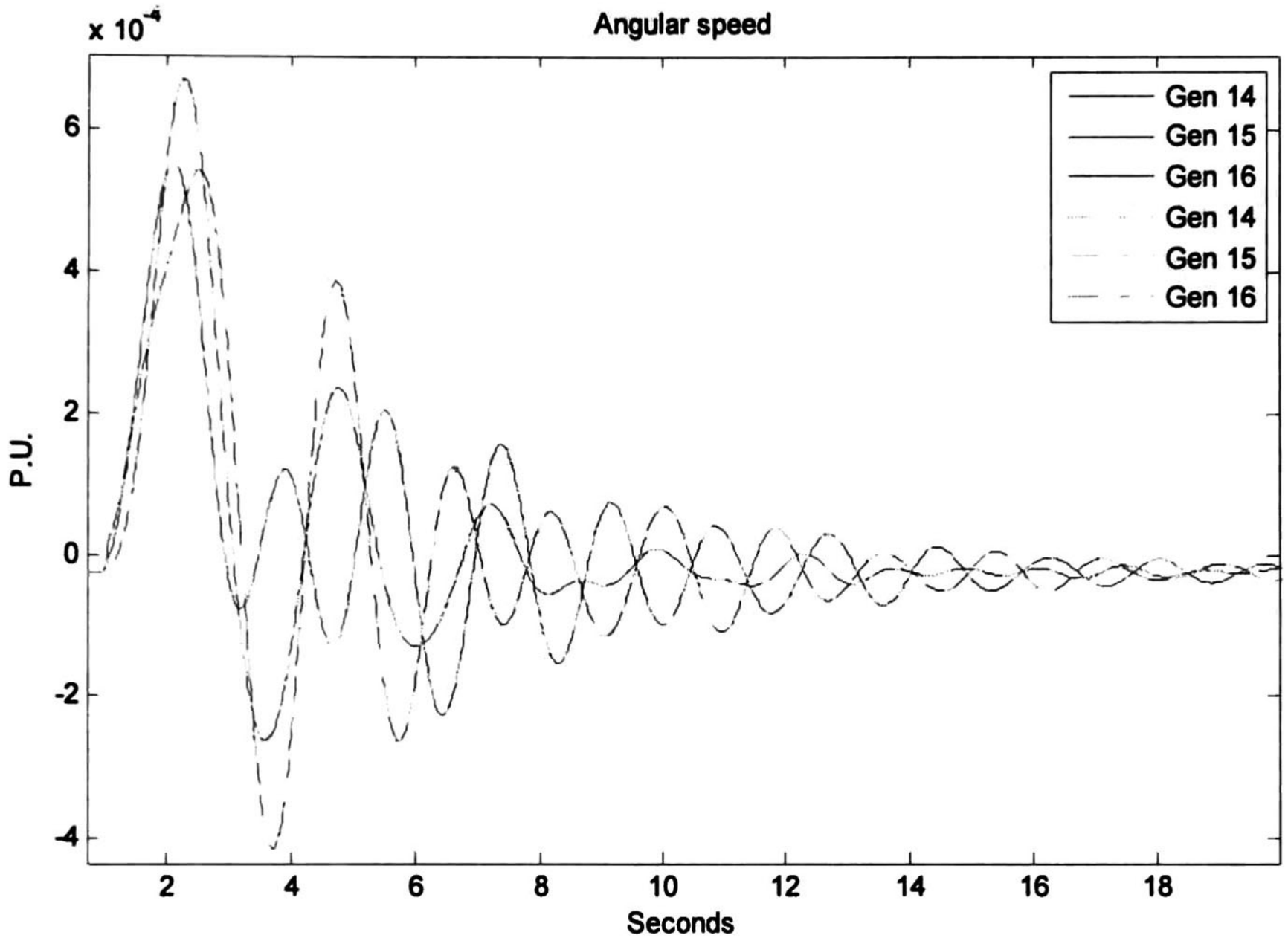

Figure 6.4. Dynamic behavior of the rotor angle position of the original model and of the ROM.

One the objectives of referring the rotor angle deviations to the center of inertia and to remove the direct current component of each one of the signals is because the proper orthogonal decomposition (POD), is more efficient for signals than do not have direct component, i.e., that the energy percentage is approximately a 99.99% in the majority of the cases.

6.2.3 Construction of Snapshots

The technique in Chapter 4 was applied to determine fault-dependent nonlinear ROMs. In all cases, the criteria adopted to extract 99.99% of the total energy.

Following the general approach described in Chapter 3, the observation matrix was obtained from the snapshots of the simulated data, i.e.

$$\mathbf{X}(t) = [\boldsymbol{\delta}_1(t) \quad \cdots \quad \boldsymbol{\delta}_{16}(t) \quad \boldsymbol{\omega}_1(t) \quad \cdots \quad \boldsymbol{\omega}_{16}(t)]^T$$

where $\boldsymbol{\omega}_i(t) = [\omega_i(t_1) \quad \omega_i(t_2) \quad \cdots \quad \omega_i(t_N)]$, for $i = 1,2,...,16$, and **N** is the number of snapshots. In the present simulations, proper orthogonal decomposition is carried out on 2000 snapshots. The snapshots are equally spaced.

Application of the proposed technique results in a second-order representation characterized by 23 states. Figure 6.5 shows the spectra of selected signals computed to capture 99.99 % of the signals' energy.

Here, the horizontal axis shows the number of singular values required to attain 99.99 % of the average total energy while the vertical axis shows the energy captured by each singular value. Singular values 1 through 5 are seen to capture nearly 99% of the total energy. Singular value 1 has the largest participation with about 89% of the energy.

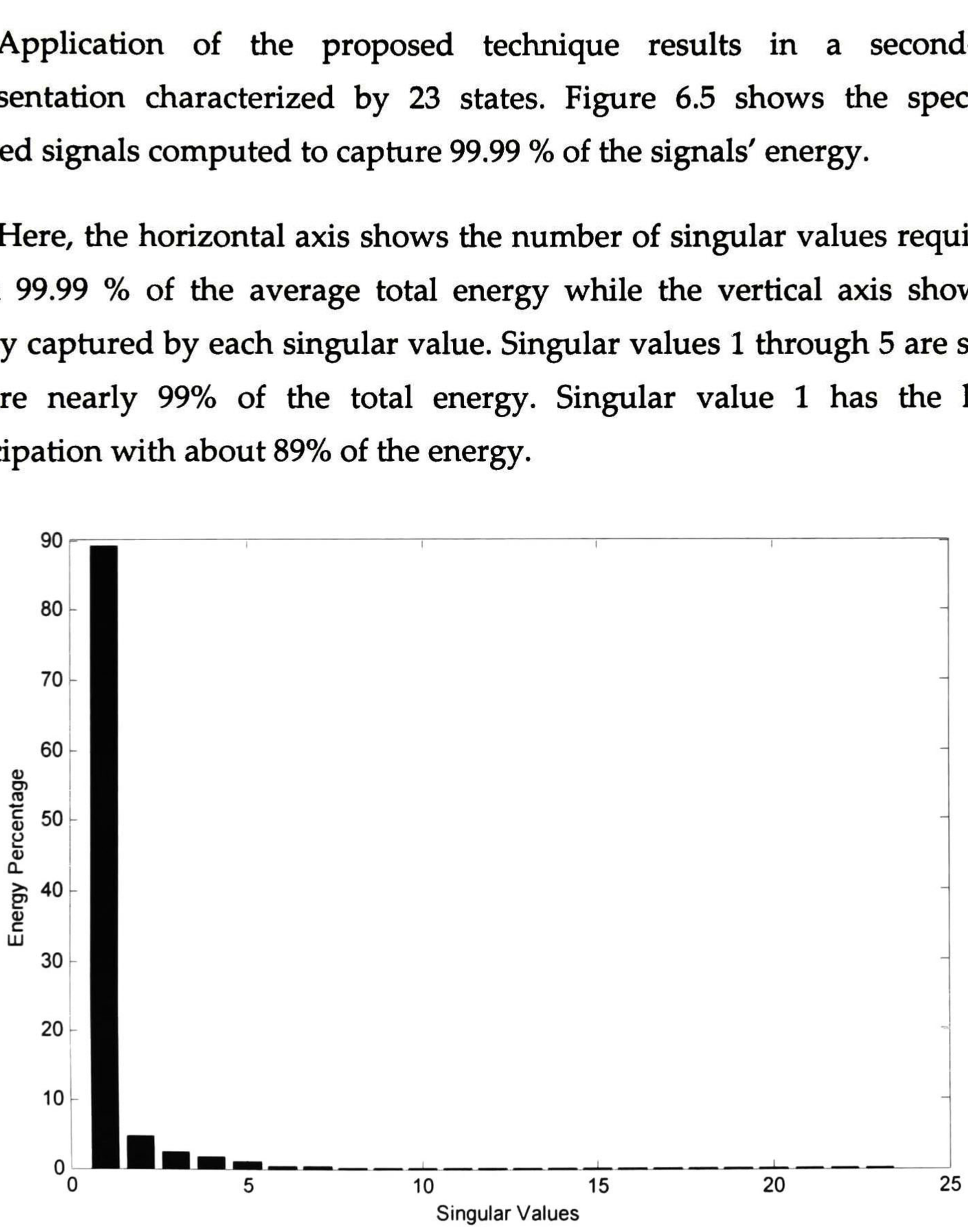

Figure 6.5. Energy percentage of each singular value of the ROM.

6.2.4 Reduced-Order Simulations

To verify the ability of the method to extract the dominant features of complex oscillations, detailed numerical simulations for the original system model and the reduced-order representation were conducted. The equations that describe the original model and the ROM are given in the Chapter 5.

Examination of system results in Figure 6.6 through Figure 6.11 shows that the ROM accurately approximates system behavior for the entire time window. Again, we emphasize that the formulation of the center of inertia provides a more accurate system description thus giving confidence to the adopted model.

In all cases the nonlinear ROM is seen to accurately describe system behavior thus giving confidence to the proposed model.

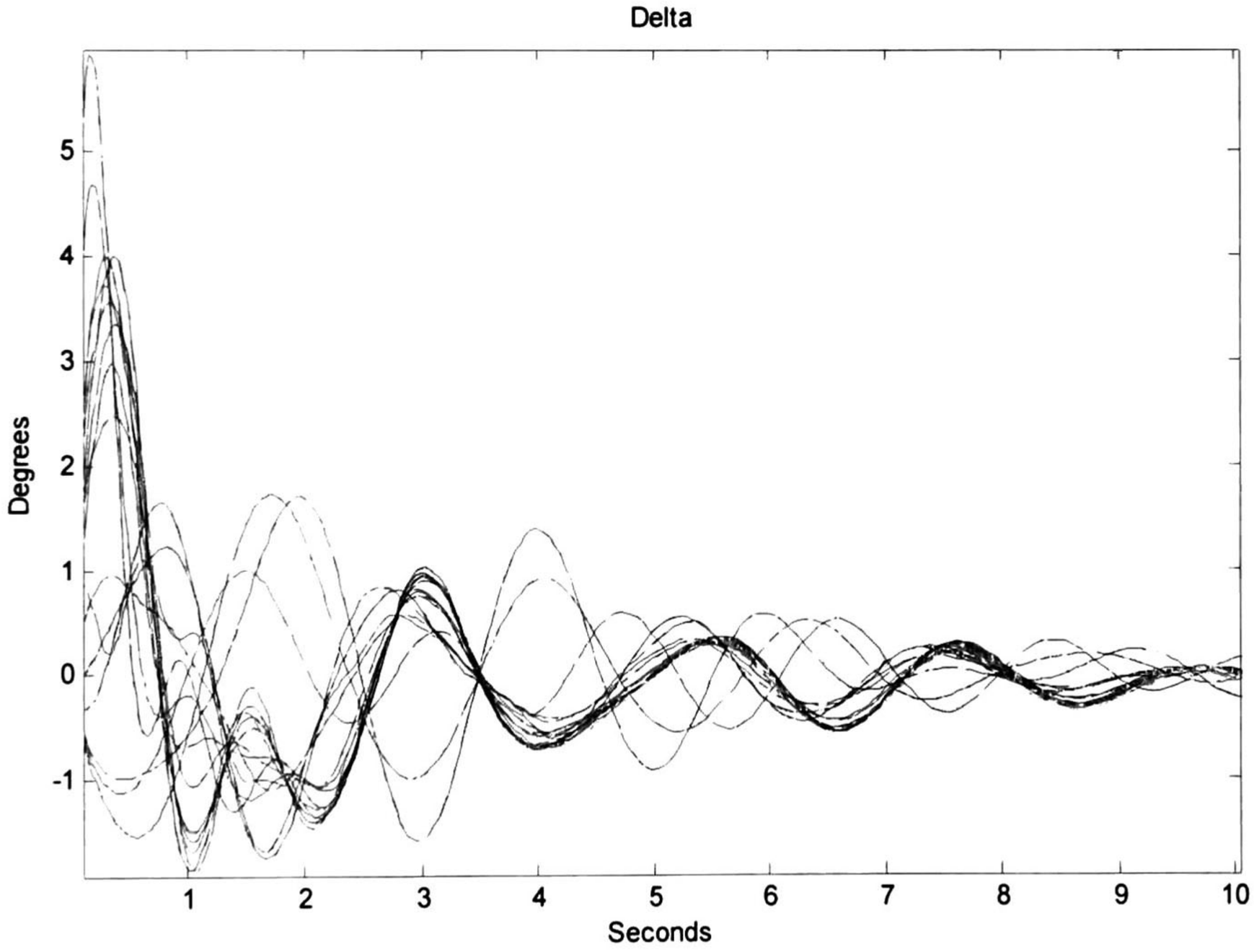

Figure 6.6. Dynamic behavior of the angle of the generators given by the original model and the ROM.

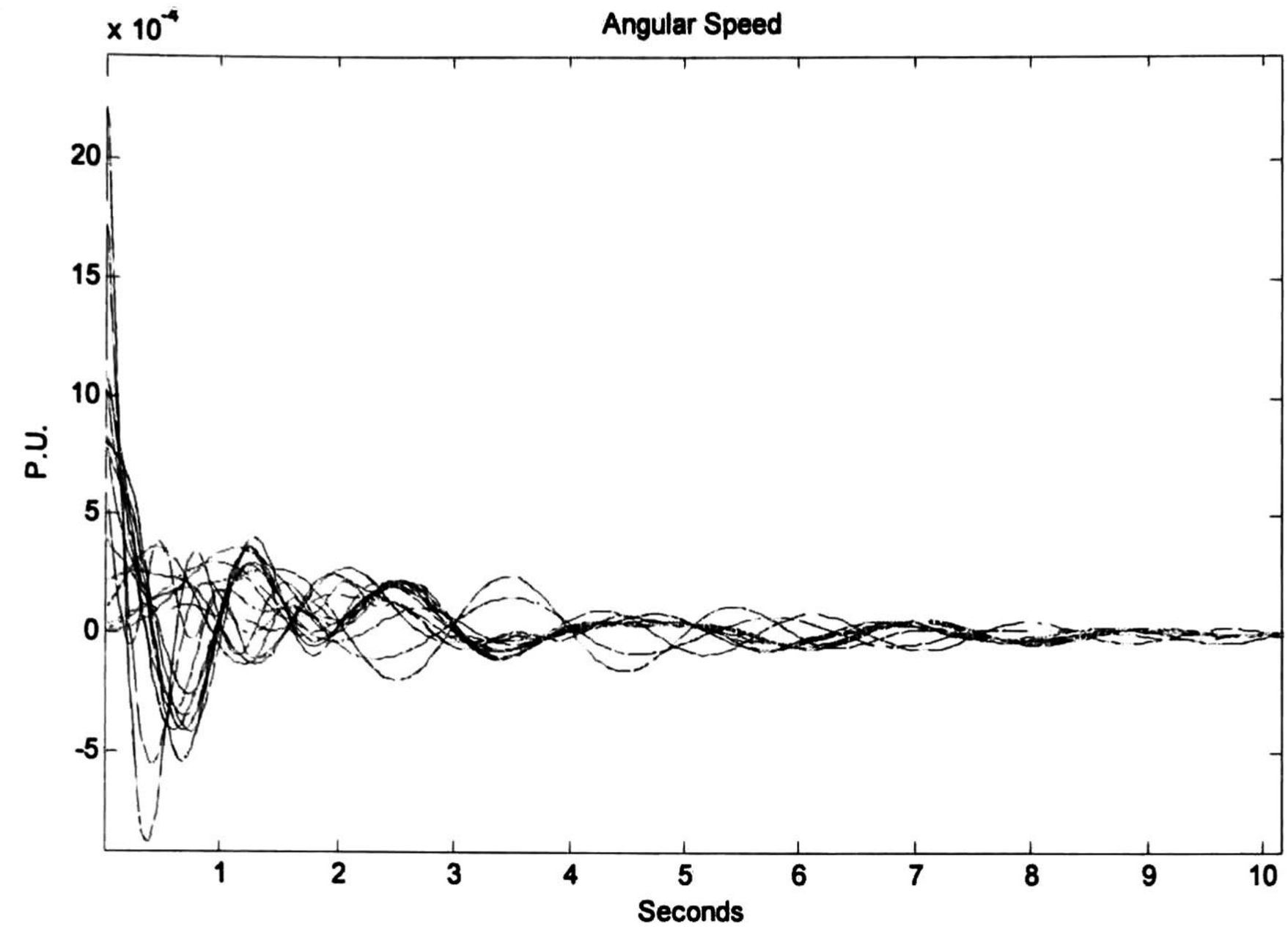

Figure 6.7. Dynamic behavior of the angular speed of the generators given by the original model and the ROM.

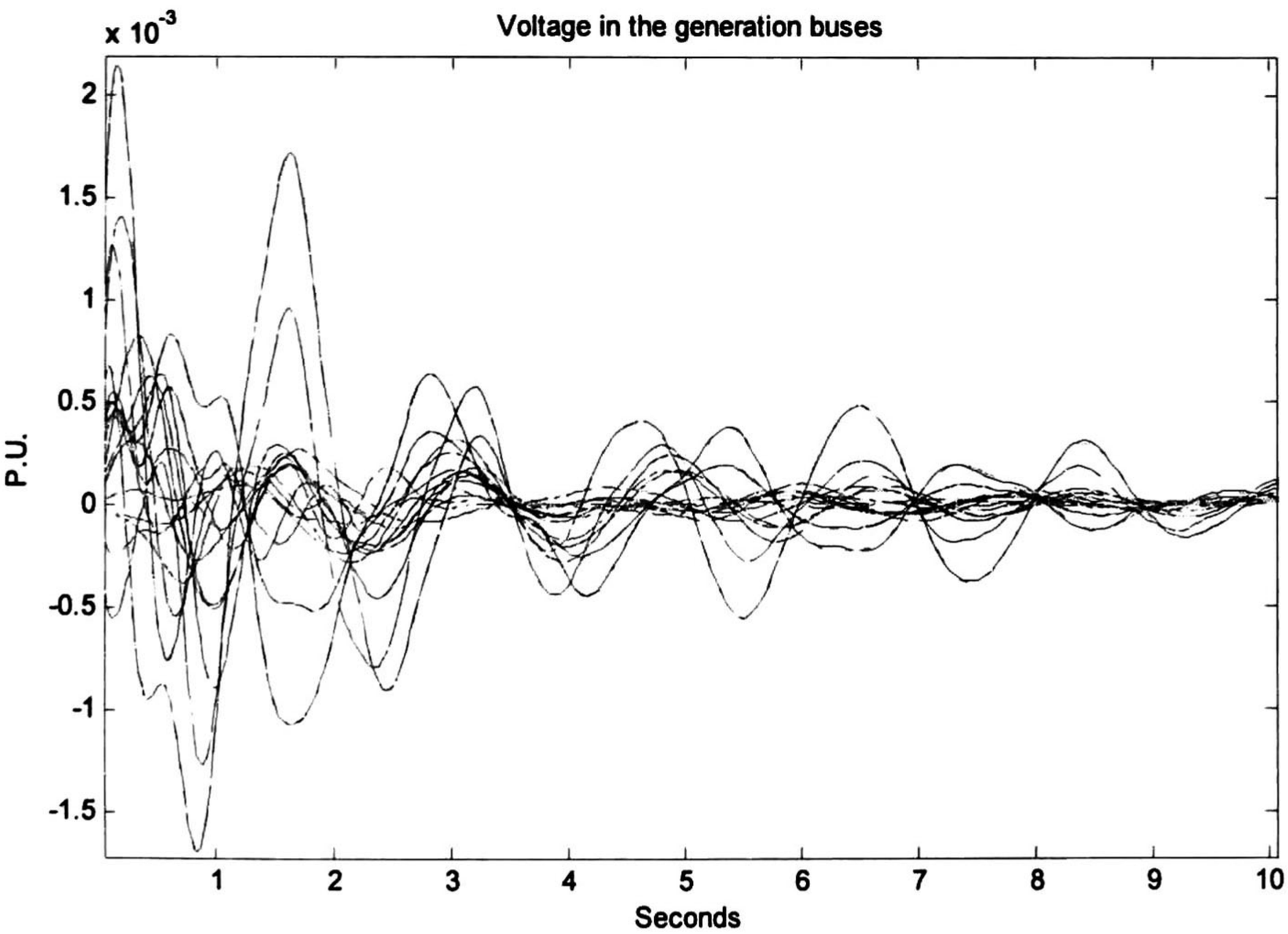

Figure 6.8. Dynamic behavior of the voltage magnitude in the generation buses, given by the original model and the ROM.

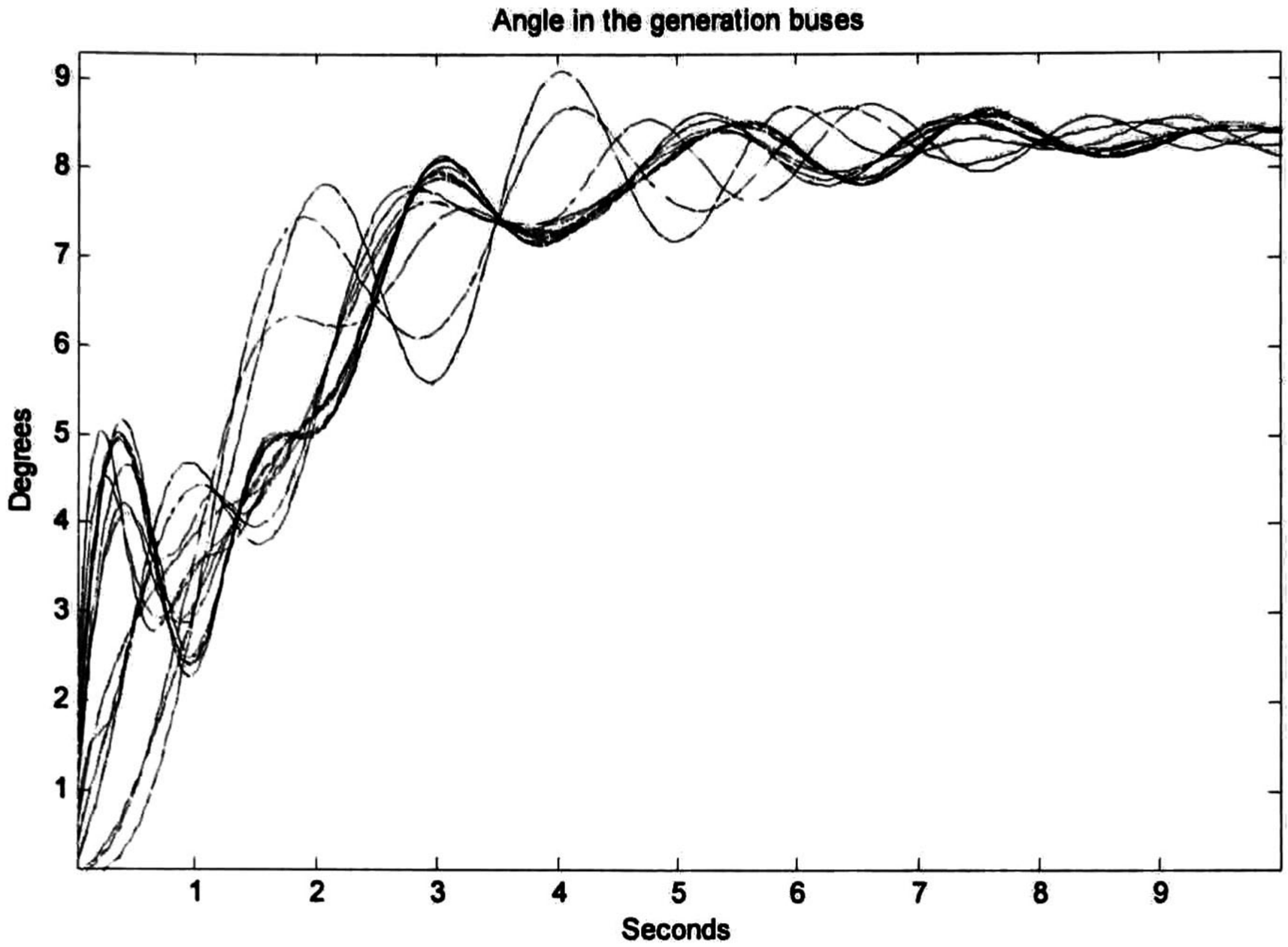

Figure 6.9. Dynamic behavior of the angle in the generation buses, given by the original model and the ROM.

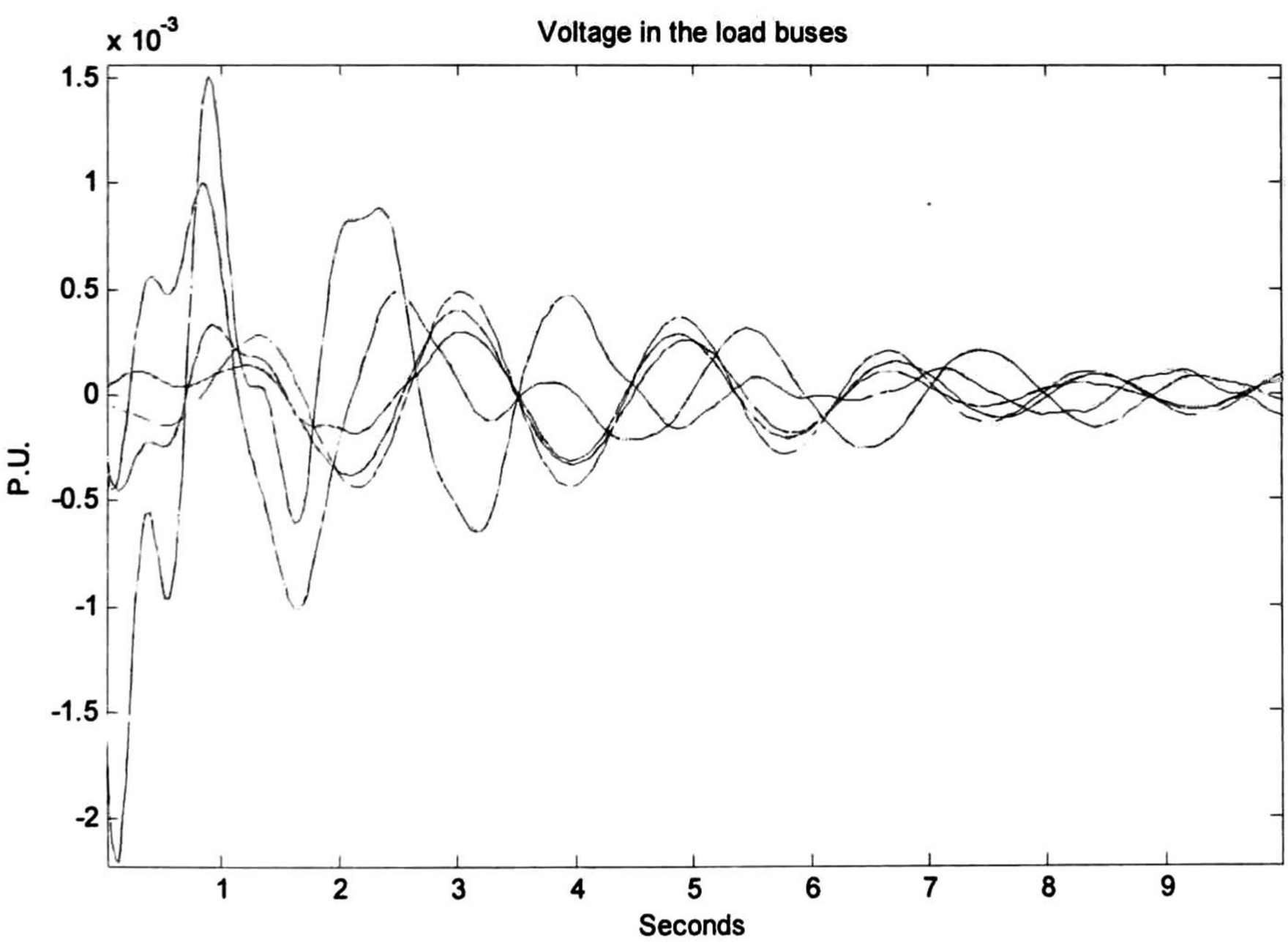

Figure 6.10. Dynamic behavior of the voltage magnitude in the load buses 40-42, 50 and 52, given by the original model and the ROM.

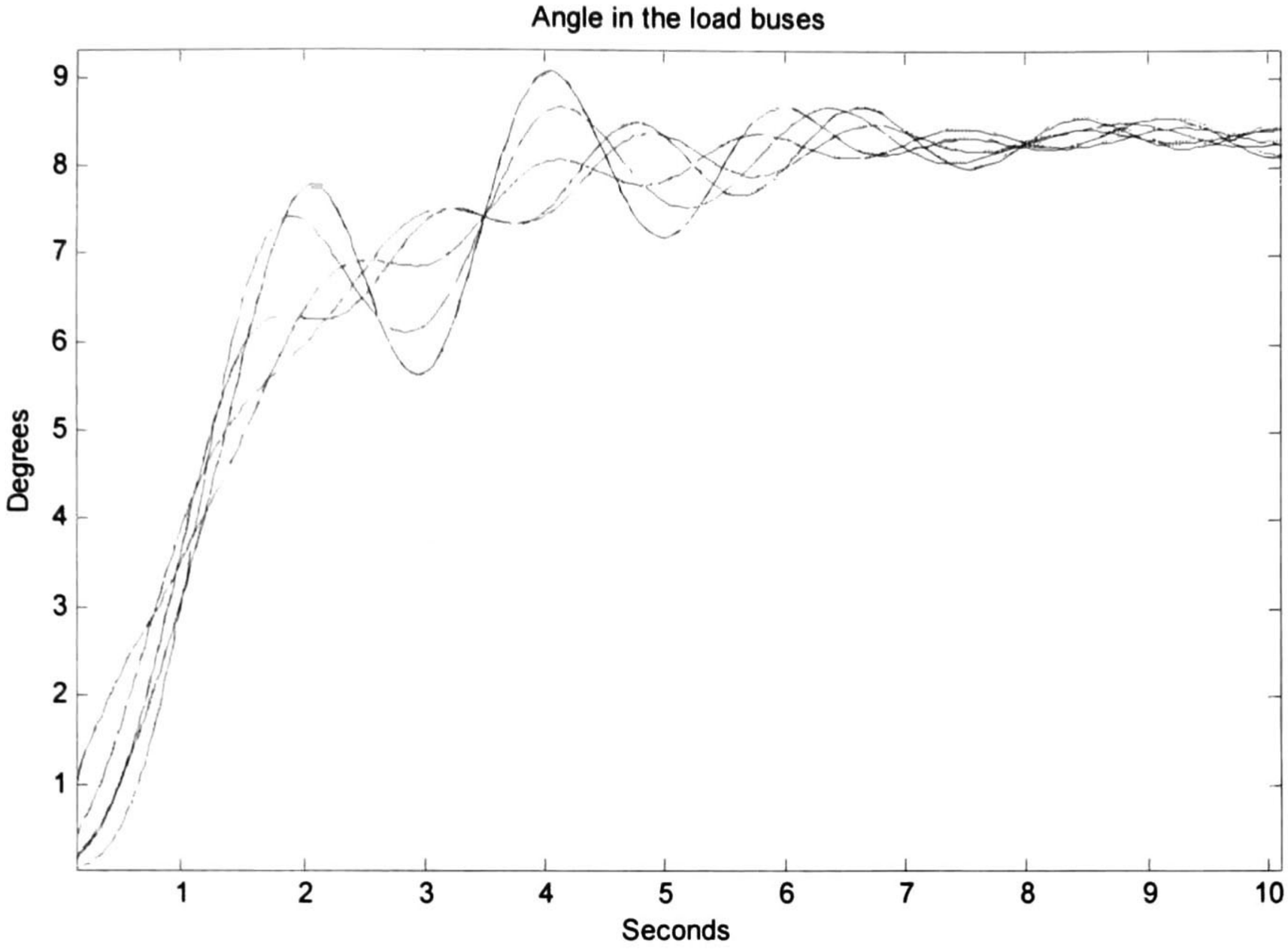

Figure 6.11. Dynamic behavior of the angle in the load buses 40-42, 50 and 52, given by the original model and the ROM.

6.2.5 Physical Interpretation of the POMs

Proper orthogonal modes have a similar interpretation to linear modes. Table 6.1 shows the eigenvalues associated with the POMs. A key feature of the model is its ability to preserve the eigenvalues of the linear model.

Further insight into the nature of these modes can be gleaned from frequency spectra of the ROM. Let $\Delta\hat{\mathbf{x}} = \hat{\boldsymbol{\varphi}}\hat{\mathbf{z}}$ be a transformation that eliminates the cross-coupling between the state variables. Application of this transformation to (6.2) yields the uncoupled model

$$\dot{\hat{\mathbf{z}}} = \hat{\boldsymbol{\Lambda}}\hat{\mathbf{z}} + \hat{\boldsymbol{\psi}}\hat{\mathbf{A}}_{uc}\Delta\mathbf{u} + \hat{\mathbf{H}}_{xxc\Lambda}\left(\hat{\mathbf{z}} \otimes \hat{\mathbf{z}}\right) \tag{6.3}$$

Neglecting second-order terms yields the linear ROM

$$\dot{\hat{\mathbf{z}}} = \hat{\boldsymbol{\Lambda}}\hat{\mathbf{z}} \tag{6.4}$$

where $\hat{\boldsymbol{\Lambda}} = diag\left[\hat{\lambda}_1 \quad \hat{\lambda}_2 \quad \cdots \quad \hat{\lambda}_{23}\right]$.

The linear system given in (6.4) has a solution of the form that follows

$$\hat{z}_k(t) = \hat{z}_{k0} e^{\hat{\lambda}_k t}$$

$$\Delta \mathbf{x} = \mathbf{W} \Delta \hat{\mathbf{x}} = \mathbf{W} \hat{\boldsymbol{\varphi}} e^{\hat{\Lambda} t} \hat{\mathbf{z}}_0 \tag{6.5}$$

where $\hat{\mathbf{z}}_0 = \hat{\mathbf{z}}(0)$, while that original model has a solution of the form

$$\Delta \mathbf{x} = \boldsymbol{\varphi} e^{\Lambda t} \mathbf{z}_0 \tag{6.6}$$

Figure 6.12 and **Figure 6.13** shows the results of the Eqns 6.5 and 6.6. Solid lines represent the time evolution of the original model while broken lines correspond to the time evolution of the ROM. Again, results are in good agreement showing the correctness of the analysis.

Table 6.1. Eigenvalues of the original model and of the ROM

Original Model		Reduced Order Model	
Eigenvalues	Frequency	Eigenvalues	Frequency
$-0.9961 \pm j11.9186$	1.8969	$-1.0021 \pm j11.9083$	1.8951
$-1.5648 \pm j9.5818$	1.5250	$-1.1530 \pm j9.5072$	1.5131
$-1.2032 \pm j8.6381$	1.3748	$-0.7341 \pm j8.6653$	1.3791
$-1.1747 \pm j8.0243$	1.2771	$-1.4769 \pm j7.9856$	1.2709
$-1.0662 \pm j6.8932$	1.0971	$-1.3493 \pm j7.0376$	1.1201
$-0.2941 \pm j7.3139$	1.1640	$-0.3740 \pm j7.1663$	1.1406
$-0.0945 \pm j4.9457$	0.7871	$-0.0911 \pm j4.9430$	0.7867
$-0.7961 \pm j4.3153$	0.6868	$-0.7934 \pm j4.3105$	0.6860
$-0.3083 \pm j2.7079$	0.4310	$-0.3095 \pm j2.7081$	0.4310
$-0.1965 \pm j3.5507$	0.5651	$-0.1971 \pm j3.5508$	0.5651
-0.6745	0	-0.6910	0
-0.0000	0	-0.0005	0
$-0.9785 \pm j9.9523$	1.5840	-0.2146	0
$-1.3377 \pm j9.7723$	1.5553		
$-1.3900 \pm j7.1441$	1.1370		
$-1.4826 \pm j8.1129$	1.2912		
$-1.1726 \pm j8.2010$	1.3052		

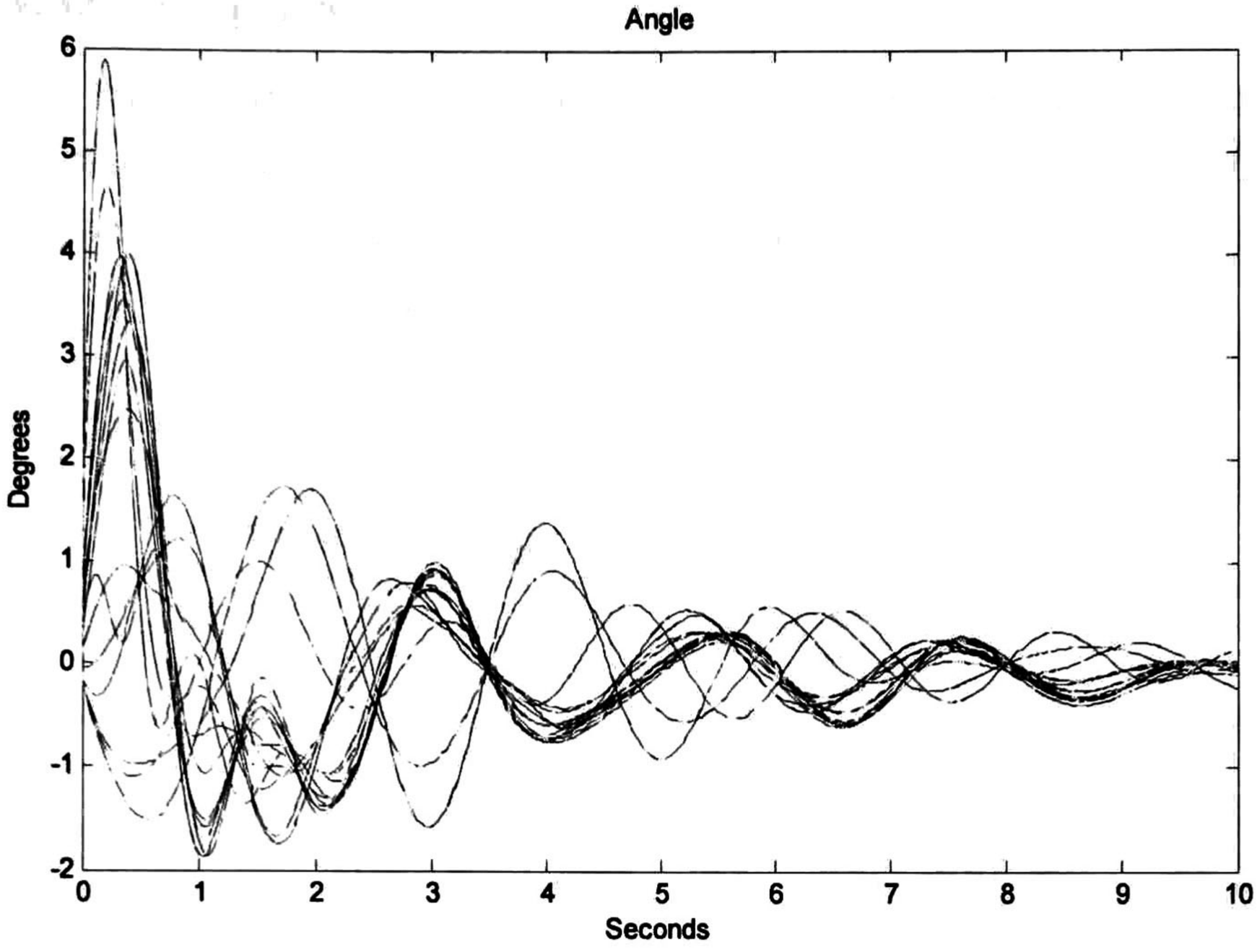

Figure 6.12. Dynamic behavior of the angle of the generators, given by the Equations 6.5 and 6.6

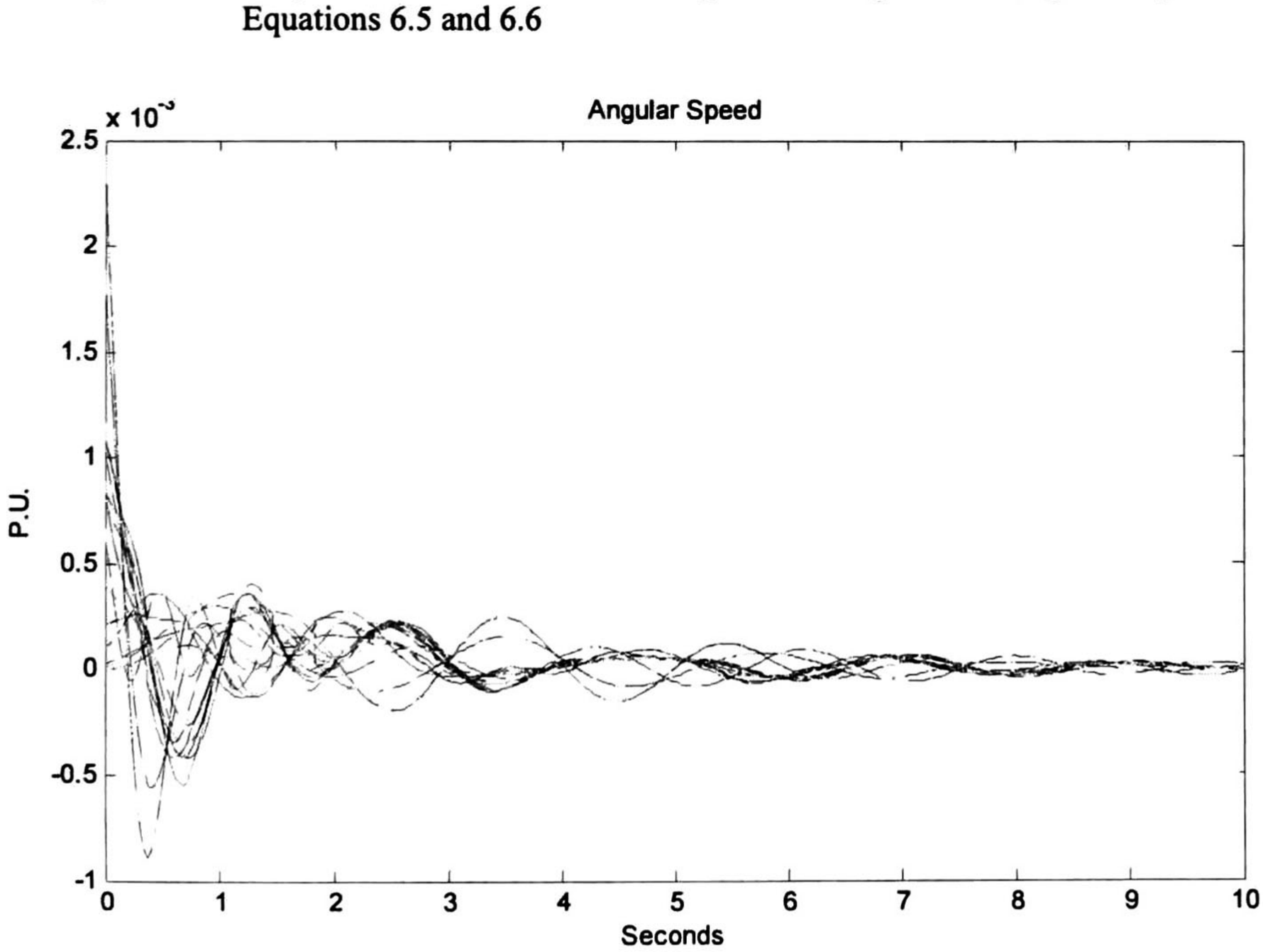

Figure 6.13. Dynamic behavior of the angular speed of the generators, given by the Equations 6.5 and 6.6.

6.2.6 Modal Properties

Based on the linear ROM, detailed studies were conducted to evaluate the ability of the method to extract modal properties. Discussion will be limited to modes 8-10. i.e., with associated eigenvalues $-0.7934 \pm j4.3105$, $-0.3095 \pm j2.7081$ and $-0.1971 \pm j3.5508$ (refer to Table 6.1):

- Mode $-0.7934 \pm j4.3105$

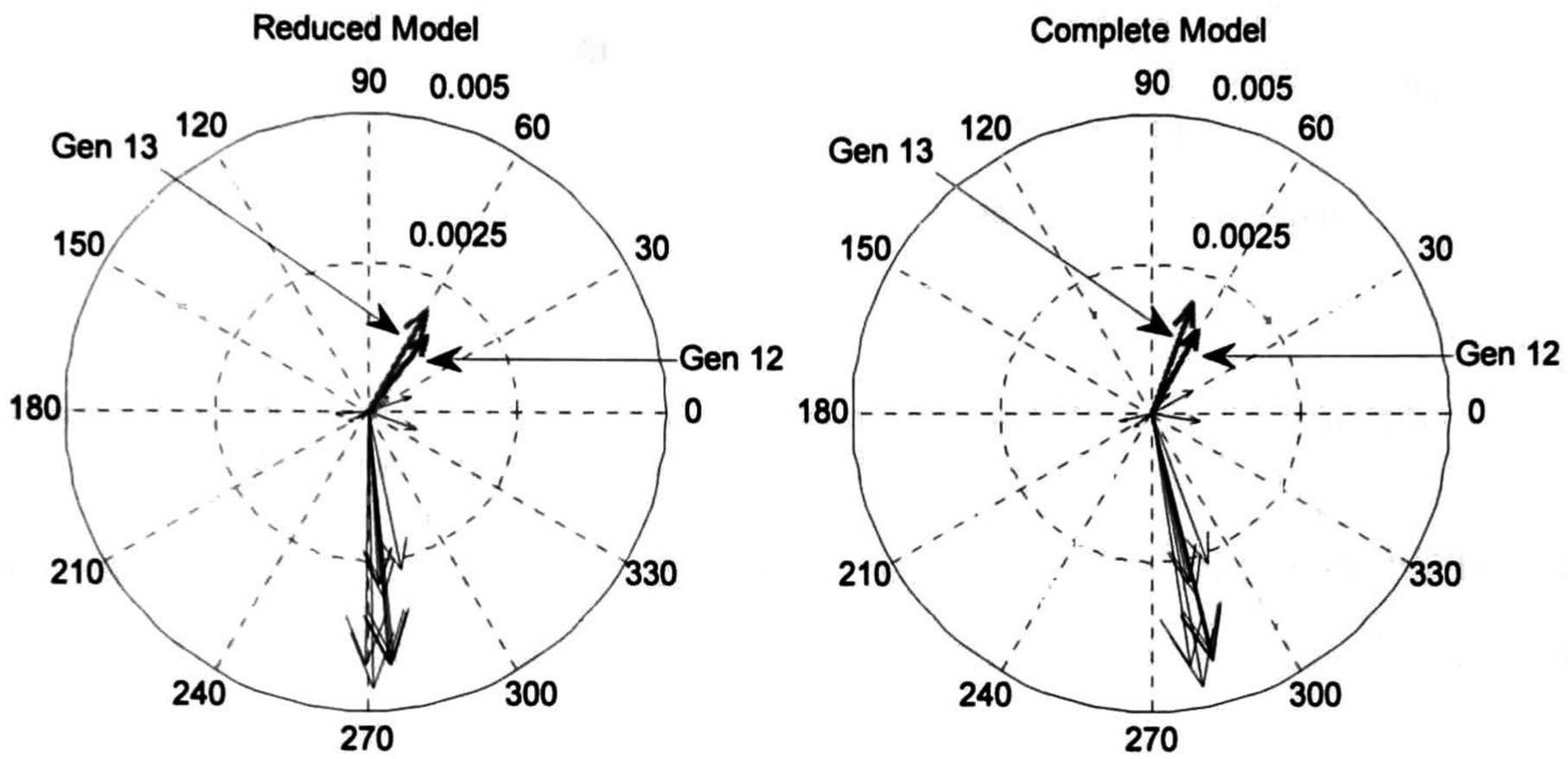

Figure 6.14. Mode shape indicates that is an inter-area mode, because the generators 12 and 13 oscillate against of the rest of the system.

- Mode $-0.3095 \pm j2.7081$

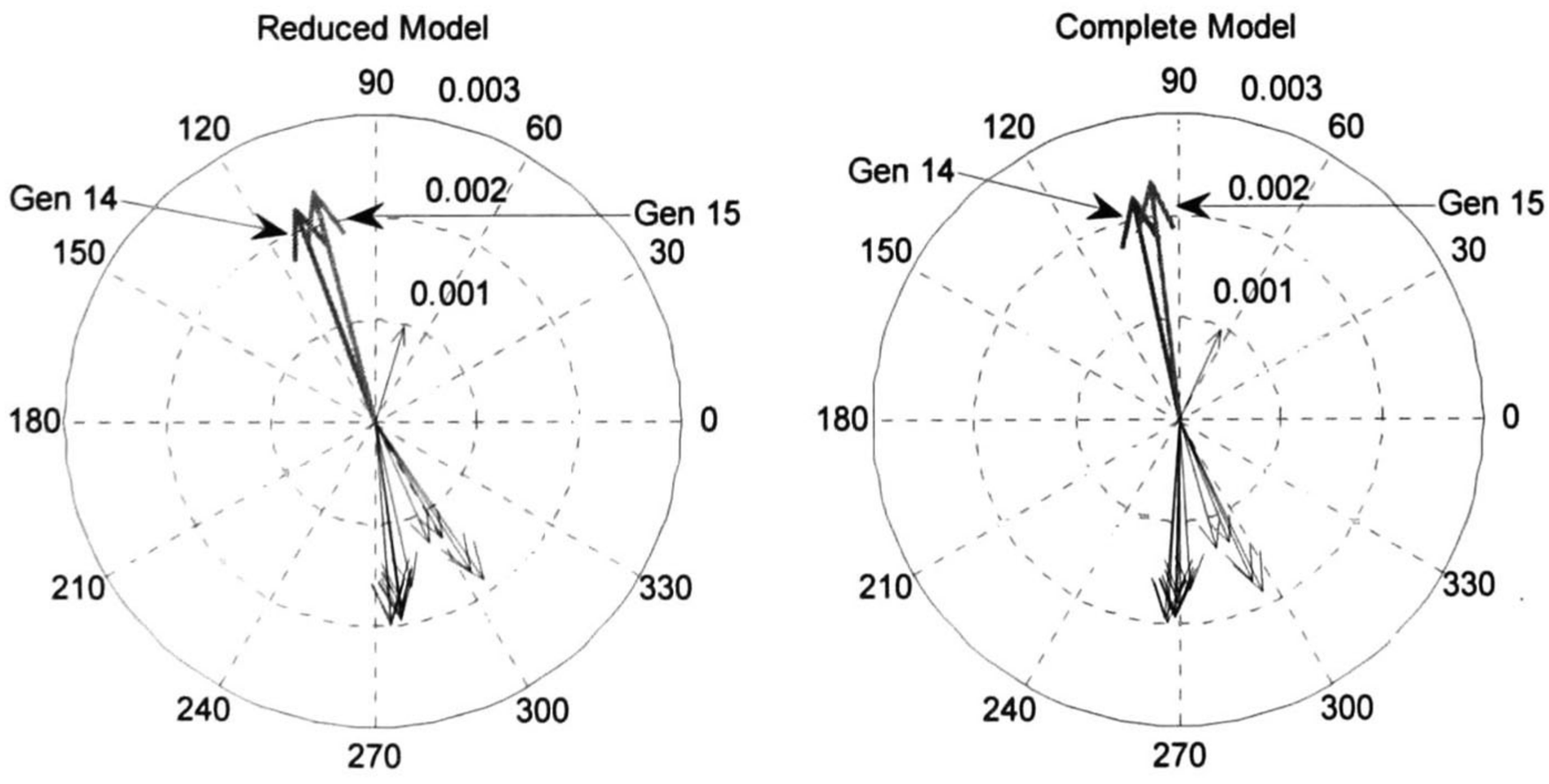

Figure 6.15. Mode shape indicates that is an inter-area mode because the generators 14 and 15 oscillate against of the rest of the system.

- Mode $-0.1971 \pm j3.5508$

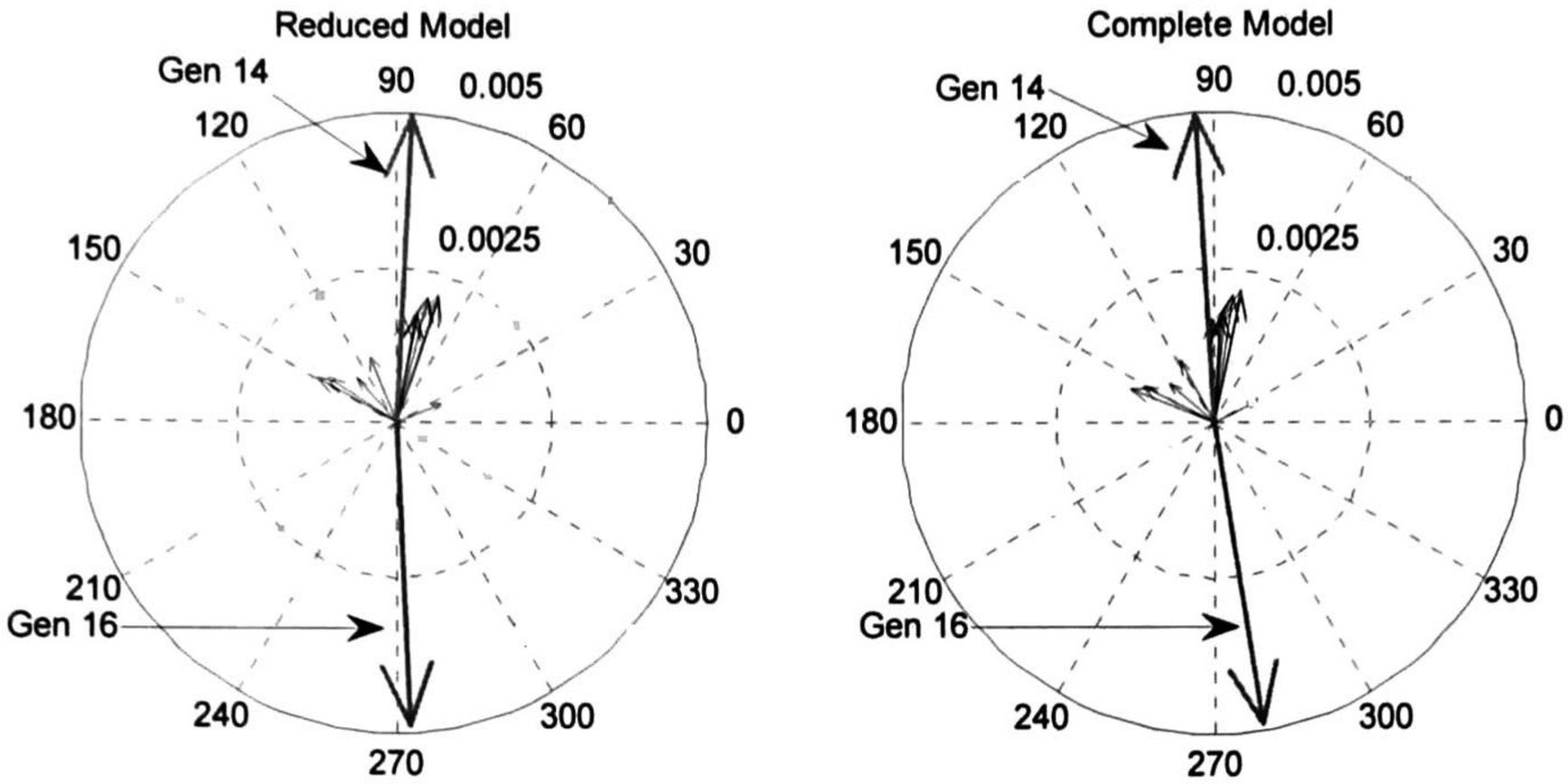

Figure 6.16. Mode shape indicates that is an inter-area mode because the generator 14 oscillates against of the generator 16.

Also of interest, Tables 6.2 and 6.3 compare the controllability and observability of the ROM with that of the original system model. Results are seen to be consistent with the full system representation

Note that in this analysis, the original model is described by

$$\begin{aligned} \Delta\dot{\mathbf{x}} &= \mathbf{A}_{xc}\Delta\mathbf{x} + \mathbf{A}_{uc}\Delta\mathbf{u} + \mathbf{H}_{xxc}(\Delta\mathbf{x} \otimes \Delta\mathbf{x}) \\ \Delta\bar{\mathbf{V}}_G &= \mathbf{B}_{xG}\Delta\mathbf{x} \\ \Delta\bar{\mathbf{V}}_L &= \mathbf{C}_{xL}\Delta\mathbf{x} \end{aligned} \tag{6.7}$$

The complete model is a model that has the same dimension that the original model, but which only conserves the eigenvalues of the reduced model and the rest is zero. For details see the chapter 5, the equation that describes the complete model is

$$\begin{aligned} \dot{\bar{\mathbf{x}}} &= \bar{\mathbf{A}}_{xc}\bar{\mathbf{x}} + \bar{\mathbf{A}}_{uc}\Delta\mathbf{u} + \bar{\mathbf{H}}_{xxc}(\bar{\mathbf{x}} \otimes \bar{\mathbf{x}}) \\ \Delta\bar{\mathbf{V}}_G &= \hat{\mathbf{B}}_{xG}\mathbf{W}^{*}\bar{\mathbf{x}} = \bar{\mathbf{B}}_{xG}\bar{\mathbf{x}} \\ \Delta\bar{\mathbf{V}}_L &= \hat{\mathbf{C}}_{xL}\mathbf{W}^{*}\bar{\mathbf{x}} = \bar{\mathbf{C}}_{xL}\bar{\mathbf{x}} \end{aligned} \tag{6.8}$$

The reduced order model is described by

$$\begin{aligned}
\Delta\dot{\hat{\mathbf{x}}} &= \hat{\mathbf{A}}_{xc}\Delta\hat{\mathbf{x}} + \hat{\mathbf{A}}_{uc}\Delta\mathbf{u} + \hat{\mathbf{H}}_{xxc}\left(\Delta\hat{\mathbf{x}} \otimes \Delta\hat{\mathbf{x}}\right) \\
\Delta\overline{\mathbf{V}}_G &= \hat{\mathbf{B}}_{xG}\Delta\hat{\mathbf{x}} \\
\Delta\overline{\mathbf{V}}_L &= \hat{\mathbf{C}}_{xL}\Delta\hat{\mathbf{x}}
\end{aligned} \tag{6.9}$$

In interpreting these results we remark that the original model is a global dynamic equivalent of the system, while the complete model and the ROM are dynamic models that model a specific disturbance of the system; this is the reason why the full system model and the ROM are more precise that the original model.

Table 6.2. The modes and their respective generators by means of which are more controllable

Mode	Reduced model	Complete model	Original model
	Generators	Generators	Generators
$-1.0021 \pm j11.9083$	11,10,1	11,10,1	11,10,12
$-1.1530 \pm j9.5072$	4,5,7	4,5,7	8,1,7
$-0.7341 \pm j8.6653$	11,4,10	11,4,10	10,1,8
$-1.4769 \pm j7.9856$	3,2,4	3,2,4	5,6,7
$-1.3493 \pm j7.0376$	3,2,4	3,2,4	9,5,6
$-0.3740 \pm j7.1663$	10,11,8	10,11,8	12,13,10
$-0.0911 \pm j4.9430$	15,14,16	15,14,16	15,14,16
$-0.7934 \pm j4.3105$	10,4,5	10,4,5	7,5,6
$-0.3095 \pm j2.7081$	10,8,11	10,8,11	15,7,6
$-0.1971 \pm j3.5508$	10,16,14	10,16,14	16,14,7

Table 6.3. The modes and their respective buses of generation and load where are more observable.

Mode	Reduced model		Original model	
	Generation buses	Load buses	Generation buses	Load buses
$-1.0021 \pm j11.9083$	63,64,62	32,33,51,34,38	63,62,64	32,33,51,34,38
$-1.1530 \pm j9.5072$	56,53,60	19,20,25,2,29	60,53,59	25,2,3,26,27
$-0.7341 \pm j8.6653$	56,53,60	19,25,2,20,29	53,62,60	25,2,3,31,38
$-1.4769 \pm j7.9856$	56,55,61	20,19,29,28,10	57,59,56	20,23,22,19,21
$-1.3493 \pm j7.0376$	61,54,55	29,28,10,11,12	61,57,56	29,28,20,19,26
$-0.3740 \pm j7.1663$	64,65,62	33,32,38	64,62,65	33,32,36
$-0.0911 \pm j4.9430$	67,66,68	42,41,40,52,48	67,66,68	42,41,40,52,48
$-0.7934 \pm j4.3105$	57,59,56	20,19,23,22,21	57,59,56	20,19,23,22,21
$-0.3095 \pm j2.7081$	67,66,57	42,41,20,19,23	67,66,57	42,41,20,23,19
$-0.1971 \pm j3.5508$	66,68,57	41,52,50,40,20	66,68,57	41,52,50,40,20

6.3 Detailed System Representation

For this study, each machine was represented by a fourth-order system model and equipped with a first-order excitation system. The overall state model has 80 differential equations, 136 algebraic equations.

Defining

$$\mathbf{x} = \begin{bmatrix} E'_{q1} & \cdots & E'_{q16} & E'_{d1} & \cdots & E'_{d16} & E_{fd1} & \cdots & E_{fd16} & \delta_1 & \cdots & \delta_{16} & \omega_1 & \cdots & \omega_{16} \end{bmatrix}^T$$

and

$$\mathbf{u} = \begin{bmatrix} T_{m1} & \cdots & T_{m16} & V_{ref1} & \cdots & V_{ref16} \end{bmatrix}^T$$

The nonlinear system model can be cast in the form (6.1).

6.3.1 Nonlinear ROM

Using the proposed technique the system is reduced to a 26nd-order system representation.

Figure 6.17 shows the energy spectrum obtained to capture 99.99% of the signal's energy. Note that in this case, the POD technique captures, essentially, 26 singular values of a total of 80 singular values.

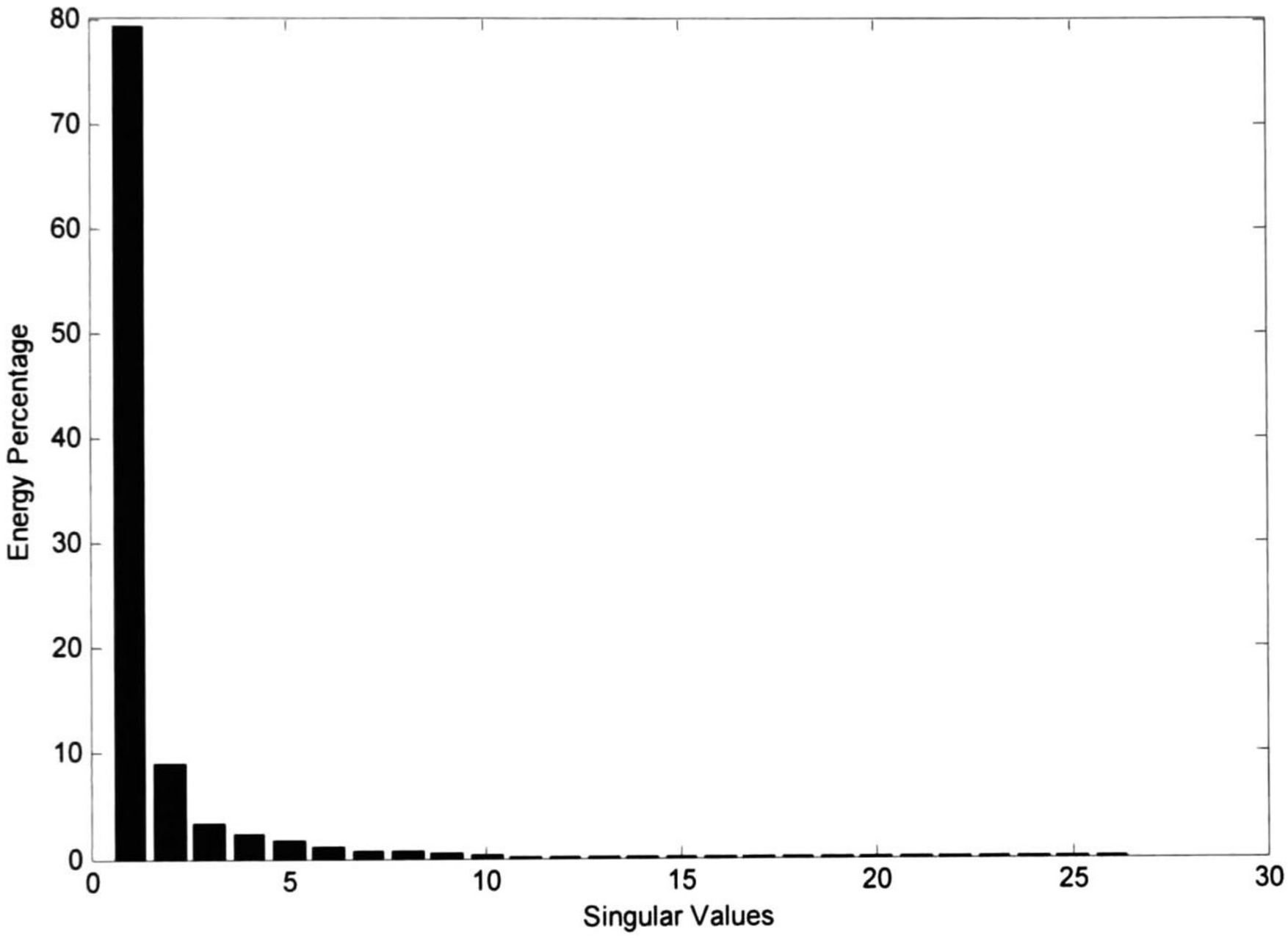

Figure 6.17. Energy percentage of each singular value of the ROM

Figure 6.18 through Figure 6.22 shows the system response to the same contingency condition in section 6.2. For the purposes of comparison, the same energy criterion is adopted in both set of simulations.

Simulation result show that the ROM is able to capture the essential system behavior. While no directly discussed in the work, the efficiency of the method increases as the order of the model increases. In these plots, the solid lines indicate the original system response while the dashed lines indicate the ROM response.

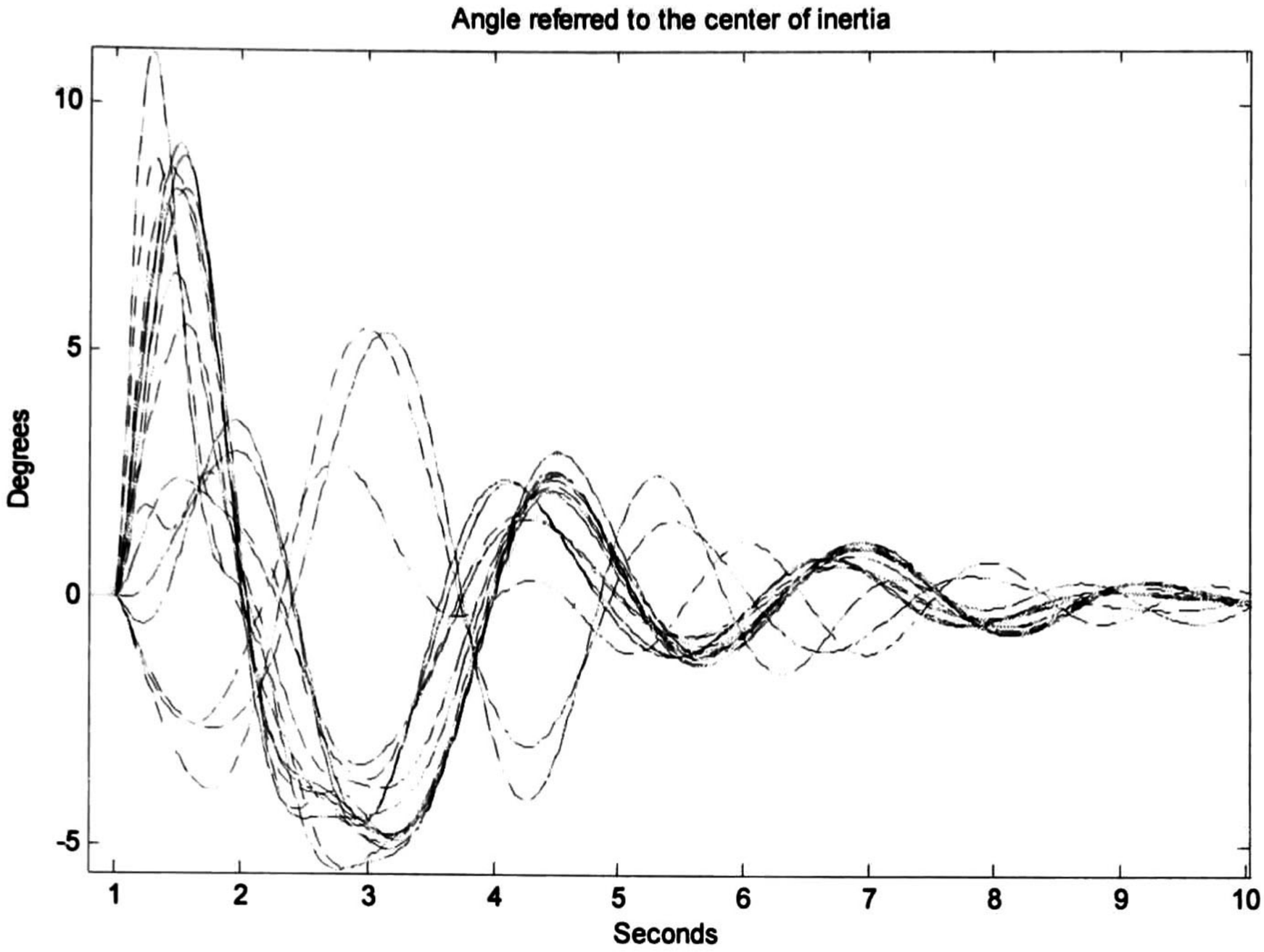

Figure 6.18. Dynamic behavior of the angle of the generators, given by el original model and the ROM.

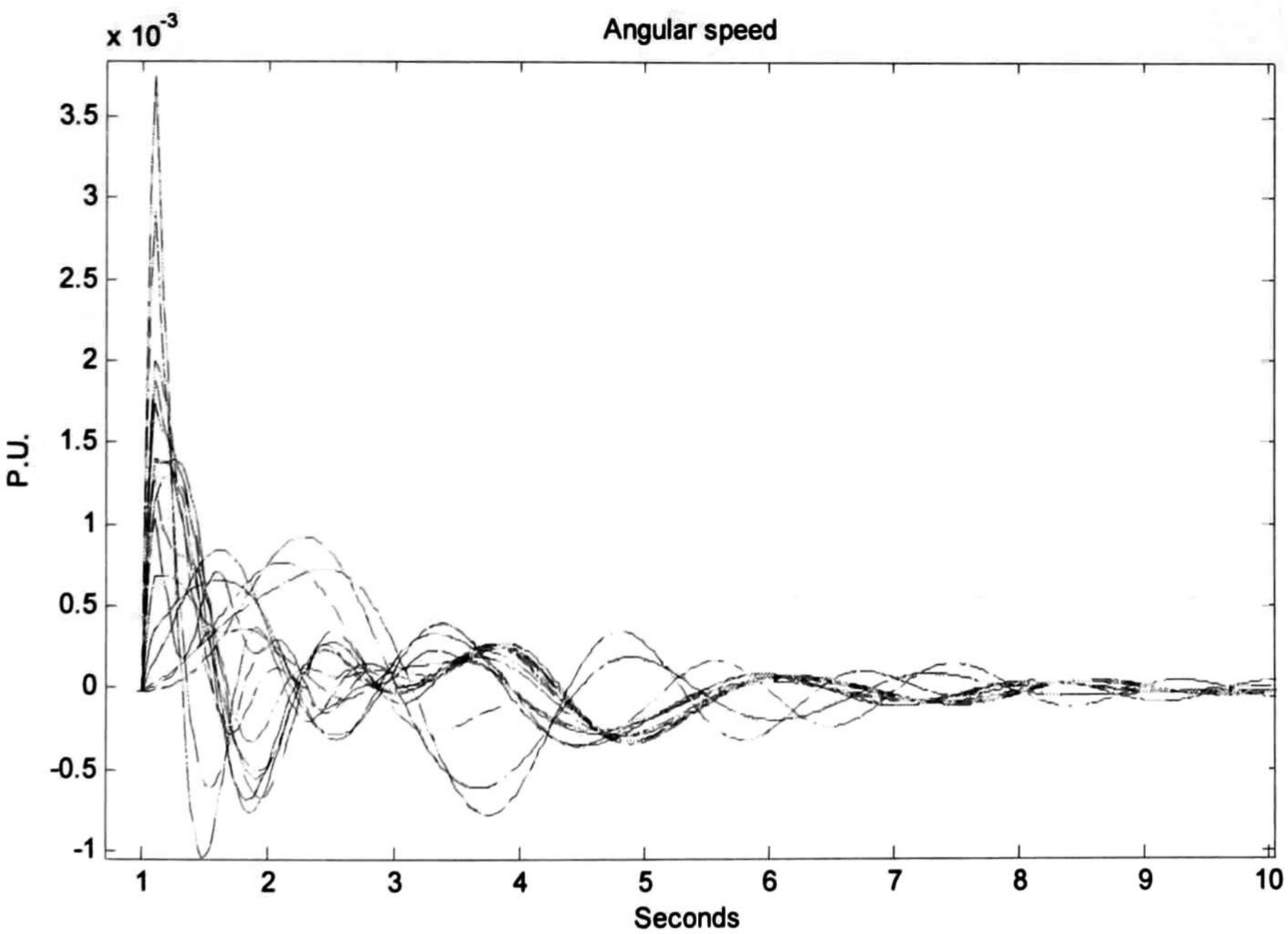

Figure 6.19. Dynamic behavior of the angular speed of the generators, given by the original model and the ROM.

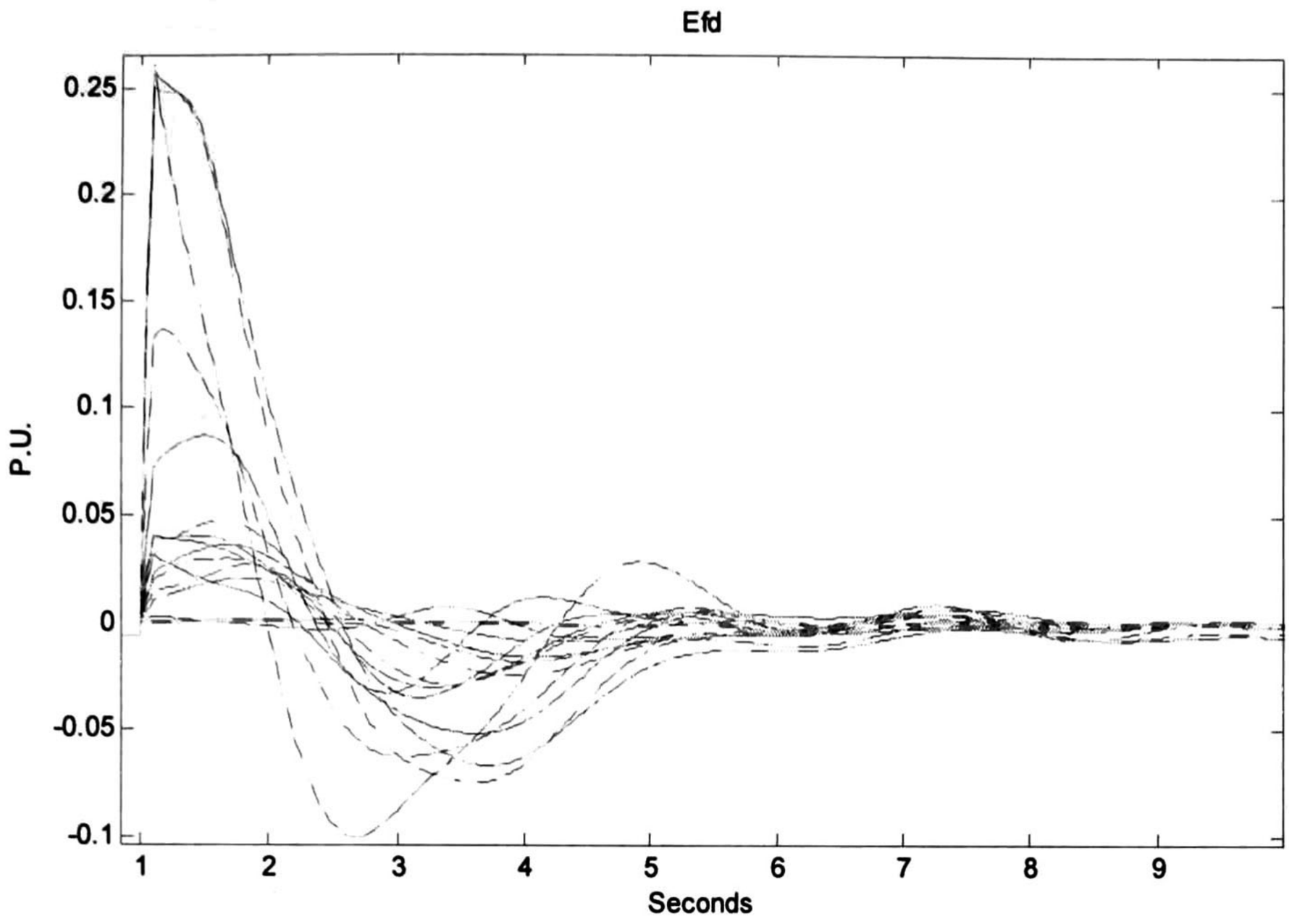

Figure 6.20. Dynamic behavior of the voltage E_{fd}, given by the original model and the ROM.

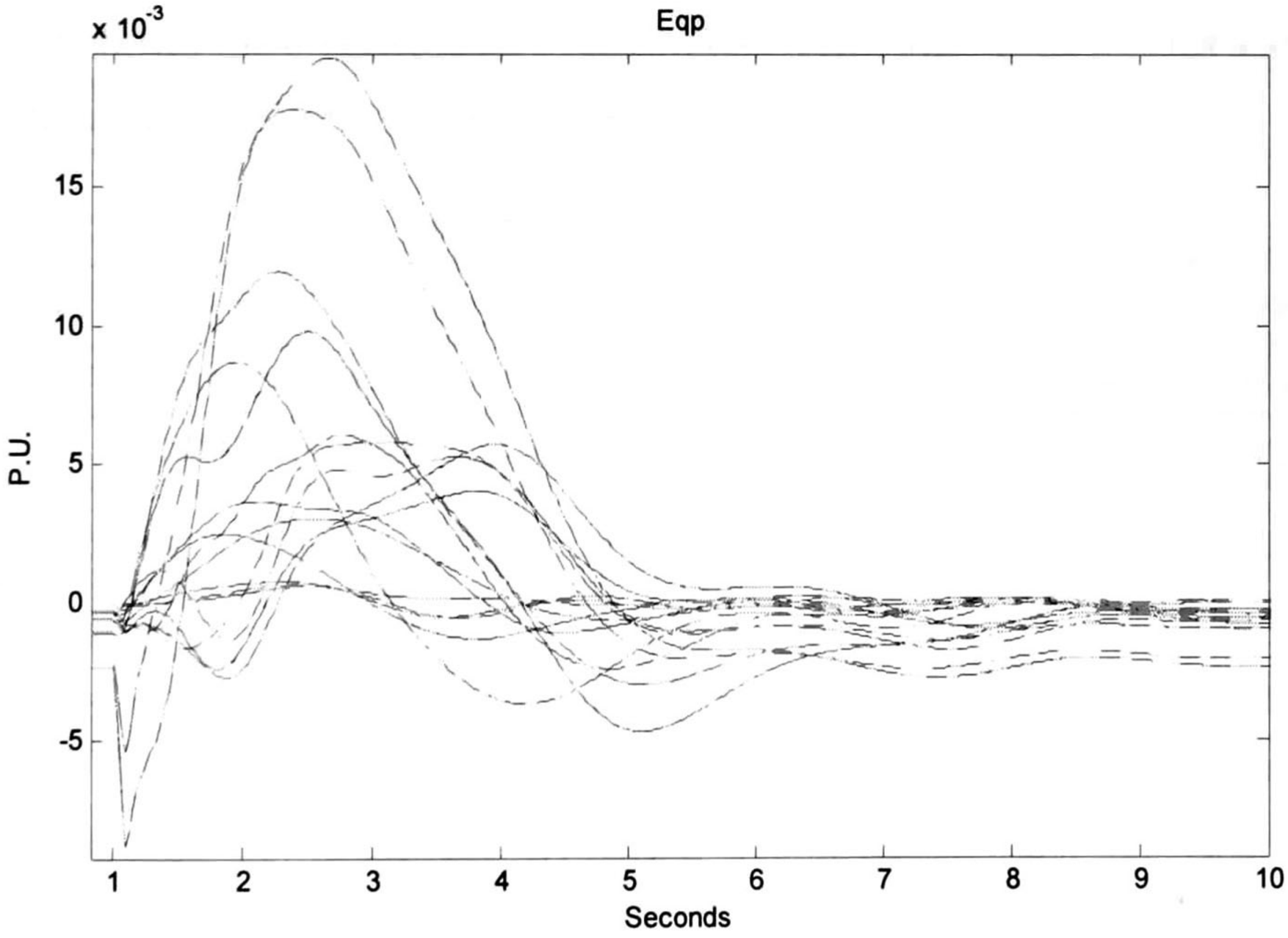

Figure 6.21. Dynamic behavior of the voltage E'_q, given by the original model and the ROM.

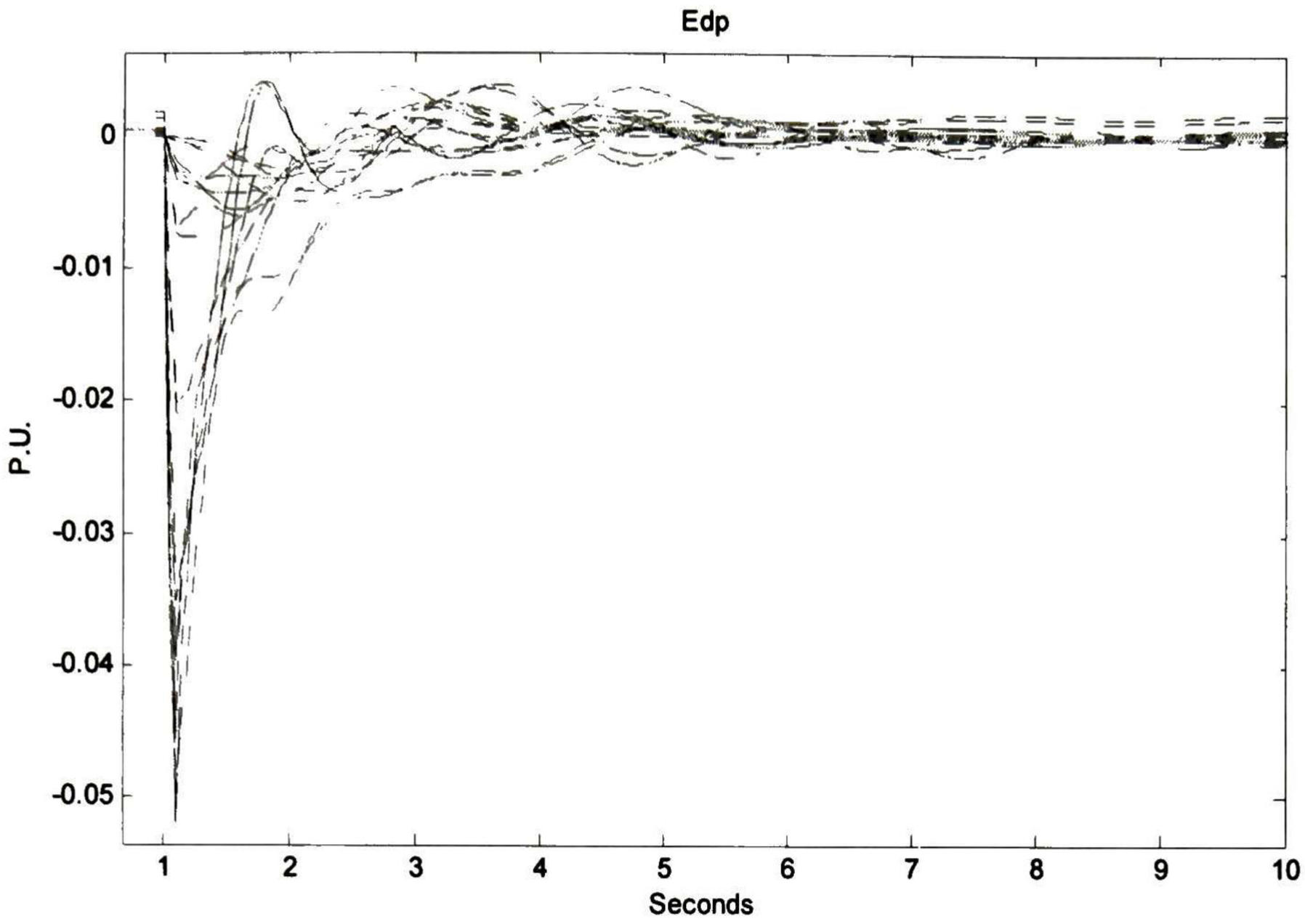

Figure 6.22. Dynamic behavior of the voltage E'_d, given by the original model and the ROM.

Proper orthogonal modes have a similar interpretation to linear modes. Table 6.4 shows the eigenvalues associated with the POMs. This is for an energy percentage of the 99.99% of the snapshots.

Table 6.4. Eigenvalues of the ROM.

Number	Eigenvalue	Frequency	Number	Eigenvalue	Frequency
1	-1.2764 ± 9.7851	1.5573	9	$-0.2749 \pm j2.6653$	0.4242
2	$-1.8783 \pm j8.6989$	1.3845	10	$-0.0363 \pm j1.3546$	0.2156
3	-7.5025	0	11	$-1.2994 \pm j0.6109$	0.0972
4	$-0.8894 \pm j7.2466$	1.1533	12	-1.1864	0
5	$-1.0384 \pm j6.3237$	1.0064	13	-0.0009	0
6	$-0.5151 \pm j4.5070$	0.7173	14	-0.3234	0
7	$-0.2452 \pm j3.5069$	0.5581	15	$-0.2624 \pm j0.3390$	0.0540
8	$-0.8545 \pm j3.1333$	0.4987			

Also of interest, the linear system given in (6.4) has a solution of the form that follows

$$\hat{z}_k(t) = \hat{z}_{k0} e^{\hat{\lambda}_k t}$$

$$\Delta \mathbf{x} = \mathbf{W} \Delta \hat{\mathbf{x}} = \mathbf{W} \hat{\boldsymbol{\varphi}} \hat{\mathbf{z}}_0 e^{\hat{\Lambda} t}$$

where $\hat{\mathbf{z}}_0 = \hat{\mathbf{z}}(0)$, while that original model has a solution of the form

$$\Delta \mathbf{x} = \boldsymbol{\varphi} \mathbf{z}_0 e^{\Lambda t}$$

Figure 6.23 and Figure **6.24** shows simulation results corresponding to Eqns. 6.5 and 6.6. Solid lines represent the time evolution of the original model while broken lines correspond to the time evolution of the ROM.

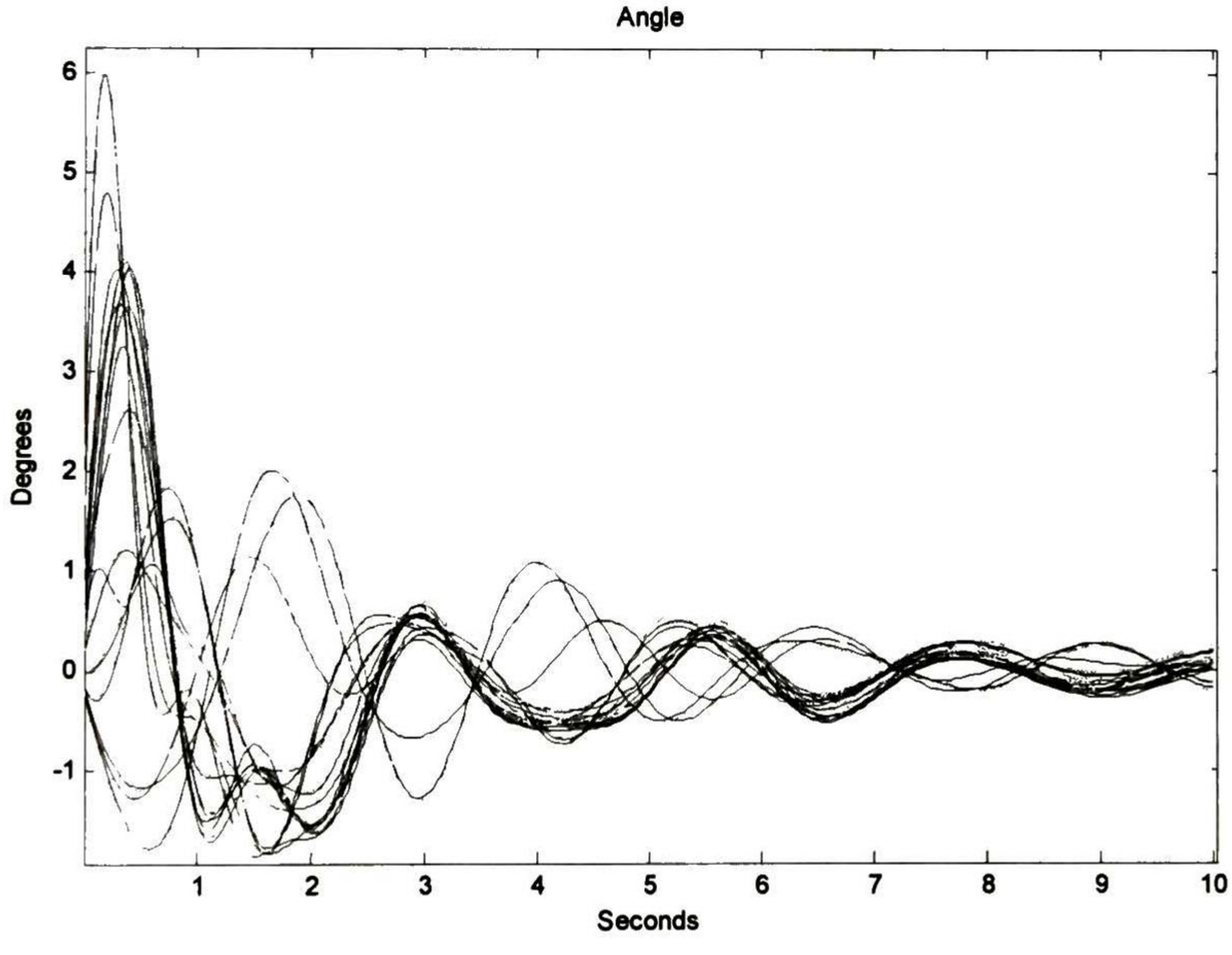

Figure 6.23. Dynamic behavior of the angle of the generators, given by the Equations 6.5 and 6.6.

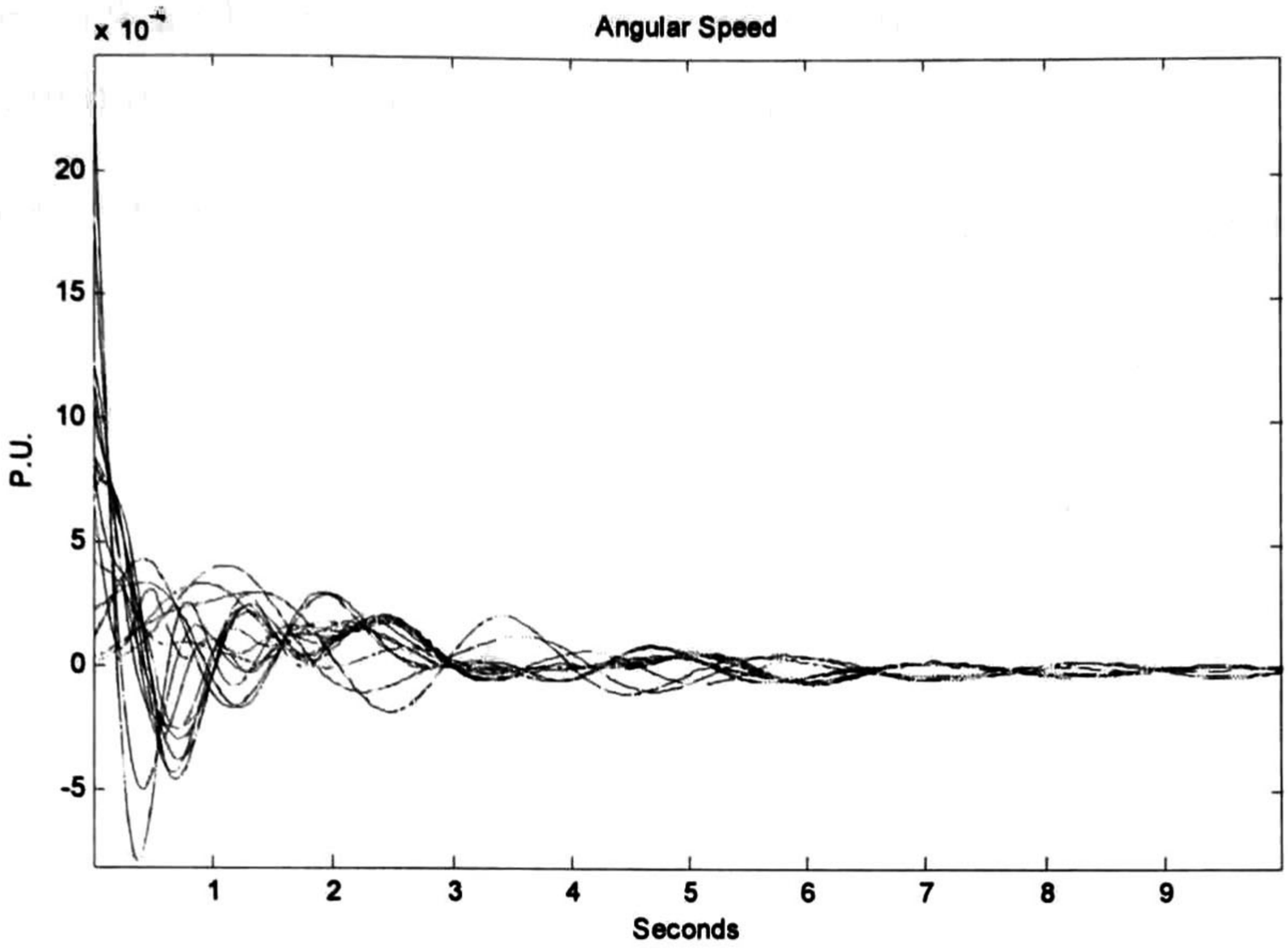

Figure 6.24. Dynamic behavior of the angular speed of the generators, given by the Equations 6.5 and 6.6.

6.3.2 Modal Properties

Based on the linear ROM, detailed studies were conducted to evaluate the ability of the method to extract modal properties. Discussion will be limited to mode $-0.2749 \pm j2.6653$

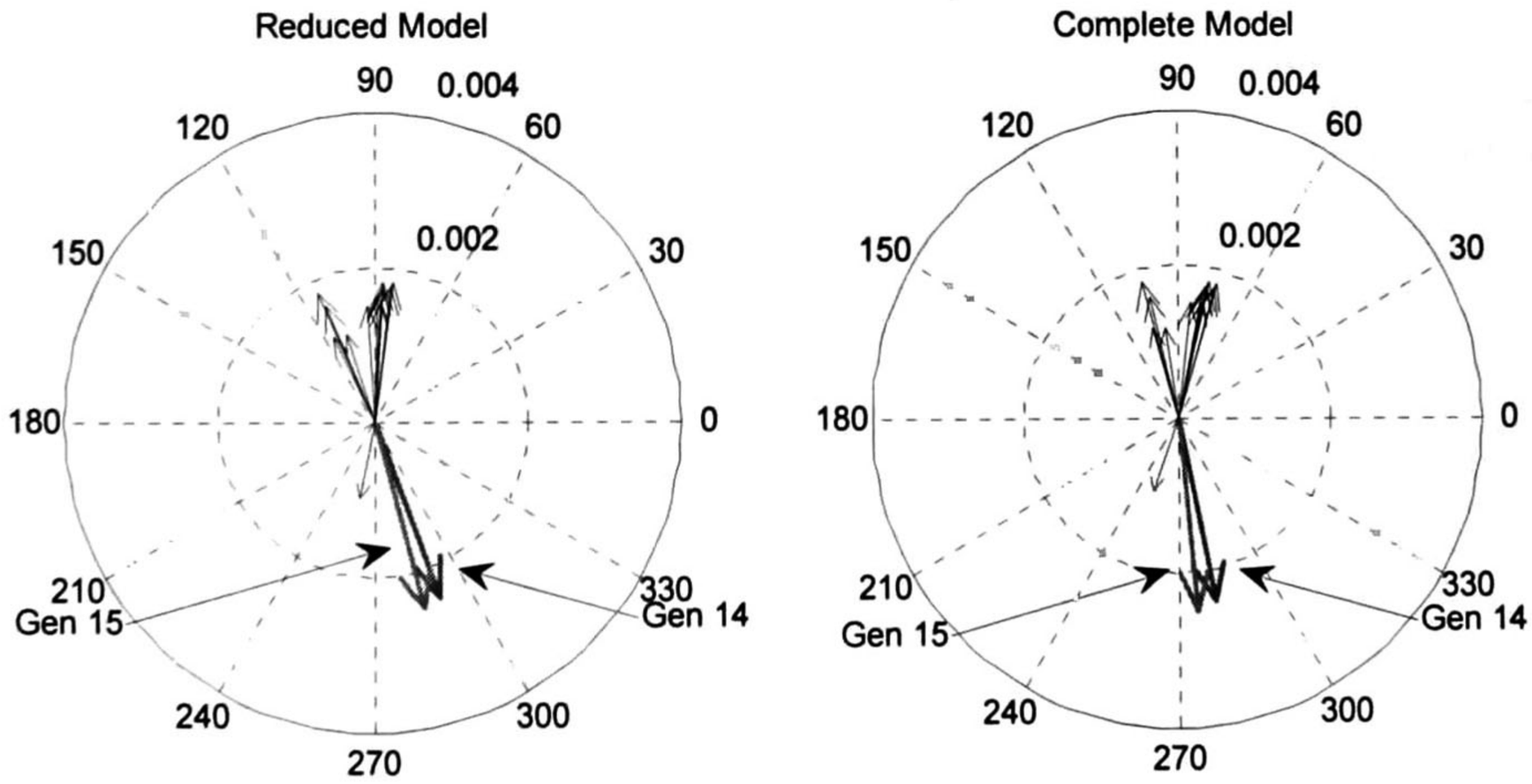

Figure 6.25. Mode shape indicate that is an inter-area mode, because the generators 14 and 15 oscillates against of the rest of the system

Tables 6.5 and 6.6 compare the controllability and observability of the ROM with that of the complete system model.

Table 6.5. The modes and their respective generators by means of which are more controllable.

Mode	Reduced model	Complete model
	Generators	Generators
-1.2764 ± 9.7851	13,14,1	13,14,1
$-1.8783 \pm j8.6989$	14,10,2	14,10,2
$-0.8894 \pm j7.2466$	13,12,14	13,12,14
$-1.0384 \pm j6.3237$	13,8,1	13,8,1
$-0.5151 \pm j4.5070$	8,1,14	8,1,14
$-0.2452 \pm j3.5069$	14,13,12	14,13,12
$-0.8545 \pm j3.1333$	8,1,13	8,1,13
$-0.2749 \pm j2.6653$	13,12,8	13,12,8
$-0.0363 \pm j1.3546$	8,14,13	8,14,13
$-1.2994 \pm j0.6109$	1,2,8	1,2,8
$-0.2624 \pm j0.3390$	1,8,2	1,8,2

Table 6.6. The modes and their respective buses of generation and load where they are more observables.

Mode	Reduced model		Complete model	
	Generation buses	Load buses	Generation buses	Load buses
-1.2764 ± 9.7851	63,64,65	32,33,37,51,34	63,64,65	32,33,37,51,34
$-1.8783 \pm j8.6989$	63,55,53	32,33,37,51,36	63,55,53	32,33,37,51,36
$-0.8894 \pm j7.2466$	55,63,54	10,11,12,37,13	55,63,54	10,11,12,37,13
$-1.0384 \pm j6.3237$	61,55,65	29,20,28,37,13	61,55,65	29,20,28,37,13
$-0.5151 \pm j4.5070$	57,59,58	20,19,22,23,21	57,59,58	20,19,22,23,21
$-0.2452 \pm j3.5069$	66,68,67	41,52,50,40,49	66,68,67	41,52,50,40,49
$-0.8545 \pm j3.1333$	57,59,56	20,19,23,22,21	57,59,56	20,19,23,22,21
$-0.2749 \pm j2.6653$	67,66,65	42,41,20,37,9	67,66,65	42,41,20,37,9
$-0.0363 \pm j1.3546$	68,67,66	52,42,50,41,37	68,67,66	52,42,50,41,37
$-1.2994 \pm j0.6109$	63,65,64	37,32,36,33,20	63,65,64	37,32,36,33,20
$-0.2624 \pm j0.3390$	67,68,66	42,52,41,50,49	63,62,57	33,32,38,46,31

As may be observed from this Table, controllability indices of the ROM are in good agreement with those of the full system models. Other results, not included in the chapter, show the proposed mode accurately capture other modal characteristics.

6.4 Summary of Results

In this chapter a number of illustrative case studies were given in which the modeling approach of previous chapters was applied to a test system.

Detailed simulation results show that POD-based projections can produce accurate reduced-order models. Because the extracted nonlinear ROM preserves the input-output characteristics, the model have the potential to be applied for control design.

Study results suggest that the analytical formulation becomes more efficient as the size of the model becomes larger. This issue is particularly relevant for assessing the accuracy of the method utilized in the paper and deserves further exploration.

6.5 References

[1] Graham Rogers, *Power System Oscillations*, Kluwer Academic Publishers, 2000.

[2] Peter W. Sauer and M. A. Pai, *Power System Dynamics and Stability*, Prentice Hall, 1998.

[3] Prabha Kundur, *Power System Stability and Control*, Mc-Graw-Hill, Inc., 12: 699-717.

Chapter 7
Conclusions

7.1 General Conclusions

The work developed in this thesis, presents a new framework for dynamic characterization of nonlinear systems described by differential-algebraic equations based on a singular value decomposition based projection framework.

A new algorithm has been presented for the reduced order model problem that preserves network structure and input-output characteristics. Using this approach, one can develop a modeling and simulation technique that retains the algebraic nature of the algebraic equations and input-output characteristics.

Other potential applications include its use in conjunction with other analysis techniques, such as normal form theory. Because the model preserves nonlinear characteristics, information about nonlinear interactions is retained which makes it useful for investigation of nonlinear aspects in complex systems. This area needs further study.

A key advantage of the proposed technique is its ability to retain the inputs and outputs of interest, thus allowing the design of system controllers. The use of this reduced nonlinear model allows, in general, for a smaller range of operation. This should be verified in practical applications involving large-scale systems.

An important research focus of this study was an examination of the accuracy of the model using energy concepts. Detailed simulation studies suggest that the proposed method is accurate, and feasible for the study and generation of reduced-order dynamic equivalents.

7.2 Future Work

The future areas of research identified in this work are:

1. The extension of the proposed technique to design system controllers.

2. The development of an analysis framework for analysis of nonlinear effects in system behavior based on normal form theory.

3. The generalization of the proposed technique to incorporate the effect of flexible ac system controllers.

4. The optimization of numerical procedures to derive the nonlinear ROMs.

CENTRO DE INVESTIGACIÓN Y DE ESTUDIOS AVANZADOS DEL I.P.N.
UNIDAD GUADALAJARA

El Jurado designado por la Unidad Guadalajara del Centro de Investigación y de Estudios Avanzados del Instituto Politécnico Nacional aprobó la tesis

Reducción no lineal de modelos de sistemas de potencia

del (la) C.

Antonino LÓPEZ RÍOS

el día 11 de Agosto de 2008.

Dr. Arturo Román Messina
Investigador CINVESTAV 3C
CINVESTAV Unidad Guadalajara

Dr. José Javier Ruíz León
Investigador CINVESTAV 3B
CINVESTAV Unidad Guadalajara

Dr. Jaime Arroyo Ledesma
Profesor Investigador Titular A
Universidad de Colima, Campus:
Delegación Regional Num 4,
Coquimatlán